August 22, 1972

To the Graduate Council:

I am submitting herewith a thesis written by John Ralph Hamilton entitled "Prediction of Semiscale Blowdown Data Using the Relap 3 Computer Code." I recommend that it be accepted for nine quarter hours of credit in partial fulfillment of the requirements for the degree of Master of Science, with a major in Nuclear Engineering.

Major Professor

We have read this thesis and recommend its acceptance:

Accepted for the Council:

Vice Chancellor for
Graduate Studies and Research

PREDICTION OF SEMISCALE BLOWDOWN DATA USING THE RELAP3 COMPUTER CODE

A Thesis

Presented to

the Graduate Council of

The University of Tennessee

In Partial Fulfillment

of the Requirements for the Degree

Master of Science

---

by

John Ralph Hamilton

March 1973

ACKNOWLEDGMENTS

The author wishes to thank the many people who helped him with this thesis. Special thanks must go to Dr. Julian E. Mott, who suggested the topic, and who gave much help and advice; to Mr. David Simpson, who labored for many hours setting up the computer codes used; to Mr. R. A. Hedrick and Dr. B. E. Bingham of the Babcock and Wilcox Company, who made many helpful suggestions; to Mr. H. W. Heiselmann of the Aerojet Nuclear Company, who supplied much useful design data; and finally, to my wife Maxine without whose patience and encouragement I could not have attempted this thesis.

1069508

ABSTRACT

This thesis compares the predictions of the RELAP3 computer code with semiscale model loss-of-coolant accident data. The test runs used are single-loop semiscale tests 825 and 845. The results of the RELAP3 calculations show general agreement with the experimental data. The thesis includes suggestions for some possible improvements in RELAP3. The suggestions include ways to improve the system thermodynamic calculations, the departure from nucleate boiling calculations, and the heat exchanger calculations.

TABLE OF CONTENTS

SECTION		PAGE
I.	INTRODUCTION	1
II.	CALCULATION PROCEDURES	3
	Description of the Semiscale Facility	3
	RELAP3 Input	10
III.	RESULTS	40
	Introduction	40
	Results--Test 845	40
	Results--Test 825	65
	Comparison of FLASH3 and RELAP3 Calculations	81
IV.	DISCUSSION	88
V.	CONCLUSIONS	97
LIST OF REFERENCES		100
VITA		103

LIST OF TABLES

TABLE		PAGE
1.	Single-Loop Semiscale System Design Data	6
2.	Test Conditions--Tests 825 and 845	8
3.	RELAP3 Heat Transfer Modes	16
4.	RELAP3 DNB Correlations	19
5.	Summary of Control Volume Input Data	27
6.	Summary of Flow Path Input Data	32
7.	Time Steps--Tests 825 and 845	39
8.	Calculated Mass Distribution at 11.5 Sec.	59
9.	Calculated Mass Distribution at 22 Sec.	60
10.	Comparison of FLASH3 and RELAP3 Calculation Models	83

LIST OF FIGURES

FIGURE		PAGE
1.	Schematic of Semiscale Loop--Test 825	4
2.	Schematic of Semiscale Loop--Test 845	5
3.	Schematic of Emergency Core Coolant Injection System	7
4.	Control Volume Arrangement Used in Conservation Equations	12
5.	RELAP3 Model of Semiscale Loop--Test 825	25
6.	RELAP3 Model of Semiscale Loop--Test 845	26
7.	Semiscale Pump Characteristic	33
8.	Inlet Plenum Pressure--Test 845	41
9.	Pressurizer Pressure--Test 845	43
10.	Outlet Plenum Fluid Temperature--Test 845	44
11.	Inlet Plenum Fluid Temperature--Test 845	46
12.	Core Fluid Temperature--Test 845	47
13.	Inlet Plenum Flow Rate--Test 845	48
14.	Inlet Plenum Flow Rate--Test 845, Initial Part of Transient	50
15.	Inlet Nozzle Flow Rate--Test 845	51
16.	Leak Flow Rate--Test 845	52
17.	Core Fluid Density--Test 845	54
18.	Inlet Plenum Fluid Mass-Test 845	55
19.	Inlet Plenum Mixture Level--Test 845	56

FIGURE PAGE

20. Volume 12 Calculated Fluid Mass--Test 845 57
21. Clad Temperature--Test 845 61
22. DNB History--Test 845 63
23. Heat Exchanger Heat Removal Rate--Test 845 64
24. Heat Exchanger Tube Bundle Pressures--Test 845 66
25. Heat Exchanger Tube Bundle Fluid Mass--Test 845 67
26. Inlet Plenum Pressure--Test 825 68
27. Heat Exchanger Outlet Plenum Pressure--Test 825 69
28. Heat Exchanger Outlet Plenum Mixture Level--Test 825 . . . 70
29. Inlet Plenum Fluid Temperature--Test 825 72
30. Core Flow Rate--Test 825 73
31. Outlet Nozzle Flow Rate--Test 825 74
32. Hot Leg Pipe Flow Rate--Test 825 75
33. Core Fluid Density--Test 825 77
34. Inlet Nozzle Fluid Density--Test 825 78
35. Clad Temperatures--Test 825 79
36. DNB History--Test 825 80
37. FLASH3 Control Volume Arrangement (from Reference 10) . . . 82
38. FLASH3 Inlet Plenum Pressure 84
39. FLASH3 Inlet Nozzle Flow Rate 85
40. FLASH3 Clad Temperature 87
41. Heat Flux Diagram--Test 825 92

LIST OF SYMBOLS

SYMBOL	DEFINITION
A	Flow area, sq ft
A_{HT}	Heat transfer surface area, sq ft
a	Acoustic velocity, ft/sec
b	Constant in equation (II-7)
C_D	Discharge coefficient, dimensionless
C_0	Constant in equations (II-7) through (II-9)
CAV	Pump cavitation multiplier, dimensionless
CD	Pump coastdown multiplier, dimensionless
D_e	Hydraulic equivalent diameter, ft
D_h	Heated equivalent diameter, ft
DP	Parameter in equation (II-22), psi
f	Moody friction factor
G	Mass flux, $lb_m/hr/sq\ ft$
g	32.2 ft/sec/sec
g_c	$32.2\ (lb_m - ft)/(lb_f - sec^2)$
H	Enthalpy, BTU/lb_m
H_f	Enthalpy of saturated liquid, BTU/lb_m
H_g	Enthalpy of saturated vapor, BTU/lb_m

SYMBOL	DEFINITION
H_{fg}	Latent heat of vaporation, BTU/lb_m
Hd	Pump head, ft
Hd_R	Reference pump head, ft
$Hd_{shutoff}$	Pump shutoff head, ft
h	Heat transfer coefficient, BTU/hr-sq ft-^oF)
h_{FC}	Forced convection heat transfer coefficient, BTU/(hr-sq ft-^oF)
h_{HXT}	RELAP3 heat exchanger coefficient, BTU/hr/^oF
h_m	Heat exchanger tube metal conductance, BTU/(hr-sq ft-^oF)
h_{pri}	Heat exchanger primary fluid conductance, BTU/(hr-sq ft-^oF)
h_{sec}	Heat exchanger secondary fluid conductance, BTU/(hr-sq ft-^oF)
K	RELAP3 friction coefficient
k	Thermal conductivity, BTU/hr/ft/^oF
k_f	Thermal conductivity of saturated liquid, BTU/hr/ft/^oF
L	Length, ft
M	Mass, lb_m
M_{gb}	Mass of vapor bubbles in a two-phase mixture, lb_m

SYMBOL	DEFINITION
m	Constant in equation (II-7)
N	Pump speed, rpm
N_R	Reference pump speed, rpm
N_{VH}	Number velocity heads
n	Safety factor for time step claculation
P	Pressure, lb_f/sq in
P_{vap}	Vapor pressure, psi
Pr	Prandtl number
ΔP	Pressure difference, $P_{upstream} - P_{downstream}$, lb f/sq in
Q	Volumetric flow rate, gpm or cu ft/sec
Q_R	Reference volumetric flow rate, gpm or cu ft/sec
Q_0	Initial volumetric flow rate, gpm or cu ft/sec
q	Heat rate, BTU/hr
q"	Heat flux, BTU/hr/sq ft
q''_i	Incipient boiling heat flux, BTU/hr/sq ft
q''_{NB}	Nucleate boiling heat flux, BTU/hr/sq ft
q''_{NBi}	Nucleate boiling heat flux at incipient boiling point, BTU/hr/sq ft
Re	Reynold number, dimensionless

SYMBOL	DEFINITION
T	Temperature, ^{o}F
T_{bulk}	Bulk fluid temperature, ^{o}F
T_{FC}	Forced convection surface temperature, ^{o}F
T_{NB}	Nucleate boiling surface temperature, ^{o}F
T_{pri}	Heat exchanger primary fluid temperature, ^{o}F
T_{sat}	Saturation temperature, ^{o}F
T_{sec}	Heat exchanger secondary fluid temperature, ^{o}F
T_{surf}	Surface temperature, ^{o}F
t	Time, sec
U	Internal energy, BTU/lb_m
V	Velocity, ft/sec
v	Specific volume, ft^3/lb_m
(Vol)	Volume, ft^3
$(Vol)_m$	Volume of a two-phase mixture, ft^3
W	Flow rate, lb_m/sec
W_0	Initial flow rate, lb_m/sec
X	Quality, dimensionless
Z	Elevation, ft
Z_{cm}	Center of mass elevation, ft
Z_{jun}	Junction elevation, ft

SYMBOL	DEFINITION
Z_m	Mixture elevation, ft
ρ	Density, lb_m/cu ft
ρ_f	Density of saturated liquid, lb_m/cu ft
ρ_g	Density of saturated vapor, lb_m/cu ft
μ	Viscosity, lb_m/hr/ft
μ_f	Viscosity of saturated liquid, lb_m/hr/ft
μ_g	Viscosity of saturated vapor, lb_m/hr/ft
Subscripts	
i	Control volume index
j	Flow path index

I. INTRODUCTION

Computer simulation of the postulated loss-of-coolant accident is an important part of the safety analysis of water-cooled nuclear reactors. Aerojet Nuclear Company has recently published the results of some loss-of-coolant accident experiments in a small semiscale model. This data makes it possible to compare the computer code predictions with test data.

This thesis compares the predictions of the RELAP3 (1)* computer code with some of the previously mentioned loss-of-coolant accident model test data. The thesis analyzes the variance between the computer predictions and the experimental data, and suggests some possible improvements in RELAP3.

Reference (1) presents a detailed description of the RELAP3 code. Briefly, RELAP3 is a Fortran IV computer code designed to simulate severe transients, such as the postulated loss-of-coolant accident, in water-cooled nuclear reactors. RELAP3 can also be used to simulate loss-of-coolant accident experiments in small models, and the analysis of this kind of simulation is the subject of this thesis.

References (2) and (3) report the results of the two experiments used in the study. Both tests were run in the single-loop, semiscale blowdown facility. Reference (4) describes this facility, and Section II

---

*The numbers in parentheses refer to reference citations in the "List of References."

includes schematic drawings of the test loop, as well as a summary of the loop's design features. Briefly, the test apparatus consists of a model reactor vessel equipped with electric heaters, and a heat exchange loop containing a heat exchanger, a coolant circulating pump, and a pressurizer. The system fluid volume is about 13 cu ft. Rupture disks provide a quick-opening leak path to the atmosphere, which is needed to simulate a loss-of-coolant accident. There are several possible rupture disk locations, which allows the simulation of vessel inlet and outlet pipe ruptures.

II. CALCULATION PROCEDURES

A. DESCRIPTION OF THE SEMISCALE FACILITY

Loop components. Figures 1 and 2 are schematic drawings of the single-loop semiscale facility. Table 1 presents a summary of the system design data. The heat exchanger has system coolant on the tube side, and the shell-side fluid is water at atmospheric pressure. The model core contains 120 cartridge-type electric heaters. The coolant circulating pump has a variable speed drive for flow rate control, and a valve in the cold leg pipe gives additional flow rate control. The pressurizer is in two sections, one above the other. The upper section is the pressurizer vessel, and the lower one is the extension vessel. The pressurizer vessel contains electric heaters for control of system pressure.

Emergency core coolant system. The emergency core coolant system for test 845 consists of an accumulator containing 2.6 cu. ft. of water and 1.4 cu. ft. of nitrogen cover gas at a pressure of 615 psig. A check valve in the pipe connecting the accumulator with the vessel inlet plenum controls the start of the fill flow. A throttle valve provides flow rate control. Figure 3 is a schematic drawing of the emergency core coolant system.

Test 825. Table 2 gives the initial conditions and the sequence of events for tests 825 and 845. Reference (2) reports the results of

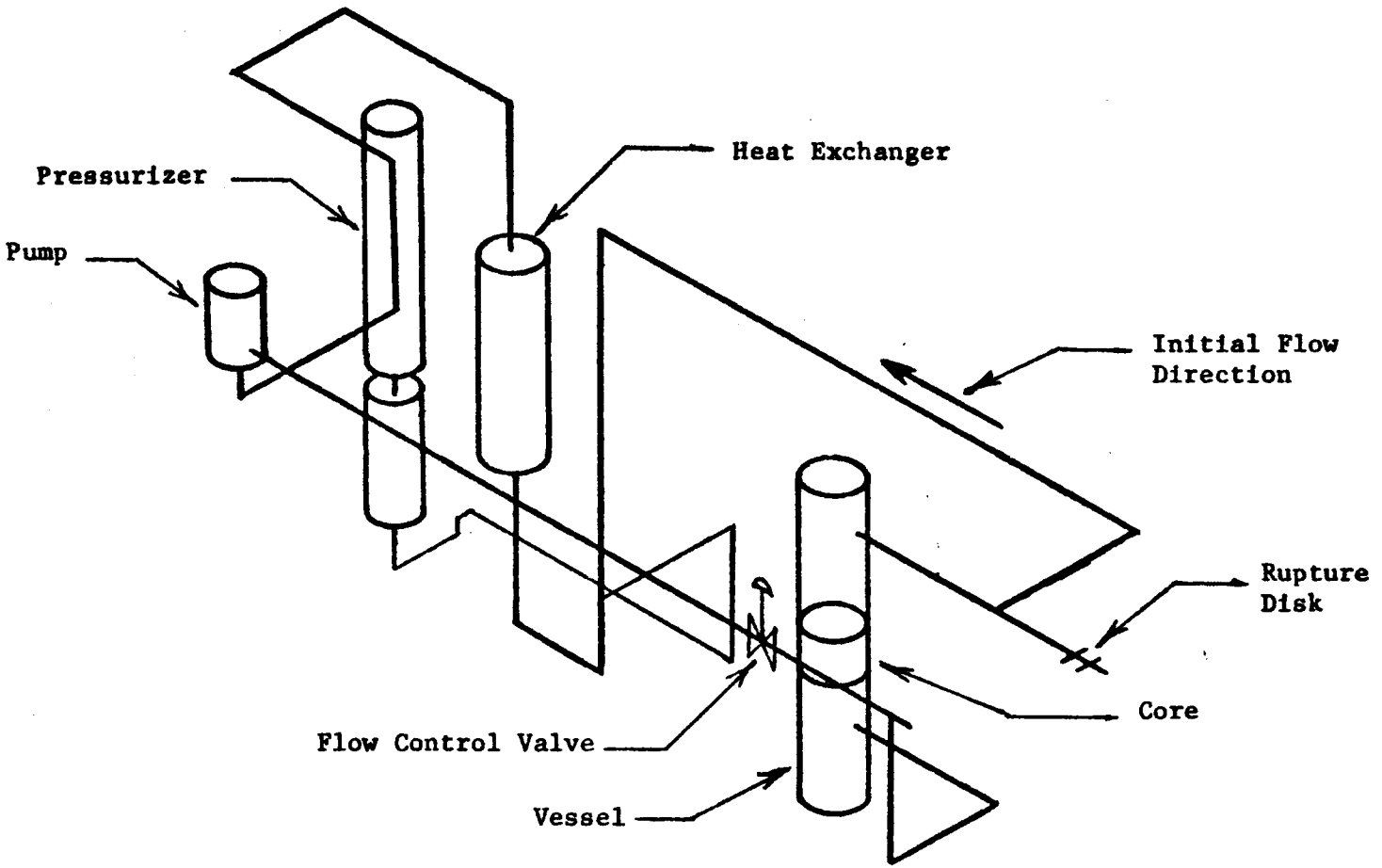


Figure 1. Schematic of semiscale loop--test 825.

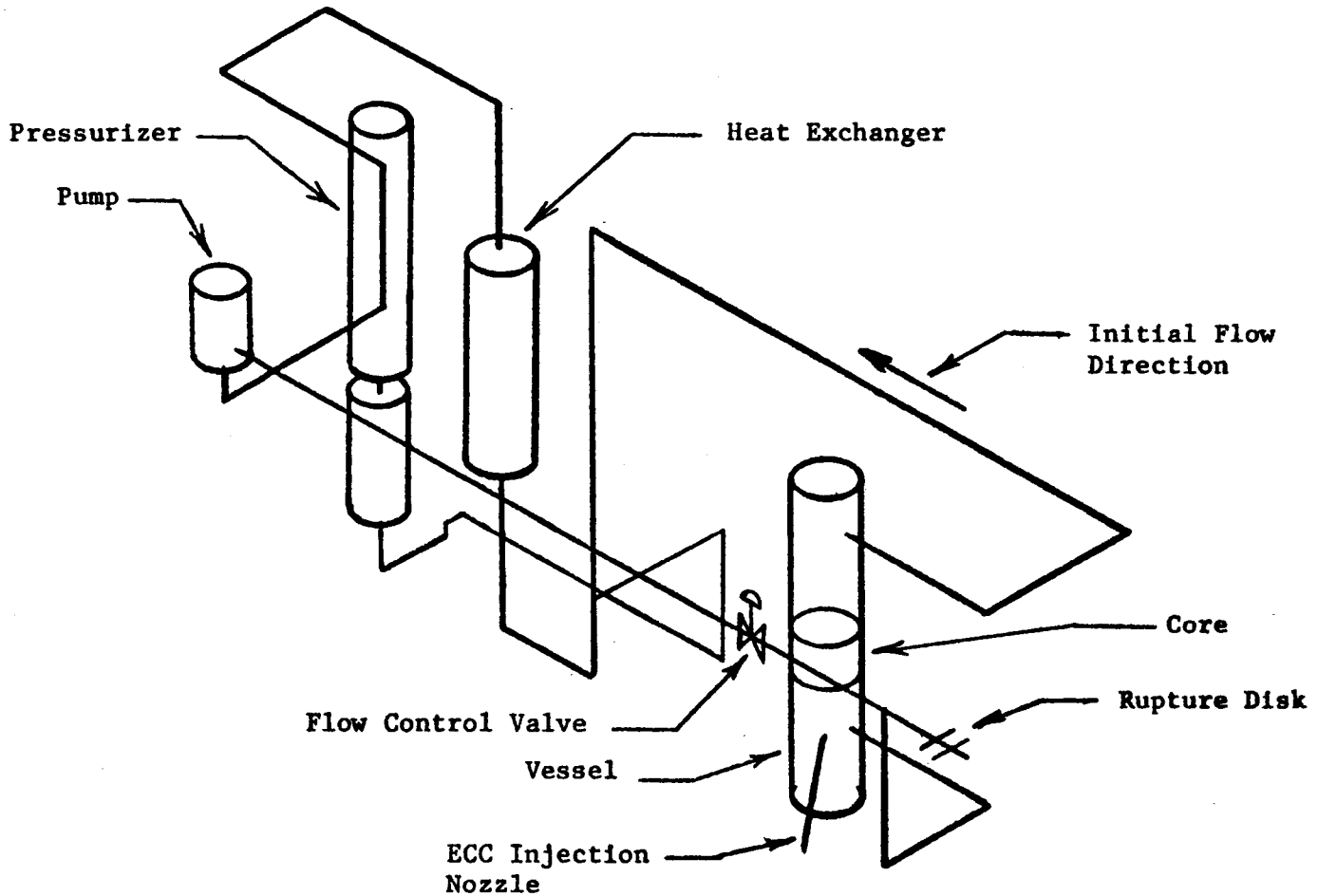


Figure 2. Schematic of semiscale loop--test 845.

TABLE 1

SINGLE-LOOP SEMISCALE SYSTEM DESIGN DATA

Item	Value
Vessel	
Inside Diameter, in.	14.5
Inside Height, in.	64
Core	
Number Heaters	120
Heater Diameter, in.	0.44
Heater Length, in.	9
Heater Pitch, in.	31/32 (triangular)
Piping	
Schedule	5 in. XX strong
Inside Diameter, in.	4.063
Flow Area, sq. ft.	0.09
Heat Exchanger	
Number Tubes	43
Tube Diameter, in.	0.75
Tube Length, in.	37.5

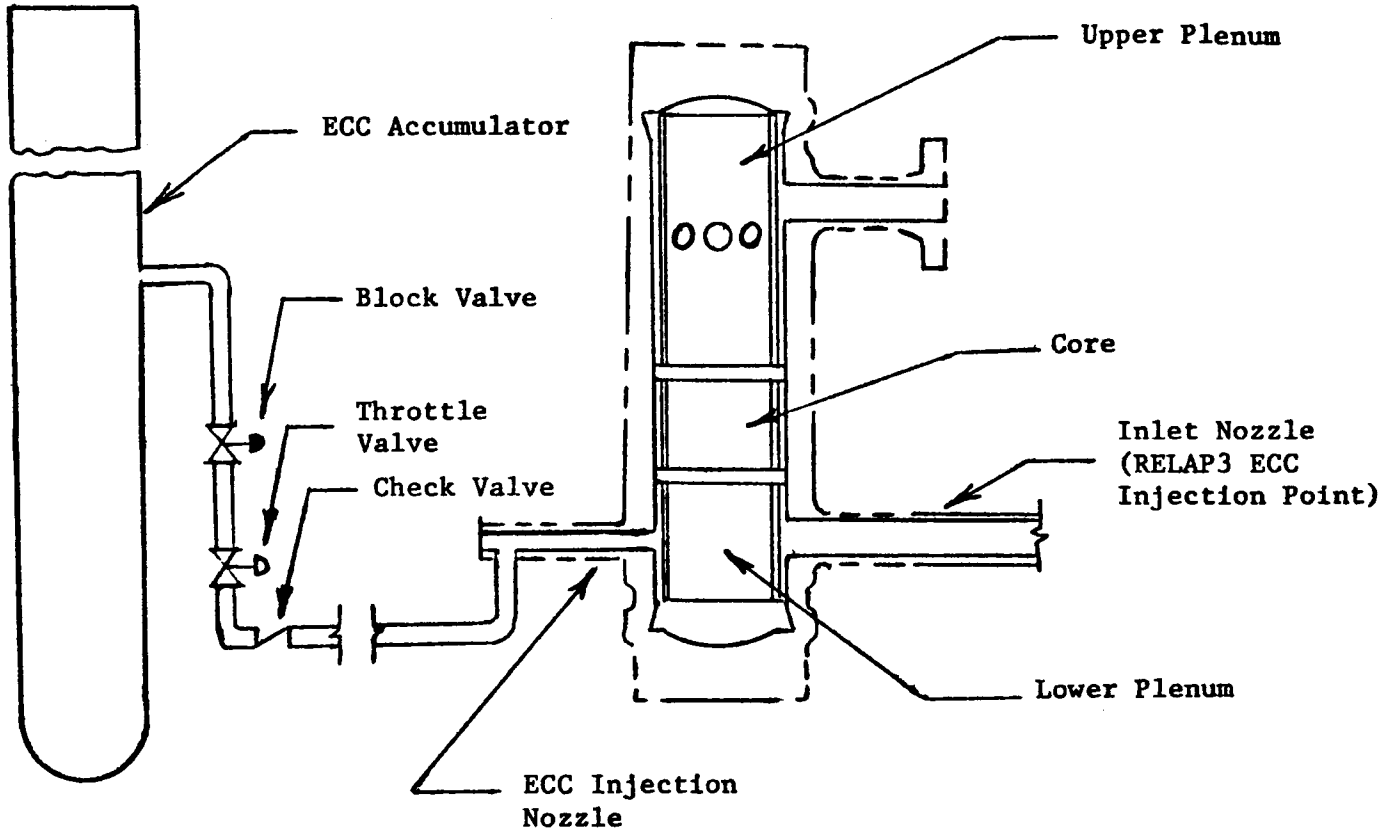


Figure 3. Schematic of emergency core coolant injection system.

TABLE 2

TEST CONDITIONS--TESTS 825 AND 845

Item	Test 825	Test 845
Initial Pressure, psia	2282	2192
Initial Temperature, ^{o}F		
Hot Leg	600	590
Cold Leg	560	558
Initial Flow Rate, lb_m/sec.	21.4	23.3
System Pressure Drop, psi	57.8	10.10
Leak Area, sq. ft.	0.009	0.027
Sequence of Events, sec. after Rupture		
Core Power Off	14	8.3
Heat Exchanger Off	0	22
Pump Power Off	16.5	0.5
ECC Injection Start	None	3.1
ECC Injection Finish	None	11.4
Blowdown Complete	40	22

test 825. For test 825, the rupture was located just downstream of the vessel (a hot leg rupture). The rupture area was 0.009 sq. ft., or 10 percent of the coolant pipe flow area. The small rupture area produced a moderate blowdown rate. Blowdown was complete about 40 seconds after rupture. The initial steady-state system pressure drop for test 825 was 57.8 psi. The flow control valve produced about 54 psi of the total.

Test 845. Reference (3) reports the results of test 845. For this test, the rupture was located just upstream of the vessel (a cold leg rupture). The rupture area was 0.027 sq. ft., or 30 percent of the coolant pipe flow area. This larger rupture area produced a rapid blowdown rate. The blowdown was complete about 22 seconds after rupture. An accumulator injected emergency core coolant into the vessel inlet plenum during the blowdown. The average injection flow rate was 160 gpm, and the period of injection was from 3.1 to 11.4 seconds after rupture. The initial steady-state system pressure drop for test 845 was 10.1 psi. The flow control valve contributed 5.6 psi of the total.

Test data reported. References (2) and (3) include selected test data in the form of curves, and a summary of the test conditions. Data reported includes pressures, fluid temperatures, material temperatures, flow rates, fluid densities, and fluid qualities at selected locations around the loop. The data presented does not give much information about the behavior of the pump or heat exchanger. However, the reports present considerable data taken in and around the reactor vessel. This data allows detailed analysis of the behavior of the core and the emergency core coolant.

B. RELAP3 INPUT

General Considerations

Equipment used. There are many different revisions of RELAP3. The one used here is RELAP3, version 36, dated June 14, 1971. The University of Tennessee's computer is an IBM Model 360/65.

Source of data. One of the objectives of this thesis was to find out how well RELAP3 would predict experimental data. To do this, the RELAP3 input had to be prepared without reference to the test data. The only portions of the test reports (references (2) and (3)) used to prepare the input were:

1. Section I, "INTRODUCTION."
2. Section II, "HARDWARE CONFIGURATIONS AND TEST CONDITIONS."
3. Section III, "SEQUENCE OF EVENTS FOR SEMISCALE TESTS. . . ."
4. Appendix A, "DATA RECORDED."

Several other references provided general background information which was of great help in developing the RELAP3 model of the semiscale loop. References (4) through (9) were especially useful for this purpose. Conversations with experienced analysts working in the field of blowdown analysis were very valuable, particularly the author's conversations with Dr. B. E. Bingham and Mr. R. A. Hedrick of the Babcock & Wilcox Company.

RELAP3 input and output. RELAP3 models a thermal-hydraulic system as a series of control volumes connected by simple pipe flow paths. The

user supplies the geometric data for these control volumes and flow paths as input. The user also inputs the initial conditions and the boundary conditions for the transient. For example, to run a loss-of-coolant accident simulation, the user would input the geometric data for the control volumes and flow paths used to describe the system. The initial conditions are the flow rates, temperatures, and pressures which exist before the start of the transient. The boundary conditions include items such as the leak area, the reactor scram curve, and the pump coastdown curve. Using the input data, RELAP3 solves the conservation of mass, energy and momentum equations for the system in finite time steps. Output includes flow rates, pressures, temperatures, in the flow paths and control volumes as a function of time.

Equations Solved

Conservation equations. RELAP3 solves the conservation equations in the forms shown below (1). Figure 4 shows the control volume for which the equations were derived.

1. Conservation of mass:

$$\frac{dM_i}{dt} = \sum_{j=1}^{J} W_{ij} \quad .^{*} \qquad \text{(II-1)}$$

---

*The subscript i in this and other equations refers to the control volume index, and the subscript j is the flow path index.

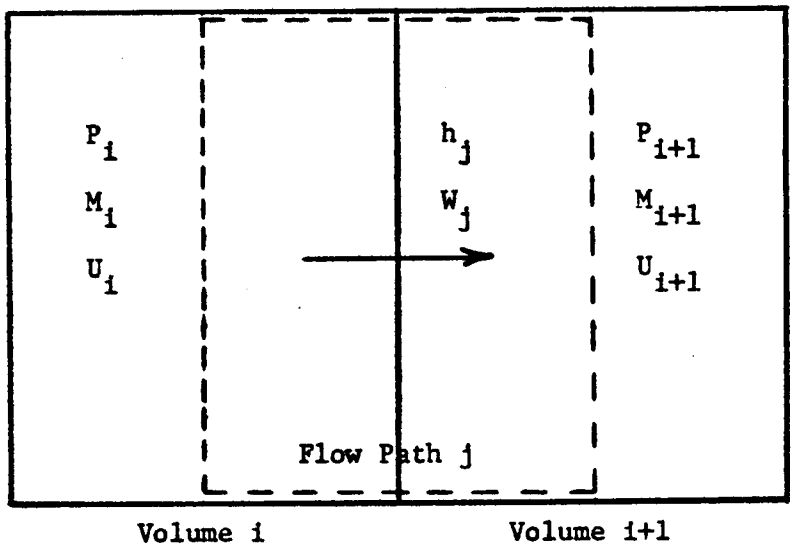


Figure 4. Control volume arrangement used in conservation equations.

2. Conservation of energy:

$$\frac{dU_i}{dt} = \sum_{j=1}^{J} W_{ij} H_{ij} + q_i \ . \qquad \text{(II-2)}$$

The derivation of the energy equation assumes that there is no transfer of energy to or from the fluid except in volumes designated as core or heat exchanger control volumes.

3. Conservation of momentum:

$$\frac{1}{144 g_c} \left(\frac{L}{A}\right) \frac{dW_j}{dt} = P_i - P_{i+1} + \Delta P_{pump}$$

$$+ \frac{g}{g_c} \int_{Z_{cm,i}}^{Z_{cm,i+1}} \frac{\rho dZ}{144}$$

$$- \frac{K_j W_j |W_j|}{\rho_j} \ . \qquad \text{(II-3)}$$

The formulation of the momentum equation assumes one-dimensional, constant-area flow. It also assumes that pressure losses are proportional to the fluid velocity squared, and that the density is constant over each time step.

Pressure search. RELAP3 computes the fluid pressure in each control volume at each time step by a trial-and-error procedure (1). RELAP3 uses an estimated pressure to compute an enthalpy from the following equation.

$$H_i = \frac{U_i}{M_i} + P_i \frac{(Vol)_i}{M_i} \ . \qquad \text{(II-4)}$$

RELAP3 computes a specific volume from the following equation.

$$v_i = \frac{(Vol)_i}{M_i} . \qquad (II-5)$$

The steam tables are stored in RELAP3 in the form of data sets. RELAP3 solves for the control volume pressure by matching the specific volumes obtained from the steam tables using the trial pressure and enthalpy to the specific volume obtained from equation (II-5).

Time steps. Reference (1) recommends that the maximum time step size be calculated from (1):

$$\Delta t)_{max} = \frac{2\pi}{na}\sqrt{\frac{(Vol)L}{A}} . \qquad (II-6)$$

From this equation, the maximum allowable time step size is inversely proportional to a, the acoustic velocity in the fluid. If the fluid is single-phase liquid, the acoustic velocity will be large, and the time step will be small. If the fluid is a two-phase mixture, the time step can be somewhat larger, since the acoustic velocity will be smaller.

The maximum allowable time step also depends on the VL/A ratio of the flow paths. The flow paths having the smallest associated volume and the smallest L/A ratio governs the size of the time step.

Phase separation. RELAP3 includes a phase separation model which is based on the partial density of bubbles in a control volume. RELAP3 assumes that the partial bubble density varies with elevation according to the equation (1):

$$\rho_{gb} = M \frac{Z}{Z_m} + b \qquad \text{(II-7)}$$

where

$$m = 2\, C_0 \frac{M_{gb}}{(Vol)_m} \qquad \text{(II-8)}$$

$$b = (1 - C_0) \frac{M_{gb}}{(Vol)_m} . \qquad \text{(II-9)}$$

The constant C_0 is arbitrary and is input by the user such that $0 \leq C_0 \leq 1.0$. Reference (1) recommends that the user input $C_0 = 0.8$ for large, low-velocity volumes such as plenums. For high-velocity volumes such as pipes, reference (1) recommends that the user input $C_0 = 0.0$.

The user must also input a bubble rise velocity. This is the velocity of the bubbles at the volume's mixture level. Reference (1) recommends a bubble rise velocity of 3 ft/sec for large low-velocity volumes such as plenums. For high-velocity volumes such as pipes, reference (1) recommends a bubble rise velocity of zero.

Fuel pin heat transfer coefficients. The heat transfer modes considered in RELAP3 and the correlations used to calculate the heat transfer coefficients are tabulated in Table 3. Table 3 also includes the range of conditions under which each heat transfer mode is used. The correlations are listed below.

Mode 1. Sieder-Tate correlation.

$$h_{FC} = \frac{0.023\, k_f}{D_e} Re^{0.8} Pr^{0.33} \times \left[\frac{\mu_f(T_{bulk})}{\mu_f(T_{sat})}\right]^{0.14} \qquad \text{(II-10)}$$

TABLE 3

RELAP3 HEAT TRANSFER MODES

Mode No.	Type of Heat Transfer	Correlation	Range of Use
1	Subcooled Forced Convection	Sieder-Tate	$X < 0.0$ $T_{surf} < T_{NB}$ (see text)
2	Subcooled Nucleate Boiling	Thom	$X < 0.0$ $T_{surf} = T_{NB}$ (see text)
3	Nucleate Boiling	Interpolates on X between Mode 2 and Mode 4	$0 < X < 0.1$
4	Forced Convection Boiling	Shrock & Grossman with Wright Constants	$0.1 < X < 0.6$
5	Forced Convection Boiling	Interpolates on X between Mode 4 and Mode 6	$0.6 < X < 1.0$
6	Single Phase Steam	Dittus-Boelter	$X \geq 1.0$
7	Stable Film Boiling	Dougall-Rohsenow	$q'' \geq q''_{DNB}$

where $\mu_f(T_{bulk})$ is the liquid viscosity evaluated at the bulk fluid temperature, and $\mu_f(T_{sat})$ is the liquid viscosity evaluated at the saturation temperature.

Mode 2. Thom correlation.

$$q''_{NB} = \frac{(T_{surf} - T_{sat})^2}{0.072 \exp(-P/1260)} \cdot \qquad \text{(II-11)}$$

Mode 4. Shrock and Grossmann correlation with Wright constants.

$$h = 6700 \left[\frac{q''}{G H_{fg}} + 0.00035 \left\{\left(\frac{X}{1 - X}\right)^{0.9} \left(\frac{\rho_f}{\rho_g}\right)^{0.5} \times \left(\frac{\mu_g}{\mu_f}\right)^{0.1}\right\}^{0.66}\right] . \qquad \text{(II-12)}$$

Mode 6. Dittus-Boelter correlation.

$$h = 0.023 \frac{k_g}{D_e} (Re)^{0.8} (Pr)^{0.4} . \qquad \text{(II-13)}$$

Mode 7. Dougall-Rohsenow correlation.

$$h = 0.023 \frac{k_g}{D_e} \{Re \left[\frac{\rho_g}{\rho_f} (1 - X) + X\right]\}^{0.8} (Pr)^{0.4} . \qquad \text{(II-14)}$$

RELAP3 determines the transition point between subcooled forced convection and subcooled nucleate boiling from the calculated surface temperatures (1). If the surface temperature calculated from the subcooled forced convection equations, T_{FC}, is greater than or equal to T_{NB}, the nucleate boiling surface temperature, then RELAP3 selects

subcooled nucleate boiling as the heat transfer mode. If T_{FC} is less than T_{NB}, then RELAP3 selects subcooled forced convection as the heat transfer mode. The subcooled forced convection surface temperature, T_{FC}, is calculated from:

$$T_{FC} = T_{bulk} + q''/h_{FC} \quad . \tag{II-15}$$

The nucleate boiling surface temperature, T_{NB}, is calculated from the following equation, which is a rearrangement of equation (II-11).

$$T_{NB} = T_{sat} + 0.072 \exp[-P/1260][q'']^{0.5} \quad . \tag{II-16}$$

DNB correlations. Table 4 shows the RELAP3 Departure from Nucleate Boiling (DNB) correlations used in RELAP3. Table 4 also shows the range of variables for which each correlation is used. The correlations are given by the equations shown below.

Range 1. Modified Barnett correlation.

$$q''_{DNB} = (10^6) \frac{B + E(H_f - H_{inlet})}{F + L} \quad , \tag{II-17}$$

where

$$B = 73.71\ D_e^{0.0523} \left(\frac{G}{10^6}\right)^{0.663}$$

$$\times \{1 - 0.315 \exp[-11.34\ D_e (\frac{G}{10^6})]\} \frac{888.6}{H_{fg}} \quad ,$$

$$E = 0.104\ D_h^{1.445} \left(\frac{G}{10^6}\right)^{0.691} \quad .$$

TABLE 4

RELAP3 DNB CORRELATIONS

Range	Correlation	Range of Use
1	Modified Barnett	$P < 725$ psia
2	Interpolates on Pressure between Ranges 1 and 3	725 psia $< P <$ 1000 psia
3	Barnett	1000 psia $< P <$ 1500 psia
4	Interpolates on Pressure between Ranges 3 and 5	1500 psia $< P <$ 1800 psia
5	BAW-2	$P \geq$ 1800 psia $G > 0.5(10^6)$ lb/hr sq ft
6	Average Value between Range 3 and Range 6	$P \geq$ 1800 psia $G \leq 0.5(10^6)$ lb/hr sq ft

$$F = 45.55\ D_h^{0.0817}\left(\frac{G}{10^6}\right)^{0.587} .$$

Range 2. Barnett correlation.

$$q''_{DNB} = (10^6)\ \frac{J + M(H_f - H_{inlet})}{R + L} , \qquad \text{(II-18)}$$

where

$$J = 67.45\ D_h^{0.68}\left(\frac{G}{10^6}\right)^{0.192}$$

$$\times \{1 - 0.744\ \exp[-6.512\ D_e(\frac{G}{10^6})]\} ,$$

$$M = 0.2587\ D_h^{1.261}\left(\frac{G}{10^6}\right)^{0.817} ,$$

$$R = 185\ D_e^{1.415}\left(\frac{G}{10^6}\right)^{0.212} .$$

Range 5. BAW-2 correlation.

$$q''_{DNB} = \frac{S[3.702(10^7)\ W^Z - 0.15208\ G\ H_{fg}\ X]}{12.71\ Y^N} ,$$

where

$$S = [1.15509 - 0.40703\ D_e]$$

$$W = 5.9137(10^{-7})G$$

$$Z = 0.8304 + 6.8479(10^{-4})(P - 2000)$$

$$Y = 3.0545(10^{-6})G$$

$$N = 0.71186 + 0.00020729(P - 2000) .$$

All of the above correlations were derived from steady-state data taken in long channels or rod bundles. In these correlations, the DNB heat flux is a function of mass flux, pressure, quality, and geometry.

FLASH DNB correlation. The FLASH3 (10) blowdown code includes a simple three-parameter fit DNB correlation. Section II-D, page 86, compares the results of some FLASH3 calculations from the literature with the RELAP3 results. The three-parameter fit correlation is shown below.

$$q''_{DNB} = q''_{DNB})_{\text{low quality}} \quad \text{for } X < X1 \tag{II-19a}$$

$$q''_{DNB} = [q''_{DNB})_{\text{low quality}}] \frac{H)_{X=X2} - H}{H)_{X=X2} - H_{X=X1}}$$

$$\text{for } X1 \leq X < X2 \tag{II-19b}$$

$$q''_{DNB} = 0 \text{ for } X \geq X2 \; . \tag{II-19c}$$

The constants X1 and X2 must be chosen by the user. The user must also input $q''_{DNB})_{\text{low quality}}$, the DNB flux for the system at low quality flow conditions. Note that there is no dependence on mass flux in this correlation. Once the three parameters are chosen, the DNB heat flux depends only on the local fluid quality.

Heat exchanger heat transfer rate. RELAP3 can calculate the heat transfer rate in the heat exchanger by one of two methods (1). In the first method, the heat transfer rate is input as an explicit power vs. time table. In the second method, RELAP3 calculates the heat transfer rate using approximate methods. With either method, RELAP3 uses the same

trip set point for both the core and the heat exchanger. After trip, the heat transfer rate comes from an explicit power vs. time table which is input by the user.

The equations RELAP3 uses to calculate the heat exchanger heat transfer rate are:

$$q_{HXT} = - \frac{W}{W_0} h_{HXT}(T_{pri} - T_{sec}) \qquad \text{(II-20)}$$

where

$$h_{HXT} = - \frac{q}{(T_{pri} - T_{sec})} . \qquad \text{(II-21)}$$

These equations are based on the following assumptions:

1. The overall heat transfer coefficient is directly proportional to the reactor coolant flow rate.

2. The overall heat transfer coefficient is not a function of any variable except the reactor coolant flow rate and the initial steady-state heat transfer coefficient.

3. The secondary side fluid temperature is constant.

4. Transient heat conduction in the heat exchanger tube wall is negligible.

Pump model. RELAP3 obtains the head developed by the coolant circulating pump from an input table which the user must supply. This table consists of paired heads and flow rates, so that the head at any flow can be found by interpolation. During a loss of coolant transient, a pump is likely to cavitate. Cavitation may greatly affect the head developed by the pump. RELAP3 accounts for cavitation effects by

multiplying the normal pump head by a cavitation multiplier. The following equation defines the cavitation multiplier.

$$CAV = 1 - CAVCON(DP)^2 \qquad \text{(II-22)}$$

where

$$DP = P + \frac{V^2}{2g} - P_{vap} - \frac{CD(NPSH)}{V(144)} \; . \qquad \text{(II-23)}$$

The user must input CAVCON, the cavitation constant in equation (II-22). In equation (II-23), CD is the coastdown multiplier. The coastdown multiplier is used to compute the pump head after power to the pump motor is cut off. Thus the pump head during cavitation and/or coastdown is given by:

$$Hd = Hd_{normal}(CD)(CAV) \; . \qquad \text{(II-24)}$$

The user must supply the coastdown multiplier as a function of time. RELAP3 obtains the coastdown multiplier at a particular time by interpolating between the input values. After the coastdown is complete, RELAP3 treats the pump as an ordinary flow resistance. RELAP3 computes the flow resistance from a shutdown friction coefficient which the user must supply.

Leak flow rate. RELAP3 calculates the leak flow rate from the Moody critical discharge correlation, provided the fluid at the leak junction is two phase. If the fluid is single phase, the user has the option of assuming metastable flow conditions. In this case, the leak flow rate is calculated from ordinary incompressible flow equations.

With either option, the user must provide a discharge coefficient. This discharge coefficient acts as a multiplier on the leak flow area. Reference (9) recommends a discharge coefficient of 0.6 for "large" breaks. The user must also pick a leak opening time. This is in the form of a leak area-versus-time table. RELAP3 interpolates between the values in the table to obtain the leak area at any particular time.

Preparation of Input

Source of design data. References (2), (3), (11), (12), (13), and (14) include the system design data needed to prepare input to RELAP3. References (2), (3), (11), (12), and (13) provided the control volume and flow path data. Reference (13) provided coolant pump performance data. Reference (14) provided detailed flow rate and pressure drop data.

Control volume arrangement. Figure 5 shows the RELAP3 model of the semiscale loop for test 825, and Figure 6 shows the RELAP3 model for test 845. Table 5 gives the control volume dimensions. The RELAP3 model for test 825 has 14 control volumes and 15 flow paths, while the RELAP3 model for test 845 has 15 control volumes and 17 flow paths.

Core control volumes. The RELAP3 model has only one control volume to represent the core and only one control volume to represent the heat exchanger tube bundle. More core control volumes should improve the model's accuracy, because most of the time, the temperature rise across the core is significant. This means that the heat transfer rate at the

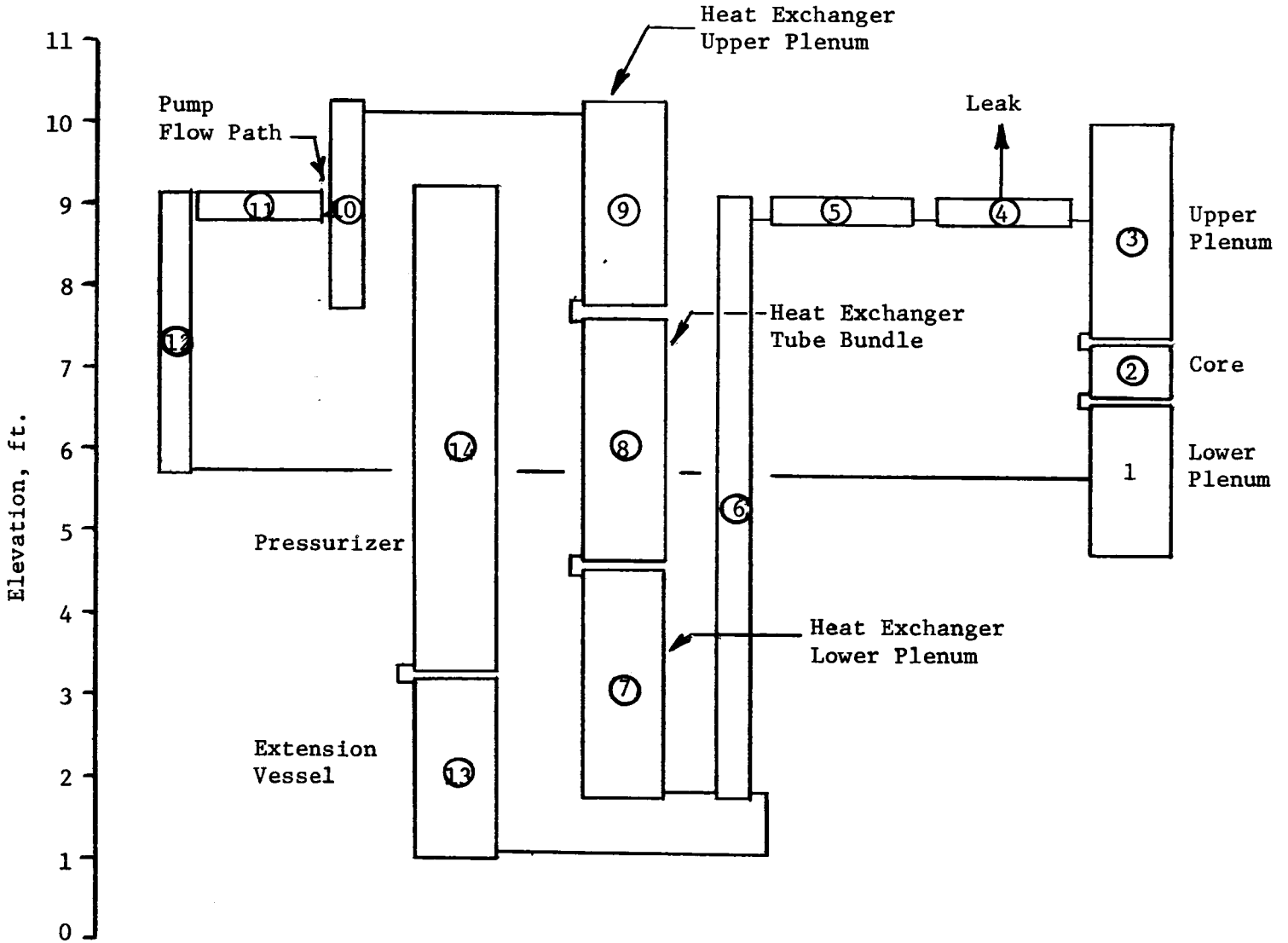


Figure 5. RELAP3 model of semiscale loop--test 825.

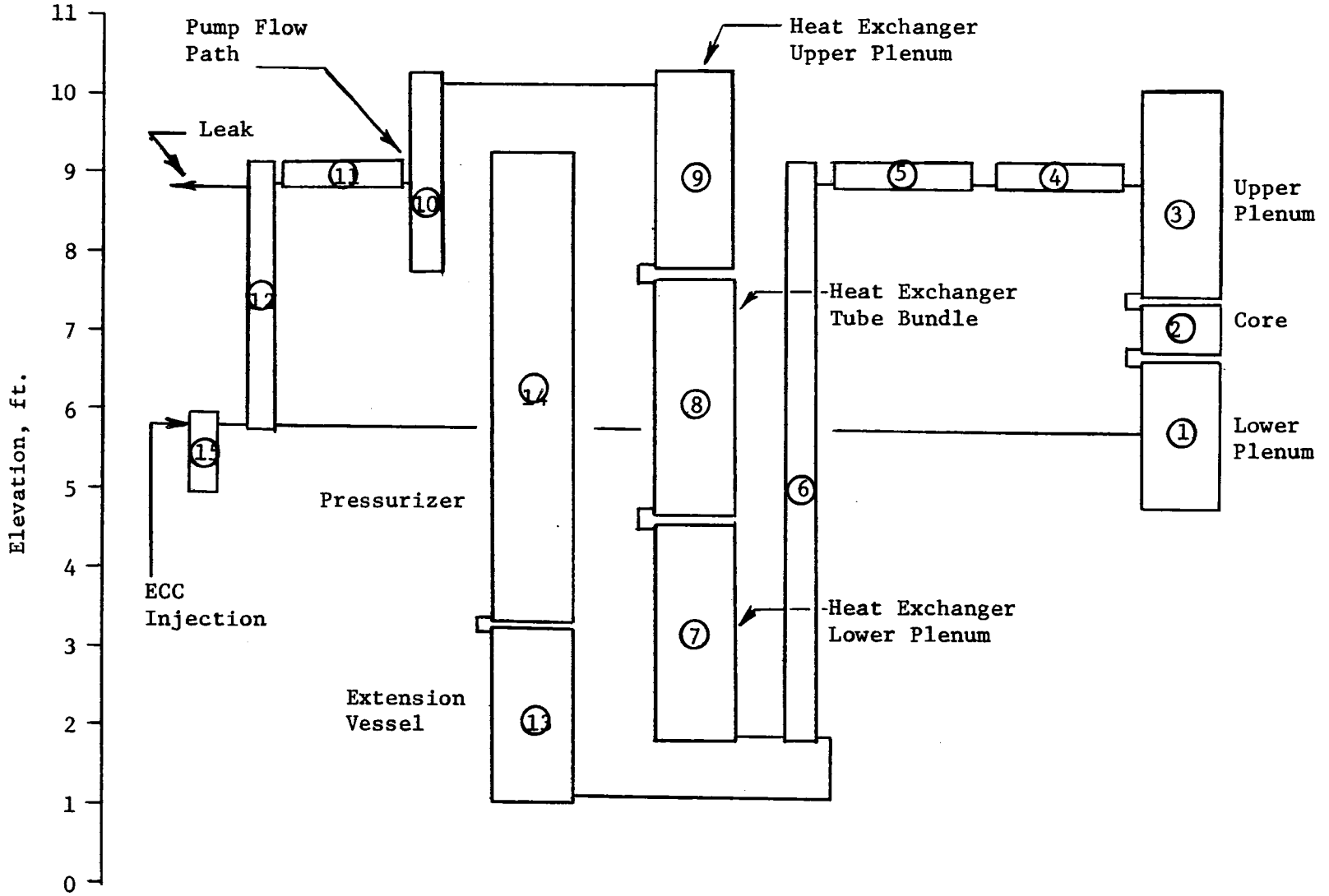


Figure 6. RELAP3 model of semiscale loop--test 845.

TABLE 5

SUMMARY OF CONTROL VOLUME INPUT DATA

Volume No.	Volume Test 825 cu. ft.	Volume Test 845 cu. ft.	Bottom Elevation, ft.	Height ft.
1	1.71	1.71	4.70	1.85
2	0.54	0.54	6.53	0.79
3	2.49	2.49	7.30	2.70
4	0.754	0.754	8.75	0.30
5	0.852	0.852	8.75	0.30
6	0.828	0.828	1.75	7.30
7	0.579	0.579	1.75	2.76
8	0.200	0.200	4.49	3.14
9	0.563	0.563	7.61	2.64
10	1.307	1.307	7.75	2.50
11	0.822	0.822	8.75	0.30
12	1.015	1.185	5.65	3.40
13	0.80	0.80	1.00	2.19
14	0.96	0.96	3.17	6.01
15*	--	0.713	4.95	1.0
Total	13.42	14.13		

*Volume 15 is the emergency coolant injection piping, which was not present on test 825.

core inlet or exit may be quite different from the rate calculated from average core conditions. However, if one did use more than one axial control volume in the core, the required time step for the calculation would be cut by at least one-half. This is because the core flow path has the least inertia of all the flow paths and thus this flow path governs the time step size. Such small time steps would lead to long and maybe impractical computer running times. For this reason, only one axial core control volume was used.

In the radial direction, the core flow should be well mixed. The support grids at the core inlet and exit cause almost all of the core flow resistance. The heaters are widely spaced, so that the lateral flow resistance is small. These factors will tend to eliminate any imbalance in flow among the various subchannels.

Heat exchanger control volumes. Only one control volume is necessary to represent the heat exchanger tube bundle because of the large temperature difference (about 380°F) between the tube side fluid and the shell side fluid. The tube side fluid temperature is about 570 to 580°F initially, while the shell side fluid temperature is about 200°F (saturation temperature at atmospheric pressure). The large temperature difference should lead to vigorous boiling on the shell side. The feedwater inlets on the secondary side appear to be designed to disperse the feedwater. These two effects should cause a uniform distribution of the secondary fluid. If the secondary fluid is uniformly distributed throughout the tube bundle, the heat flux will be uniform

throughout the tube bundle. In this event, one control volume is adequate.

The above approximation may lose validity near the end of the transient, when the primary temperature is low. However, even then, more control volumes would probably not improve the calculation.

Pipe control volumes. The control volumes that represent sections of pipe usually have their center of gravity fairly close to an instrument station on the test apparatus. This makes the RELAP3 results directly comparable to the test data. The sizes of the pipe volumes are about equal, at least on an order of magnitude basis.

Computer time. Reference (1) points out that the required computer time for a RELAP3 run varies roughly with the square of the number of volumes. Fifteen is about the maximum practical number of control volumes for The University of Tennessee's computer. The computer running time averaged 0.25 to 0.30 sec. of central processing unit (CPU) time per RELAP3 time step. At this rate, the CPU time needed for one run is six to eight hours. Such long runs require special scheduling.

Control volume pressure. RELAP3 requires as input the initial pressure at the center of gravity of each control volume. At the user's option, RELAP3 uses the control volume pressures and the initial steady state flows and densities to calculate friction coefficients for the flow paths. This makes the control volume pressures an important part of the input. The procedure used to calculate the control volume pressures is as follows:

1. Calculate the system pressure drops in detail, by hand, using the flow and temperature conditions from (4). Reconcile the calculated values to the experimental values by adjusting the most uncertain parts of the calculation.

2. Obtain friction coefficients for the flow paths using the reconciled pressure drops from step one. The friction coefficient is defined (1) as

$$K_j = \frac{\rho_j \, \Delta P_j}{W_j^2} \qquad \text{(II-25)}$$

3. Compute the control volume pressures according to the relation (1):

$$P_{1,j} = P_{2,j} + \frac{K_j W_j^2}{\rho_j}$$

$$+ \frac{\rho_2}{144} j \frac{g}{g_c} (Z_{cg} - Z_{jun})_{2,j}$$

$$- \frac{\rho_{1,j}}{144} j \frac{g}{g_c} (Z_{cg} - Z_{jun})_{1,j} \, . \qquad \text{(II-26)}$$

where the subscript 1 refers to the upstream control volume, and the subscript 2 refers to the downstream control volume.

Bubble parameters. RELAP3 requires as input a bubble gradient parameter and a bubble rise velocity. The bubble parameters used here are those recommended in (1). In low fluid velocity areas, i.e., the vessel and heat exchanger plenums, and the pressurizer, the bubble gradient parameter is 0.8 and the bubble rise velocity is 3 ft/sec. In

all other control volumes, the fluid velocities are much higher and both parameters are zero.

Flow path data. Table 6 is a summary of the flow path input. In several of the flow paths, the flow area varies with length. For these flow paths the flow path area and inertia are defined as (14):

$$A = \left(\sum_K L_K A_K\right) / \sum L_K \qquad \text{(II-27)}$$

$$L/A = \sum_K \left(L_K / A_K\right) \qquad \text{(II-28)}$$

where the subscript K refers to the constant-area segments which make up the flow path. In the flow paths where the initial flow rate was nonzero, RELAP3 calculated the friction coefficients from the steady-state pressure drops, flow rates, and densities. In the flow paths where the initial flow rate was zero, such as the pressurizer surge line, the following relation defines the friction coefficient:

$$K_j = \left(\frac{fL}{D_h} + N_{VH}\right) / \left(288\ g_c\ A^2\right) . \qquad \text{(II-29)}$$

Pump input data. The input data for the coolant circulating pump comes from (12). Figure 7 shows a dimensionless homologus characteristic curve for the semiscale pump (13). This curve can be used to derive a shutdown coefficient, as follows:

1. Extrapolation of the dimensionless-homologus pump curve yields a friction coefficient for the case where the pump speed is zero. That is, when

TABLE 6

SUMMARY OF FLOW PATH INPUT DATA

Upstream Control Volume	Downstream Control Volume	Flow Area $ft.^2$	Friction Coefficient, K	Inertia L/A
Data Common to Both Tests				
1	2	0.626	0.0698	2.74
2	3	0.626	0.0698	3.14
3	4	0.09	0.0287	30.2
4	5	0.09	0.0136	71.5
5	6	0.09	0.01005	104
6	7	0.09	0.0315	76.8
7	8	0.0663	0.0243	23.5
8	9	0.0663	0.0367	23.5
9	10	0.09	0.0307	106
10	11	0.0813	0.0127	161
11	12	0.09	not calculated	102
12	1	0.09	0.030	51.8
13	6	0.00499	64.4	3030
14	13	0.00301	20	118
Test 825 Data				
4	0 (Leak Path)	0.009	1.995	70.6
Test 845 Data				
12	9 (Leak Path)	0.027	0.222	60.4
15	12	0.025	0.219	590
0	15 (Fill Path)	0.025	--	--

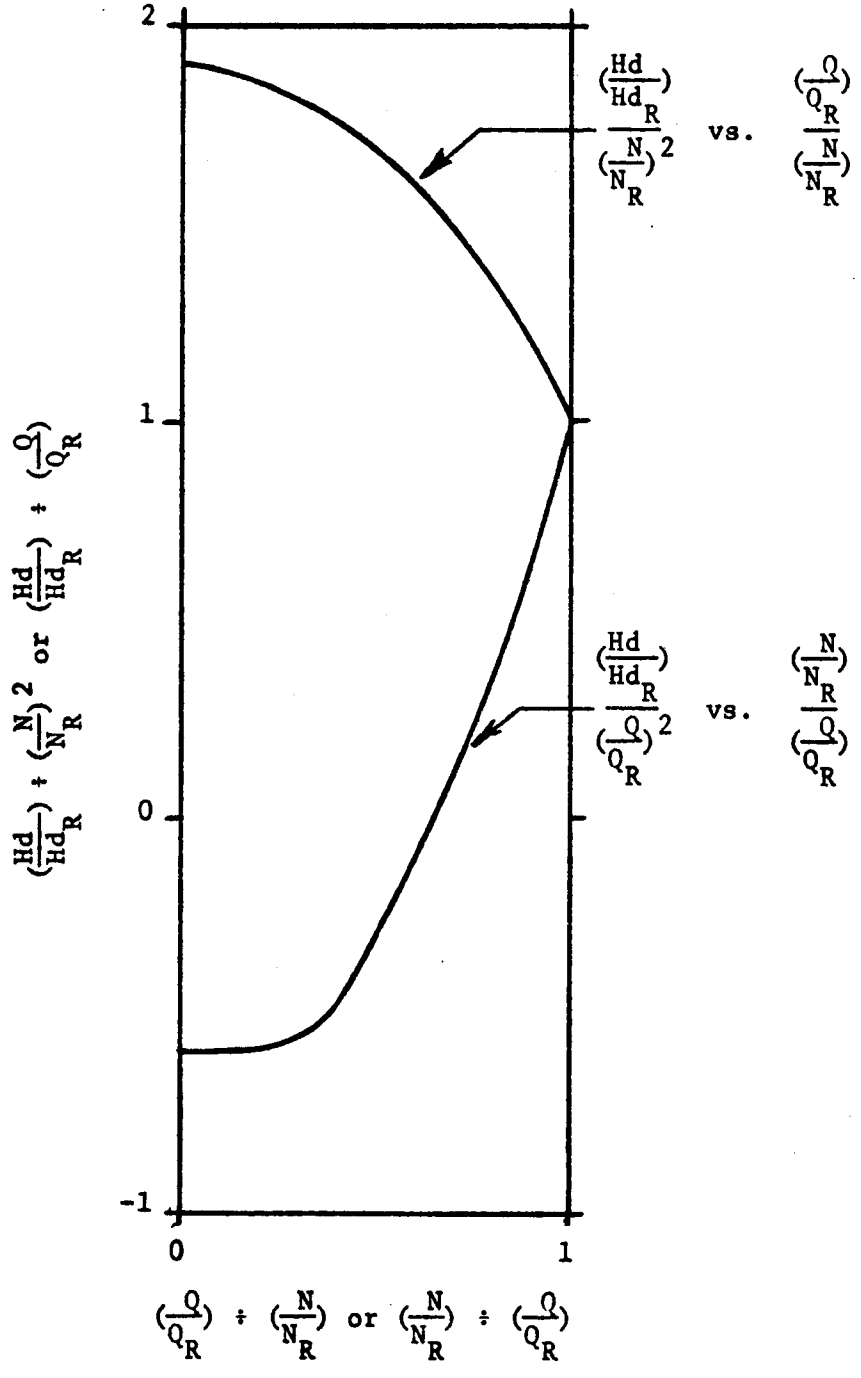


Figure 7. Semiscale pump characteristic.

$$\frac{(N/N_R)}{(Q/Q_R)} = 0, \quad \frac{(Hd/Hd_R)}{(Q/Q_R)^2} = -0.6 \ . \qquad \text{(II-30)}$$

If $\frac{(N/N_R)}{(Q/Q_R)}$ is small, then either (N/N_R) is small, or, (Q/Q_R) is large. The case of interest is the one where (N/N_R) approaches zero. Under this condition,

$$(Hd/Hd_R) = -0.6(Q/Q_R)^2 \ . \qquad \text{(II-31)}$$

If we assume that the same relation applies when either Q is positive and H is negative, or when Q is negative and H is positive we get:

$$\begin{aligned} (Hd/Hd_R) &= -0.6(Q/Q_R)^2 \text{ for } Q > 0 \\ &\qquad\qquad\quad N = 0 \\ (Hd/Hd_R) &= -0.6(Q/Q_R)^2 \text{ for } Q < 0 \\ &\qquad\qquad\quad N = 0 \ . \end{aligned} \qquad \text{(II-32)}$$

2. Substituting the values of Hd_R and Q_R into the above equations gives:

$$\begin{aligned} Hd &= -5.3(10^{-4})Q^2 \text{ for } Q > 0 \\ &\qquad\qquad\quad N = 0 \\ Hd &= +5.3(10^{-4})Q^2 \text{ for } Q < 0 \\ &\qquad\qquad\quad N = 0 \ . \end{aligned} \qquad \text{(II-33)}$$

3. Converting Q from gpm units to cu. ft./sec. units gives:

$$\begin{aligned} Hd &= -107\ A^2V^2 \text{ for } Q > 0 \\ &\qquad\qquad\quad N = 0 \\ Hd &= +107\ A^2V^2 \text{ for } Q < 0 \\ &\qquad\qquad\quad N = 0 \ . \end{aligned} \qquad \text{(II-34)}$$

By analogy, for N = 0

$$Hd = \pm N_{VH} \frac{V^2}{2g} . \qquad \text{(II-35)}$$

By equating like terms we get:

$$N_{VH} = 2g(107)A^2 . \qquad \text{(II-36)}$$

Evaluating this expression gives $N_{VH} = 45.9$. From equation (II-5), page 14, K, the friction coefficient, equals 0.742.

The pump shutdown coefficient can be used to extrapolate the head-capacity data to positive-flow negative head conditions and to negative-flow, positive-head conditions. This is done by assuming that the following relations hold

$$Hd = Hd_{shutoff} + 5.3(10^{-4})Q^2 \text{ for}$$

$$Q < 0$$
$$H > 0 \qquad \text{(II-37)}$$
$$N \neq 0$$

$$Hd = -5.3(10^{-4})(Q - Q_0)^2 \text{ for}$$

$$Q > 0$$
$$H < 0 \qquad \text{(II-38)}$$
$$N \neq 0 .$$

The extrapolated head-capacity curve insures that the pump performance is defined for all possible operating conditions. This prevents premature stoppage of a computer run.

The input value for the pump cavitation constant is 0.0005 $(psi)^{-2}$. See equation (II-23), page 23. Reference (17) presents the results of an

analysis which shows that this value gives a good simulation of pump performance during cavitation.

Fill system data. The fill (or emergency core coolant) water is injected directly into volume 15. This volume represents the fill system pipe from the vessel up to the ECC flow control valve. Volume 15 connects directly to volume 12, which is part of the cold leg pipe. This model differs slightly from the test arrangement. On test 845, the fill system piping connects with the annulus between the core flow skirt and the vessel wall. Figure 3, page 7, shows the test injection point compared to the injection point assumed for the RELAP3 calculations. In the RELAP3 model, fill water enters the system several feet downstream of the actual injection point. This approach insures that the flow resistances for the fill water flow are conservative. It is difficult to develop accurate flow resistances for the annulus between the flow skirt and the vessel, since the flow topography is unknown. One possible way to develop an accurate model would be to add an additional control volume to represent the annulus, and then estimate the flow resistance on either side of this volume. However, this new control volume would be much smaller than any of the others, which would greatly reduce the required time step size. These considerations led to the model described previously.

The fill flow rate was input as an explicit flow vs. time table. The model does not consider the discharge of the nitrogen cover from the accumulator into the system. On test 845, the nitrogen cover gas from

the accumulator was allowed to flow into the system after the fill water was exhausted. The RELAP3 model does not consider the effects of the nitrogen in the system.

Leak input data. The leak area versus time input to RELAP3 assumes the leak opening time of 0.0015 seconds, the value given in the test reports (2) and (3). The leak area is a linear function of time during this period.

The input leak discharge coefficient is 0.6. The input data assumes no liquid phase choking in the leak flow path. The friction coefficient for liquid phase flow in the leak assumes a 1.5 velocity head pressure loss across the orifice in the leak nozzle.

Channel and rod geometry data. Seven radial nodes were used for the heater pin conduction model. Thermal conductivity and specific heat data for the boron nitride insulation are averaged values obtained from (18), (19), and (20).

Heat exchanger power. This part of the input presented no particular problem for test 825, since the heat exchanger was shut off at the instant of rupture. Both the core and heat exchanger power were input as explicit power vs. time tables. However on test 845, the use of the same trip set point for the core and the heat exchanger is troublesome. Before running the calculation, there is no way to know if that is a good assumption or not. For this test, the heat exchanger remained on throughout the transient, while the core power was shut off at 8.3 seconds after

rupture. Two runs were required to get around the problem. In the first run, the heat transfer rate was input as a constant 1.1 MW. The results of this run showed that the use of the same trip set point for the core and heat exchanger is acceptable for this particular problem. By 8.3 seconds the system fluid temperatures are low enough so that there can be only a small temperature difference in the heat exchanger. Thus, beyond this point the heat transferred by the heat exchanger should be small.

Time step size. The calculated maximum time step size at the start of the blowdown is 0.0003 sec. The time steps used for the RELAP3 runs are shown in Table 7. As a check, selected portions of the transient were re-run using smaller time steps. The calculations using the reduced time steps gave essentially the same results as the original time step. A better method of verifying the time steps used in the calculation would be to re-run the entire transient using smaller time steps. This method was impractical, because of the large amount of computer time that would be needed.

TABLE 7

TIME STEPS--TESTS 825 AND 845

Time Interval (sec.)	Time Step (sec.)
Test 825	
0 - 5	0.0001
5 - 8	0.0002
8 - end	0.0005
Test 845	
0 - 2	0.0001
2 - 4	0.0002
4 - 22	0.0005

III. RESULTS

A. INTRODUCTION

This section presents the results of three RELAP3 runs, in comparison with experimental data. There were two RELAP3 runs simulating test 845. One run had a constant, 1.07 MW heat exchanger power. The other had a flow-and-temperature dependent heat exchanger power. Most of the results presented here are for the flow-and-temperature dependent case, with a few comparisons between the two. The constant power run aborted at 8.3 seconds because of low pressure in the heat exchanger tube bundle.

There was one RELAP3 run to simulate test 825. This run aborted at about 14 seconds. The calculated fluid film temperature on the heater pins exceeded 1500°F, which is the limit of the viscosity and thermal conductivity tables for steam.

B. RESULTS--TEST 845

System Parameters

System pressures. Figure 8 compares the RELAP3 predicted inlet plenum pressure with data from test 845. These results are typical of the results for other parts of the system, except for the pressurizer. Its behavior will be discussed later. The predicted pressures are higher

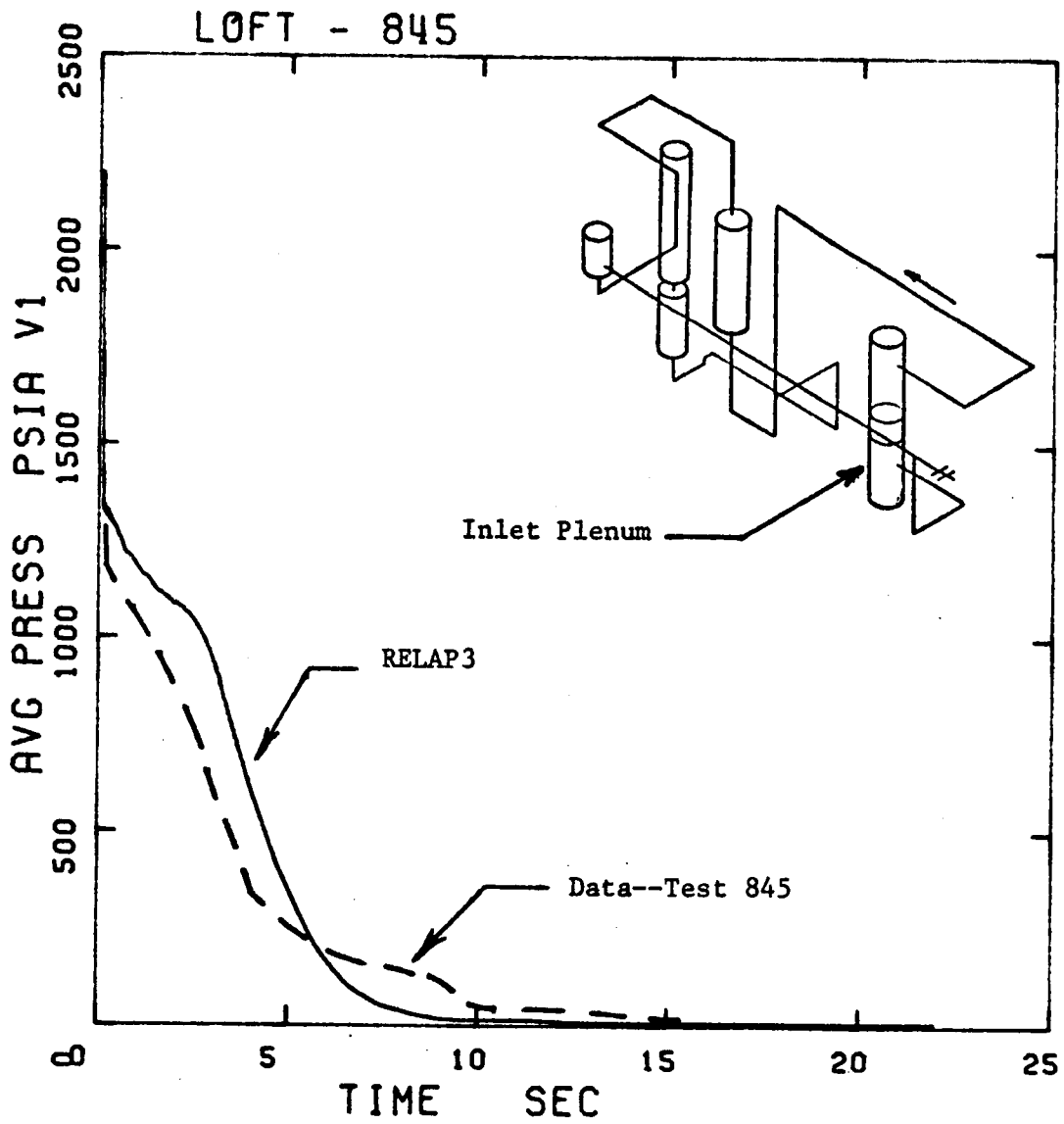


Figure 8. Inlet plenum pressure--test 845.

than the measured values for the first six seconds. After six seconds the calculated pressures are lower than the measured ones. The maximum difference between the two is 200 to 300 psi.

The estimated accuracy of the pressure data is ± 150 psi (2), (3). The error introduced in transferring the experimental data from the plots in (2) and (3) averages ± 100 psi. Combining the two errors gives a maximum error of ± 250 psi.

Pressurizer pressure. Figure 9 compares the calculated pressurizer pressure with the test data. The change in slope of the test data curve between two and nine seconds is due to the mixing of the saturated vapor from the pressurizer with the subcooled liquid in the extension vessel (3). The pressurizer pressure actually dips below system pressure for a moment at about 3.5 sec. (3). Compare the experimental pressure in the inlet plenum from Figure 8 with the pressure in the pressurizer at 3.5 seconds. The two pressures are very close to each other. The RELAP3 pressure does not follow the pressurizer pressure behavior because the initial input fluid temperatures for the pressurizer and extension vessel were the same (saturation temperature). Actually, the fluid in the extension vessel was subcooled (440°F), while the fluid in the pressurizer vessel was at a higher temperature.

Fluid temperatures. Figure 10 compares the predicted outlet plenum fluid temperature with the test data. These results are typical of most locations in the system. The temperatures agree very well out to about four seconds. After four seconds, the test fluid temperatures are above

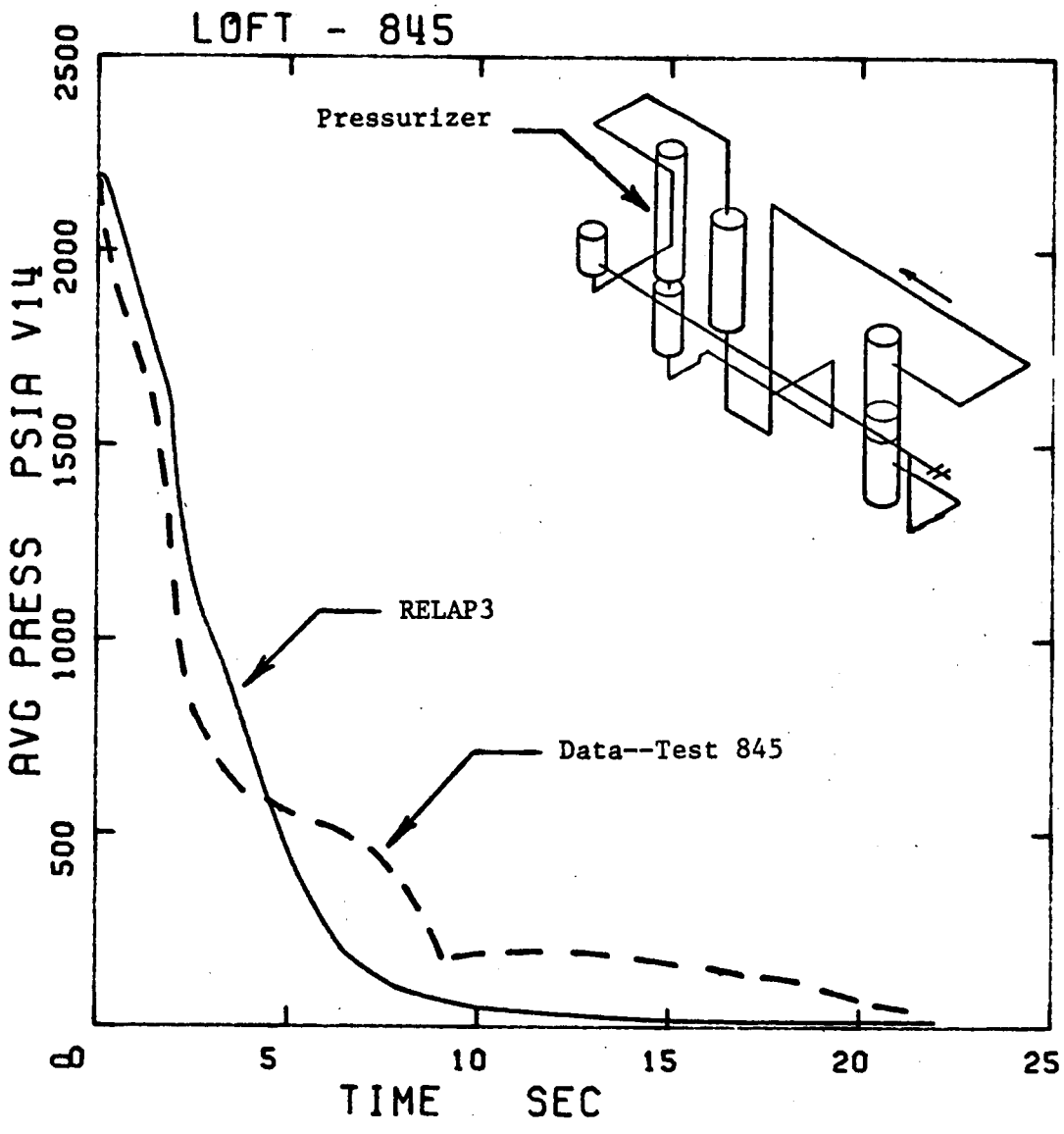


Figure 9. Pressurizer pressure--test 845.

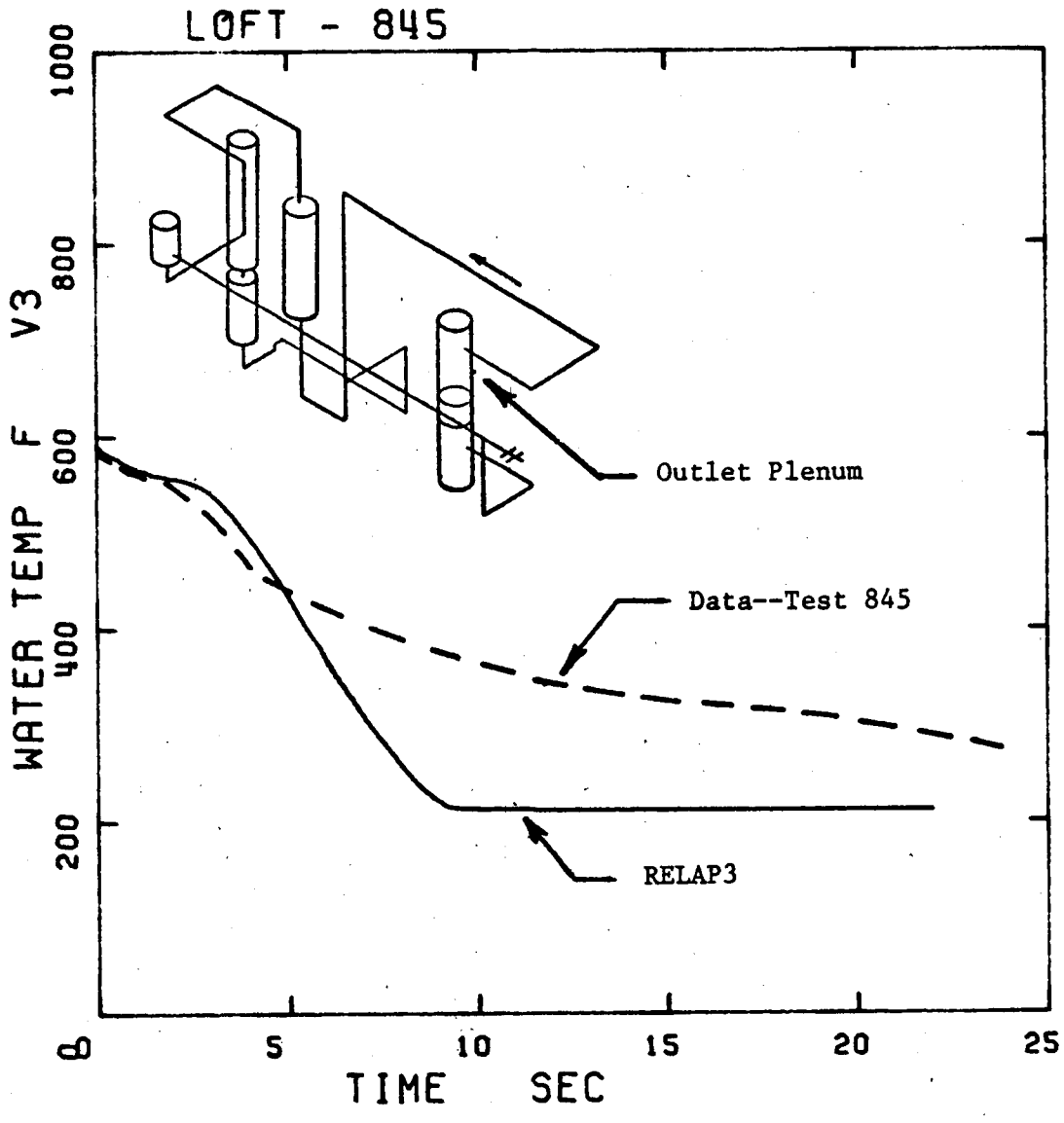


Figure 10. Outlet plenum fluid temperature--test 845.

saturation. The calculated fluid temperatures equal saturation. Figure 11 compares the inlet plenum temperatures. Note the decrease in the calculated temperature at 11.5 sec. This corresponds to the entrance of emergency core cooling water into the plenum. The test data shows no such decrease. This is because little emergency core coolant reached the lower plenum in the experiments. Instead, the emergency core coolant was entrained and carried out the leak. Figure 12 compares the fluid temperatures in the core. The momentary increases in calculated fluid temperatures occur during periods of low calculated flow. The core power was turned off at 8.3 seconds, well before the time that the temperature rises occur. However, the calculated heater temperatures are quite high by this time, which provides the necessary energy to superheat the fluid.

The dips in calculated core fluid temperature at 11.5 seconds and again at 13.3 seconds occur at the same time that emergency core coolant enters the lower plenum. The sudden backflow into the lower plenum causes the flow to reverse in the junction between the lower plenum and the core. The flow in the junction between the core and the upper plenum does not reverse. Thus, for a fraction of a second fluid enters the core from both top and bottom. The fluid entering the bottom is saturated steam. The fluid entering the top is a two-phase mixture. The combined flows mix with the superheated steam in the core, reducing the fluid temperature to saturation.

Flow rates. Figure 13 compares the calculated mass flow rate in the inlet plenum with the test data. The increase in test flow at 3.5

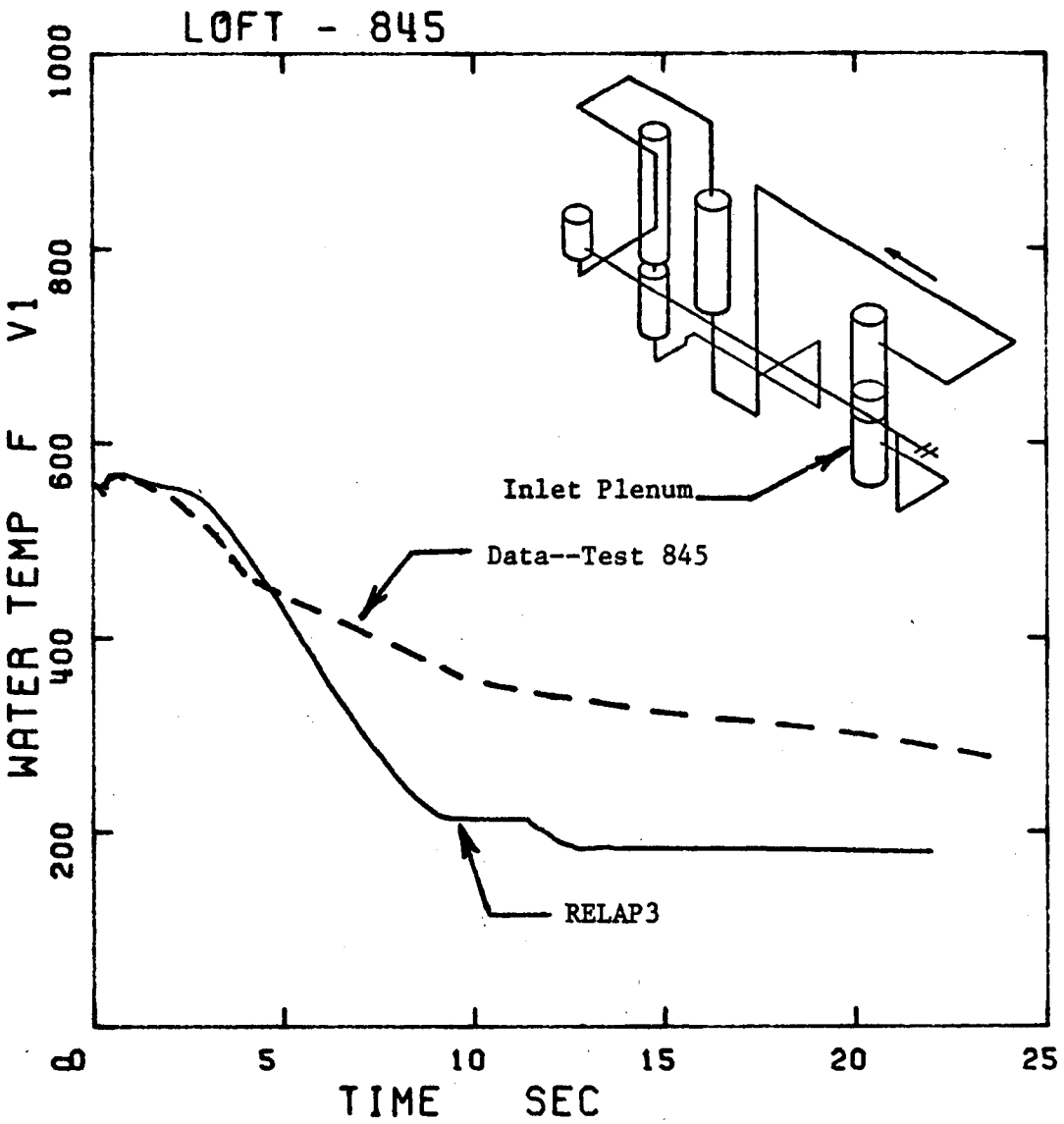


Figure 11. Inlet plenum fluid temperature--test 845.

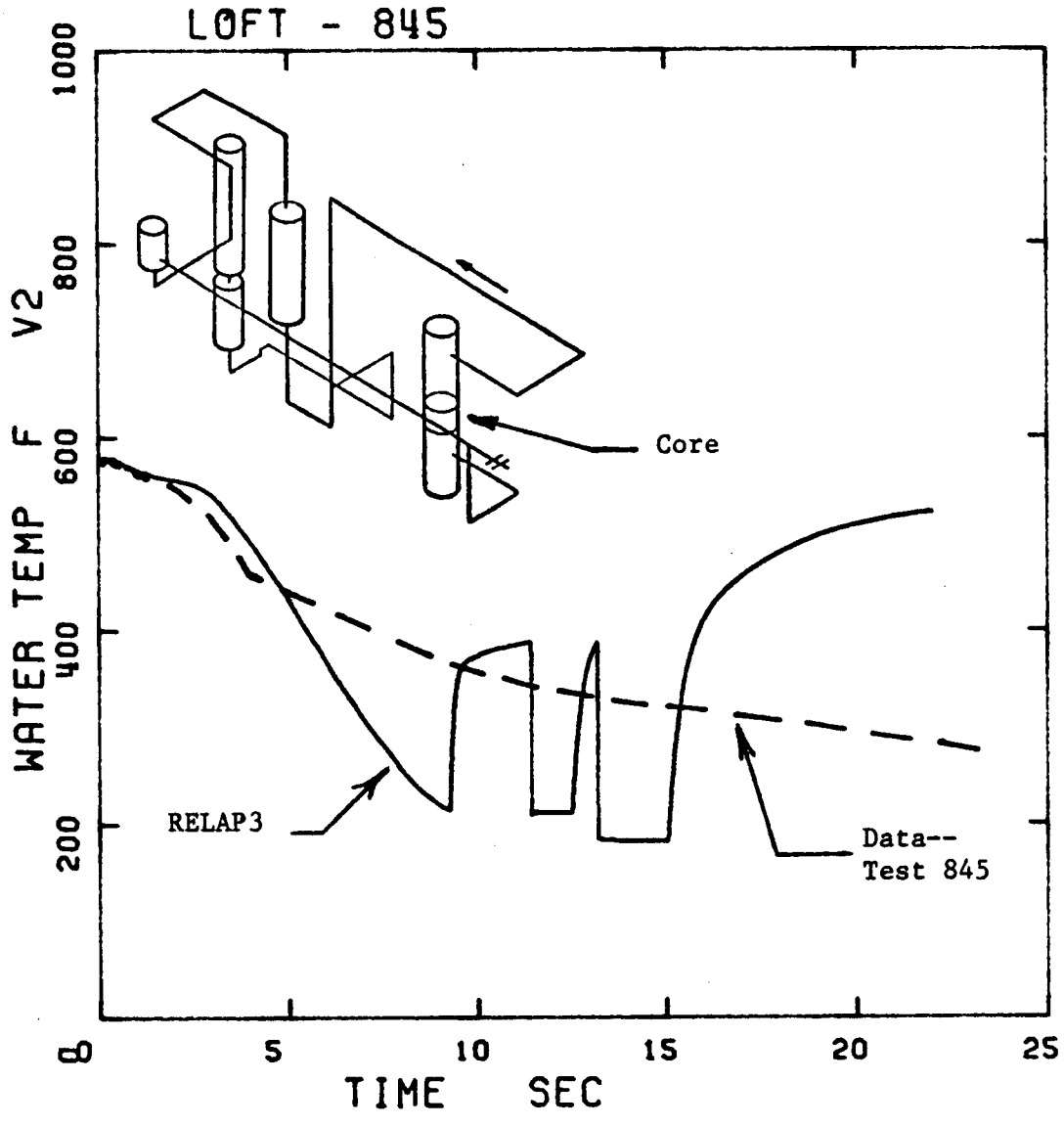


Figure 12. Core fluid temperature--test 845.

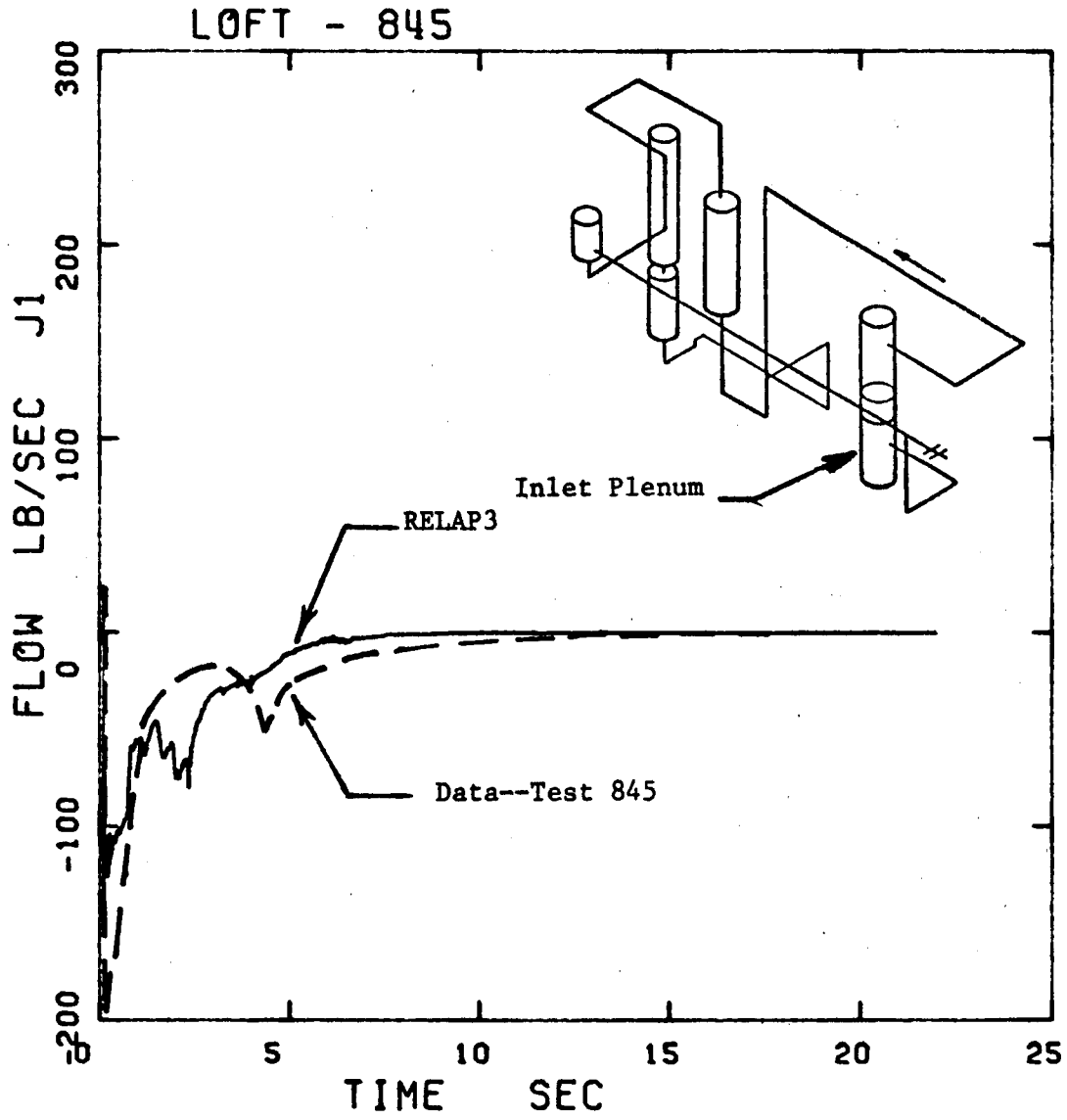


Figure 13. Inlet plenum flow rate--test 845.

sec. results from a decrease in flow out of the pressurizer (3). As we saw previously, the RELAP3 input did not consider this effect. Note that the calculated flow rate reverses direction almost immediately after rupture. Figure 14 shows the inlet plenum flow rate in the first fraction of a second of the transient. The leak begins to open at 0.1000 sec. The leak is fully open by 0.1015 sec. By 0.1033 sec., the calculated flow rate is fully reversed. Figure 15 compares the calculated flow rate in the inlet nozzle with the test data. On test 845, the ECC water was injected into the annulus between the core flow skirt and the vessel wall. Thus, the measured inlet nozzle flow rate includes the ECC water leaving the vessel. The RELAP3 model assumes that the ECC water enters the cold leg pipe. Consequently, the calculated flow rate does not include the flow of ejected ECC water. This accounts for the lower (less negative) calculated flow rate between 3.2 and 11.5 seconds. Note that the calculated flow rate shows periods of positive flow between 11.5 and 14 seconds and again at 19 seconds. This positive flow is fill water entering the inlet plenum. Volume 12 is completely full of subcooled water from the fill system and from condensation. Thus, the flow reverses back into the inlet plenum. Figure 16 shows the RELAP3 flow through the leak. The leak flow stops at 9.5 seconds. This effect is a result of the assumption of thermal equilibrium in a RELAP3 control volume. The cold fill water causes rapid steam condensation. By 9.5 seconds, this condensation has reduced the pressure in volume 12 to below the atmospheric pressure, stopping the leak flow. The leak flow resumes momentarily near 12 seconds, when volume 12 has been completely filled with water.

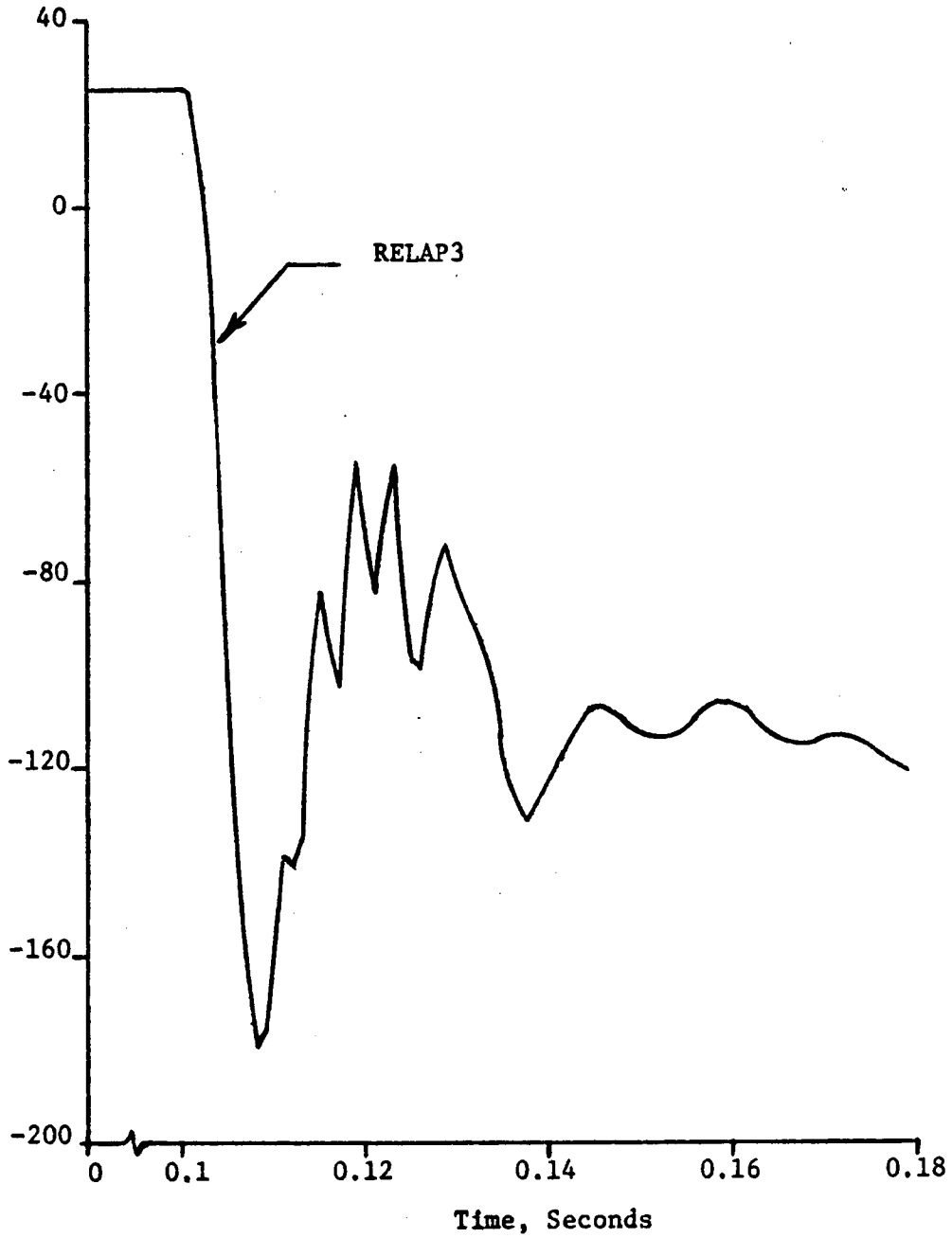


Figure 14. Inlet plenum flow rate--test 845, initial part of transient.

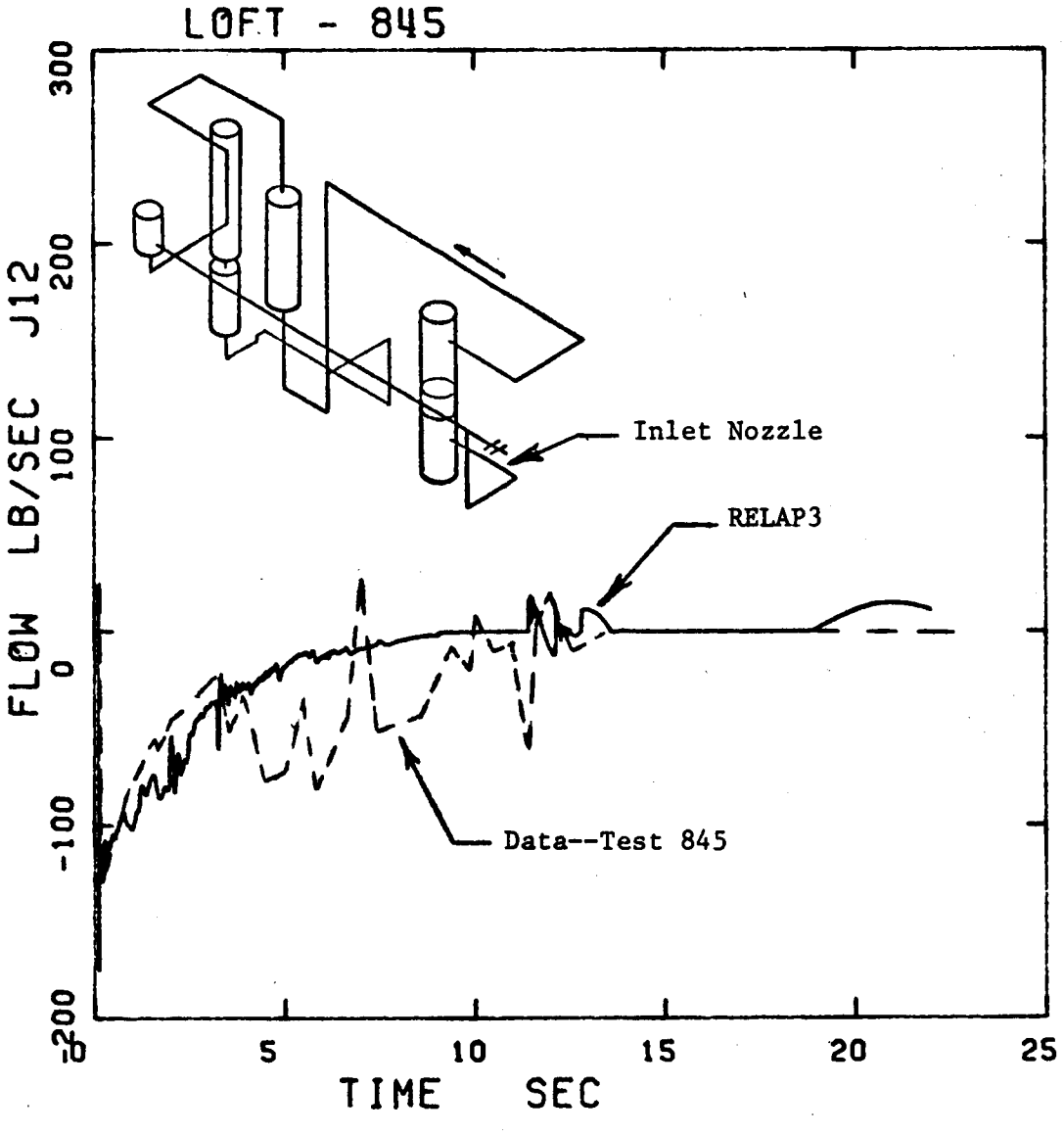


Figure 15. Inlet nozzle flow rate--test 845.

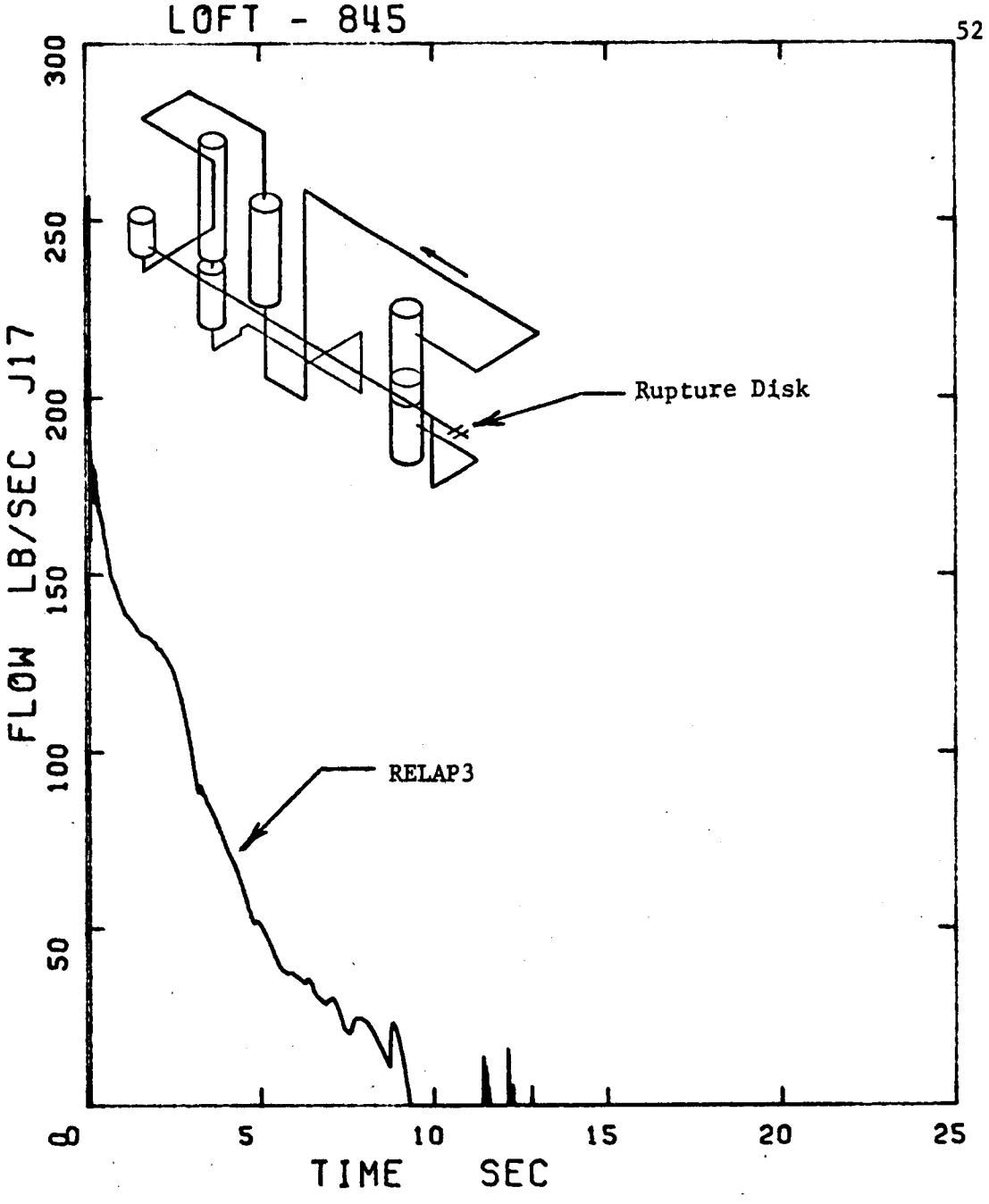


Figure 16, Leak flow rate--test 845.

Fluid density. Figure 17 compares the RELAP3 fluid density in the core with the test data. Density comparisons such as this one are of doubtful accuracy. The RELAP3 densities are averaged over the entire control volume, in this case the whole core. The test densities are measured at a particular line-of-sight through the core. One should be cautious in drawing conclusions from such a comparison. The results shown in Figure 17 are typical of most of the density comparisons.

Fluid mass. Figure 18 shows the RELAP3 calculated fluid mass in the inlet plenum. The plenum fluid mass decreases to a low value by nine seconds. At 11.5 seconds the fluid mass increases because of backflow from volume 12. Figure 19 shows the RELAP3 calculated mixture level in the inlet plenum. The level of the inlet nozzle is 0.96 ft. The mixture level falls to the level of the inlet nozzle by two seconds, and then at nine seconds, the mixture level falls to nearly zero. The sharp dip in mixture level at 9.5 seconds occurs just after the mixture level falls below the inlet nozzle. When this happens, the remaining bubbles in the mixture rise to the surface. This shrinks the mixture, and the level falls rapidly. At about 12 seconds, some of the liquid again flashes to steam, which swells the mixture level back up to the inlet nozzle. Note that the total fluid mass in the plenum (see Figure 18) remains nearly constant during the swell and shrink cycle.

Figure 20 shows the RELAP3 calculated fluid mass in volume 12. The rate of decrease of the fluid mass slows at 3.5 seconds, when the fill water flow begins. By 11.5 seconds, volume 12 is full of fill water and

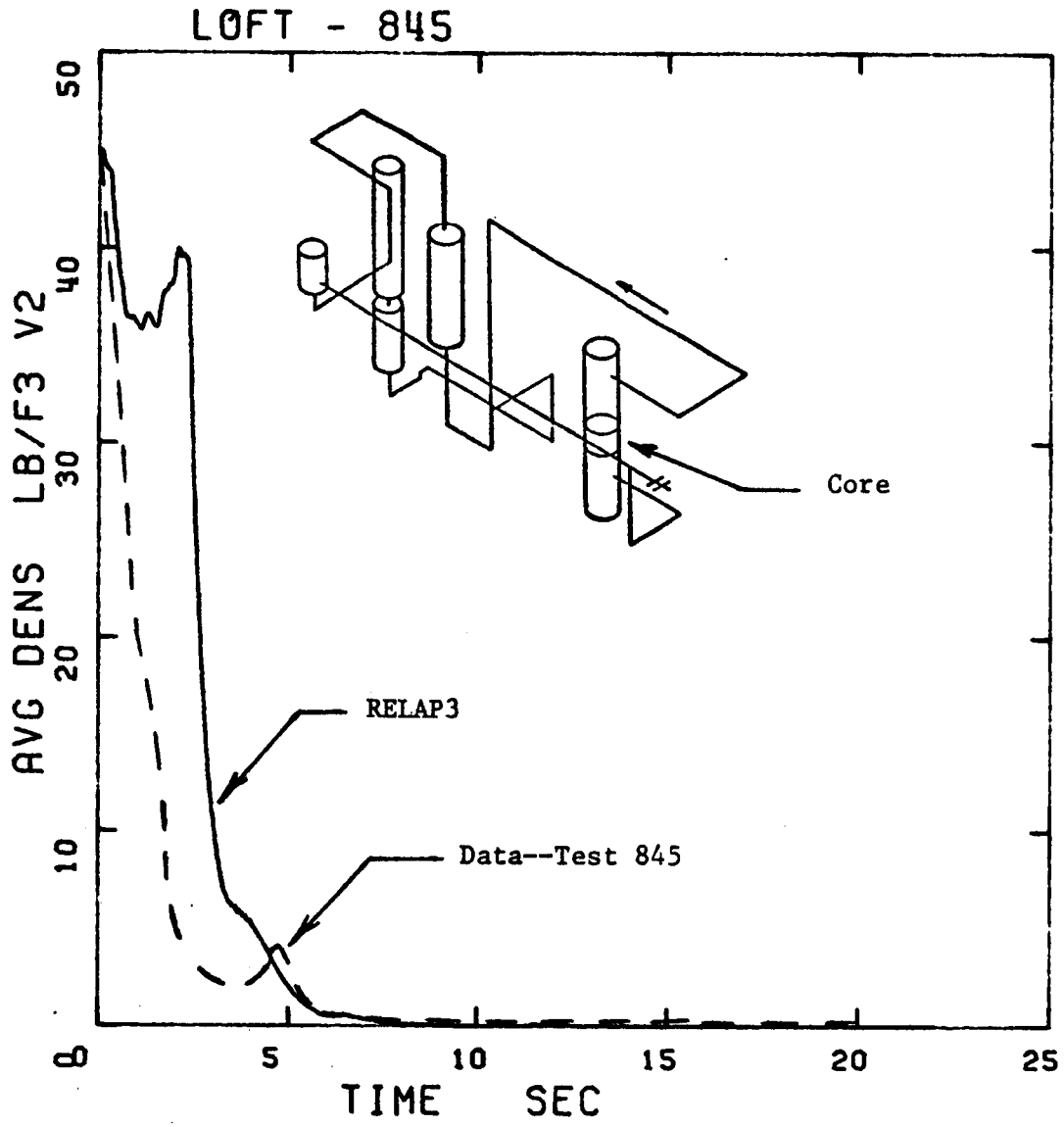


Figure 17. Core fluid density--test 845.

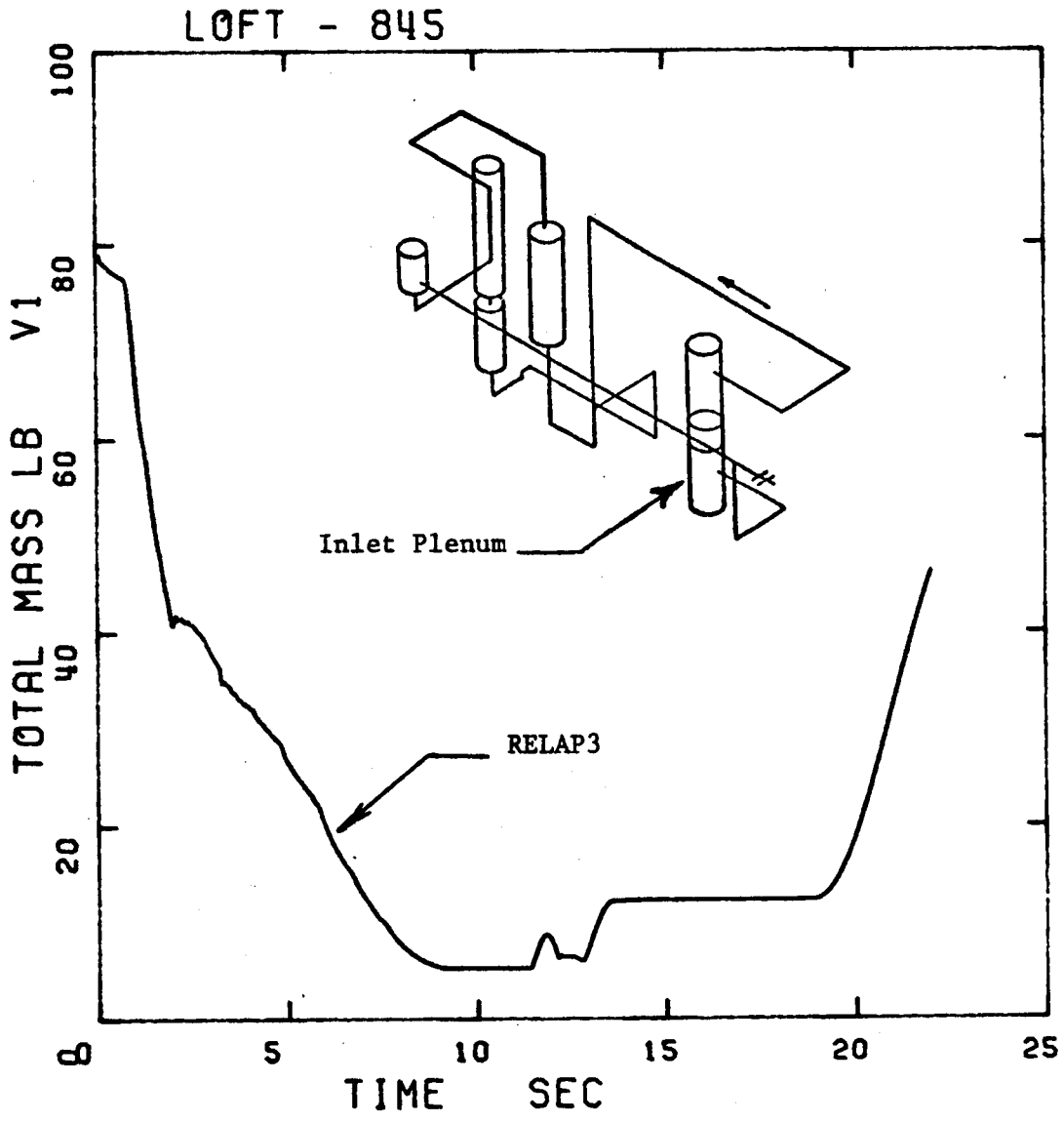


Figure 18. Inlet plenum fluid mass--test 845.

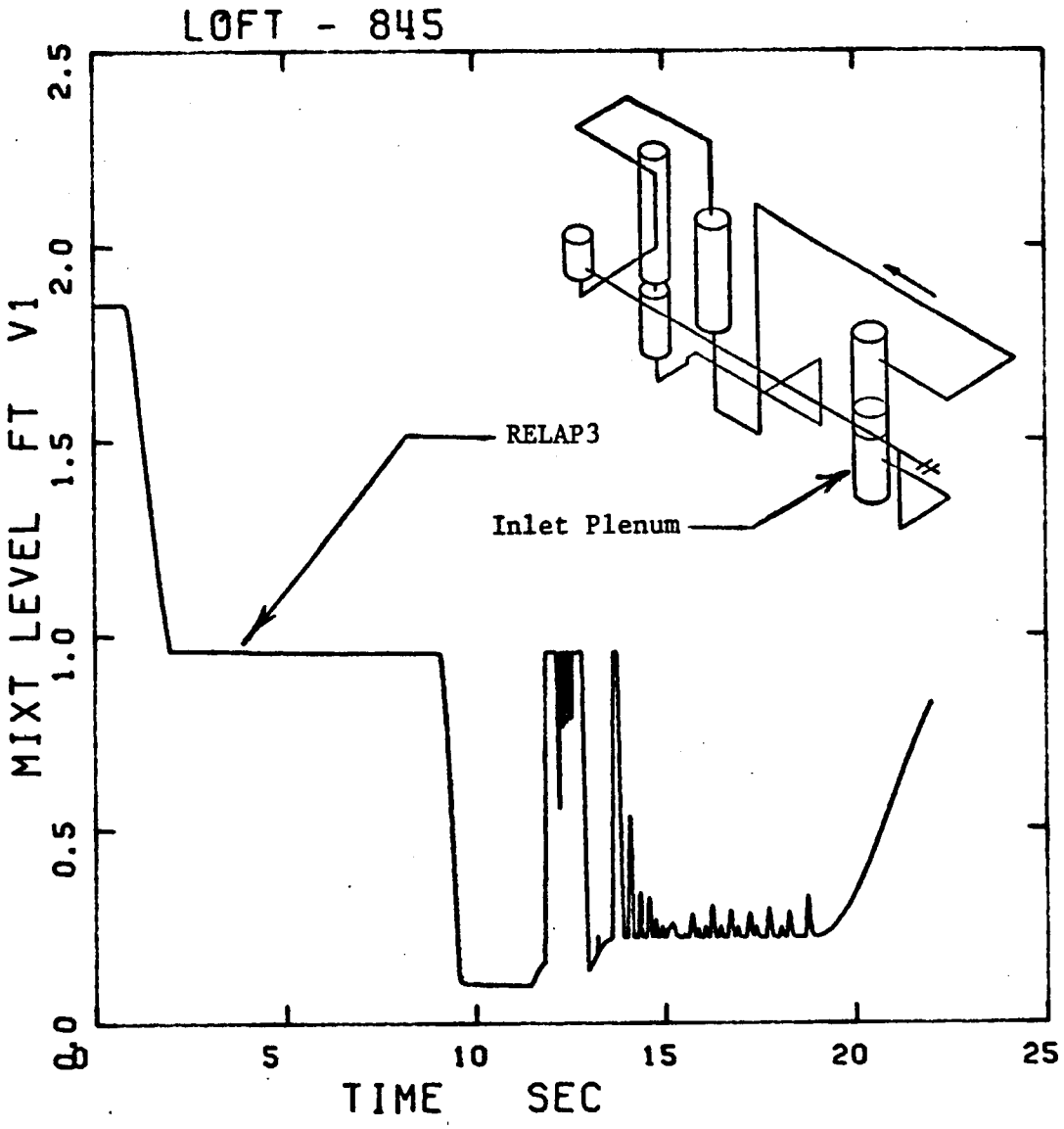


Figure 19. Inlet plenum mixture level--test 845.

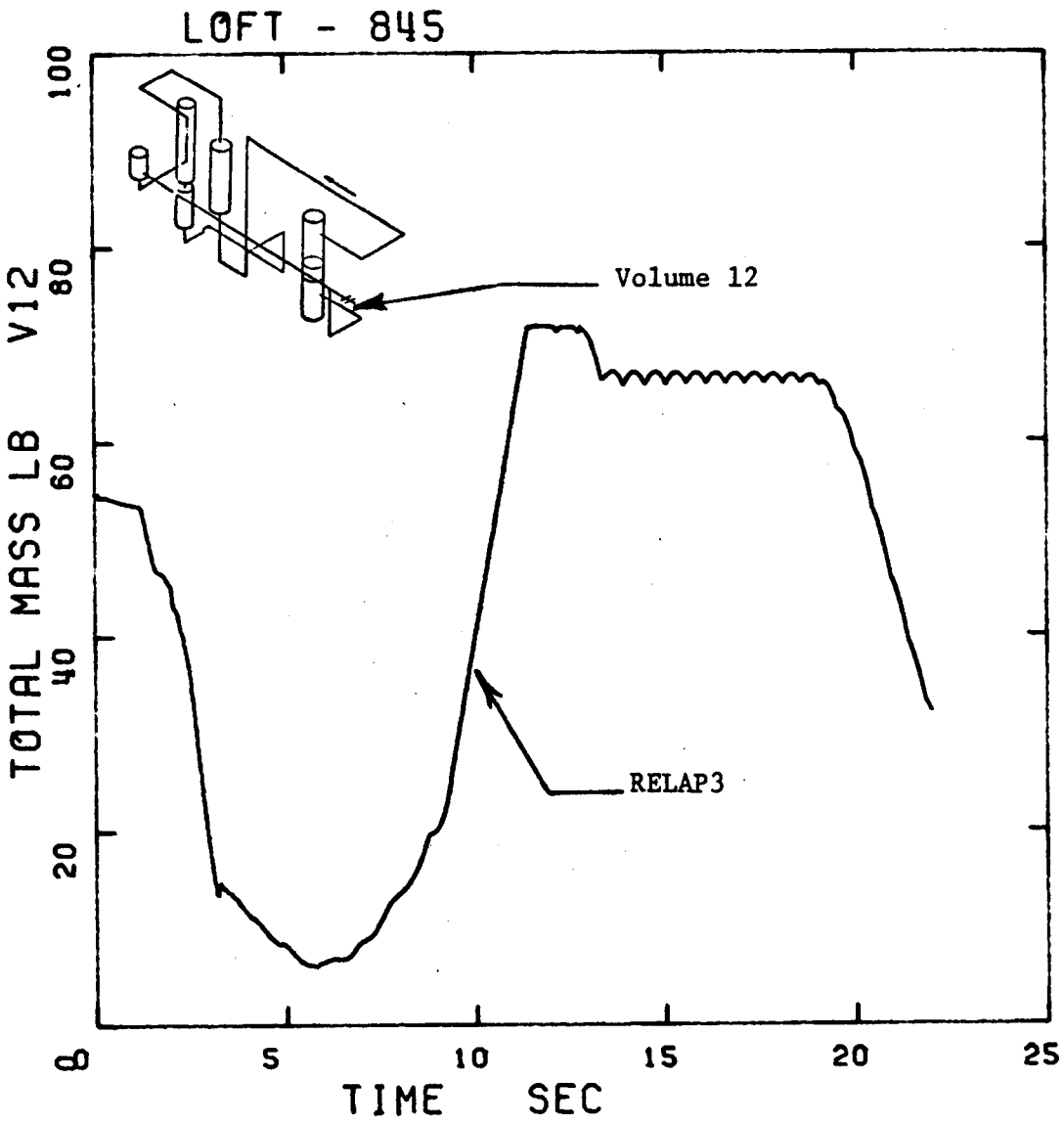


Figure 20. Volume 12 calculated fluid mass--test 845.

condensed steam. The fluid mass then decreases due to a resumption of flow out the leak, and to backflow into volume 12.

Effect of accumulator gas. The RELAP3 model does not include the effects of the nitrogen gas escaping from the accumulator. The effect of this gas would be to expell most of the liquid from volumes 12 and 15. The expulsion would start at about 11.5 seconds, at the time the present model predicts liquid backflow into the inlet plenum. Figure 3, page 7, is a schematic diagram of the emergency core coolant system, and helps explain the mechanism of the expulsion. The cover gas follows the last of the emergency core coolant into the system. The gas would expell some or all of the liquid from the section of pipe between the vessel inlet nozzle and the leak. Except for the cover gas expulsion effect, some of the liquid in the inlet pipe would probably flow back into the inlet plenum, as RELAP3 predicts it does.

Residual fluid mass. The calculated fluid mass in the system at the end of the transient is 128 lb. Table 8 and Table 9 show the fluid mass distribution at 11.5 seconds and 22 seconds, respectively. If the effect of the escaping nitrogen from the accumulator was considered, the calculated residual fluid mass would be reduced to perhaps 20 lb. The test results showed no residual water anywhere in the system.

Core Heat Transfer

Clad temperatures. Figure 21 compares the RELAP3 clad temperatures with the test data from two typical fuel pins. RELAP3 predicts departure

TABLE 8

CALCULATED MASS DISTRIBUTION AT 11.5 SEC.

Control Volume	Location	Total Mass, lb m	Liquid Mass, lb m	Pressure psia
1	Inlet plenum	5.92	5.86	14.31
2	Core	0.06	0.04	14.75
3	Outlet plenum	0.51	0.41	14.75
4	Hot leg pipe	0.04	0.02	15.02
5	Hot leg pipe	0.06	0.03	15.01
6	Hot leg pipe	0.06	0.03	15.01
7	HXT inlet plenum	0.18	0.16	15.00
8	HXT tube bundle	0.01	0.006	15.00
9	HXT outlet plenum	0.39	0.37	14.91
10	Cold leg pipe	0.18	0.13	14.98
11	Cold leg pipe	0.40	0.37	13.42
12	Cold leg pipe	71.85	71.85	10.77
13	Extension vessel	5.87	5.81	37.37
14	Pressurizer	0.17	0.08	37.35
15	Fill system pipe	43.64	43.64	57.26
Total		129.34	128.81	

TABLE 9

CALCULATED MASS DISTRIBUTION AT 22 SEC.

Control Volume	Location	Total Mass, lb m	Liquid Mass, lb m	Pressure psia
1	Inlet plenum	46.28	46.26	8.32
2	Core	0.007	0.0	8.15
3	Outlet plenum	0.63	0.53	14.70
4	Hot leg pipe	0.03	0.005	14.70
5	Hot leg pipe	0.04	0.004	14.70
6	Hot leg pipe	0.03	0.0007	14.70
7	HXT inlet plenum	0.19	0.17	14.70
8	HXT tube bundle	0.26	0.257	7.49
9	HXT outlet plenum	0.14	0.13	7.51
10	Cold leg pipe	0.09	0.07	7.75
11	Cold leg pipe	0.43	0.41	7.51
12	Cold leg pipe	32.14	32.13	7.84
13	Extension vessel	5.42	5.39	14.76
14	Pressurizer	0.12	0.08	14.71
15	Fill system pipe	42.89	42.89	4.97
Total		128.70	128.34	

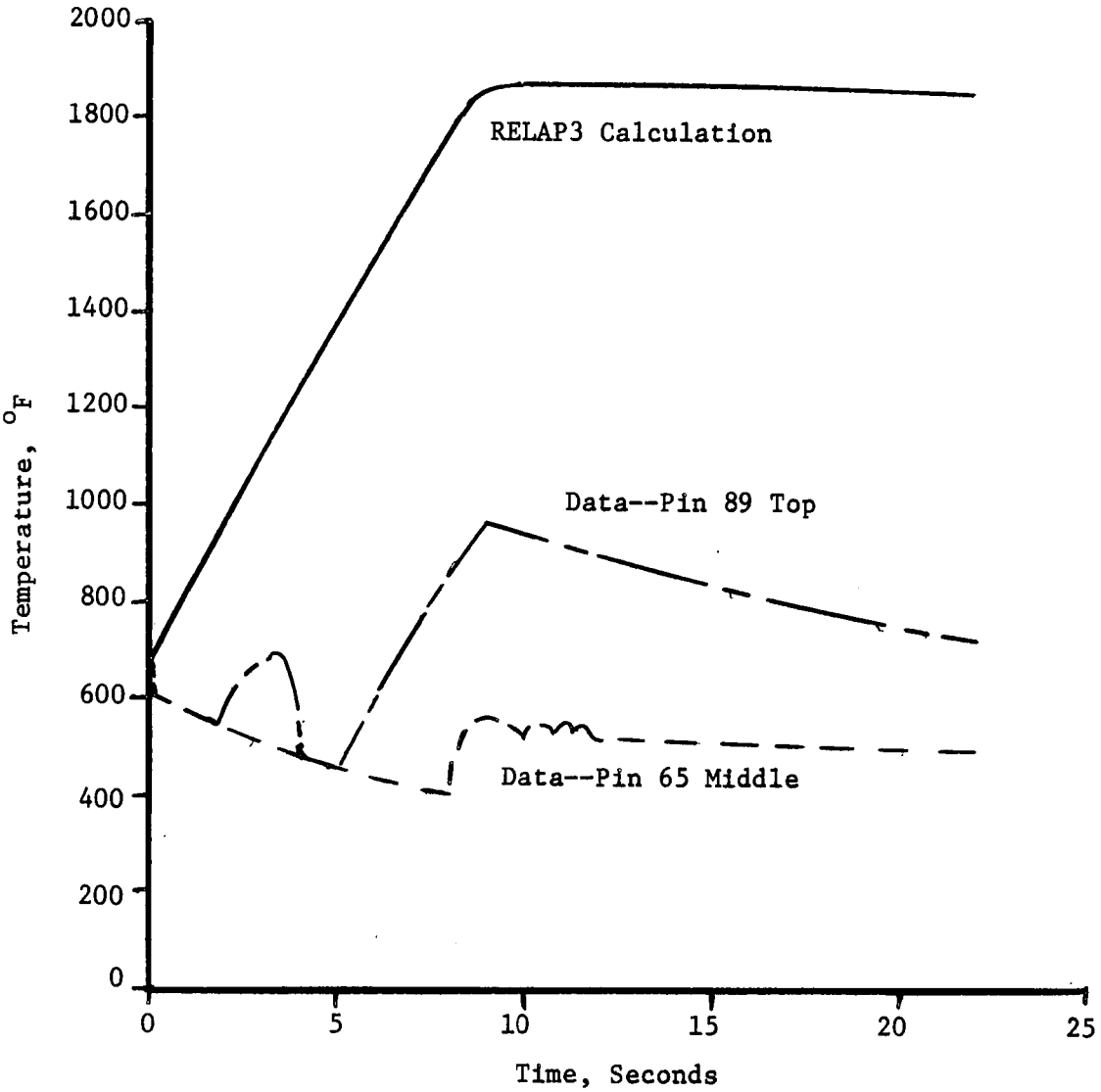


Figure 21. Clad temperature--test 845.

from nucleate boiling (DNB) at 0.1026 seconds. The leak is fully open at 0.1015 seconds. The test data shows DNB occurred from four to eight seconds after rupture, depending on the heater pin being considered. As a result of the very early DNB, RELAP3 predicts much higher clad temperatures than actually occurred in the core.

DNB calculations. Figure 22 shows the calculated surface heat flux and the calculated DNB heat flux. From time zero to 0.1019 seconds the heat transfer mode oscillates between subcooled forced convection and subcooled nucleate boiling. The heat transfer mode changes each time step. The upper bound on the surface heat flux is the heat flux for subcooled nucleate boiling. The lower bound is the heat flux for subcooled forced convection. At 0.1019 seconds, the mode oscillations stop, and the heat transfer mode is entirely subcooled nucleate boiling. The core flow reverses direction between 0.1020 seconds and 0.1033 seconds, causing a sharp dip in the DNB flux as the flow rate crosses zero. During this momentary dip, DNB occurs. The DNB flux recovery almost immediately, because of the high reverse flow rate in the core.

Heat Exchanger Results

Heat removal rate. Figure 23 shows the heat transfer rate for the two RELAP3 runs on test 845. The first run used a constant, 1.07 MW heat transfer rate. For the second run, the heat removal rate was dependent on the flow rate and the temperature difference. The flow and temperature dependent model gives very high heat removal rates in the initial part of

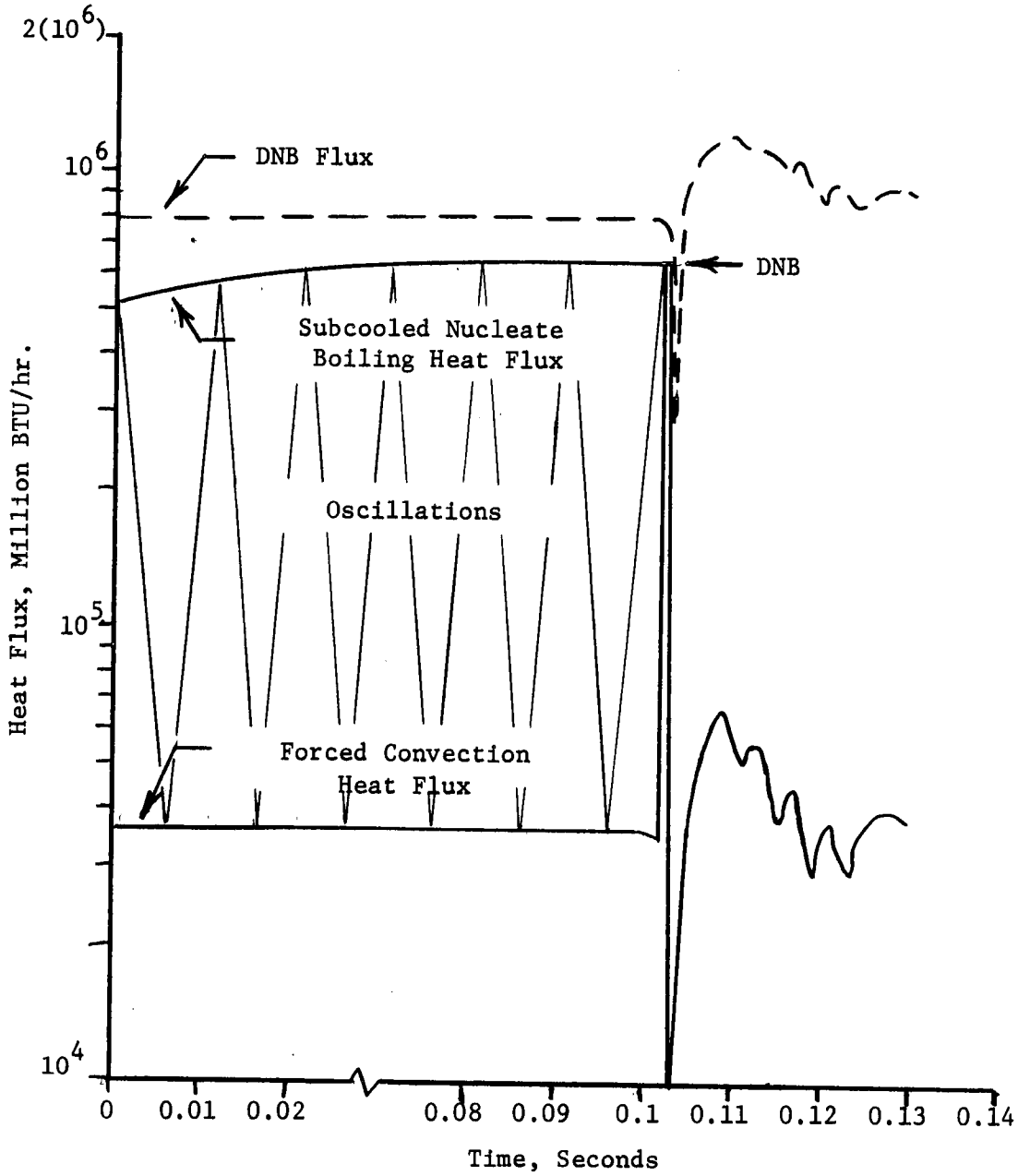


Figure 22. DNB history--test 845.

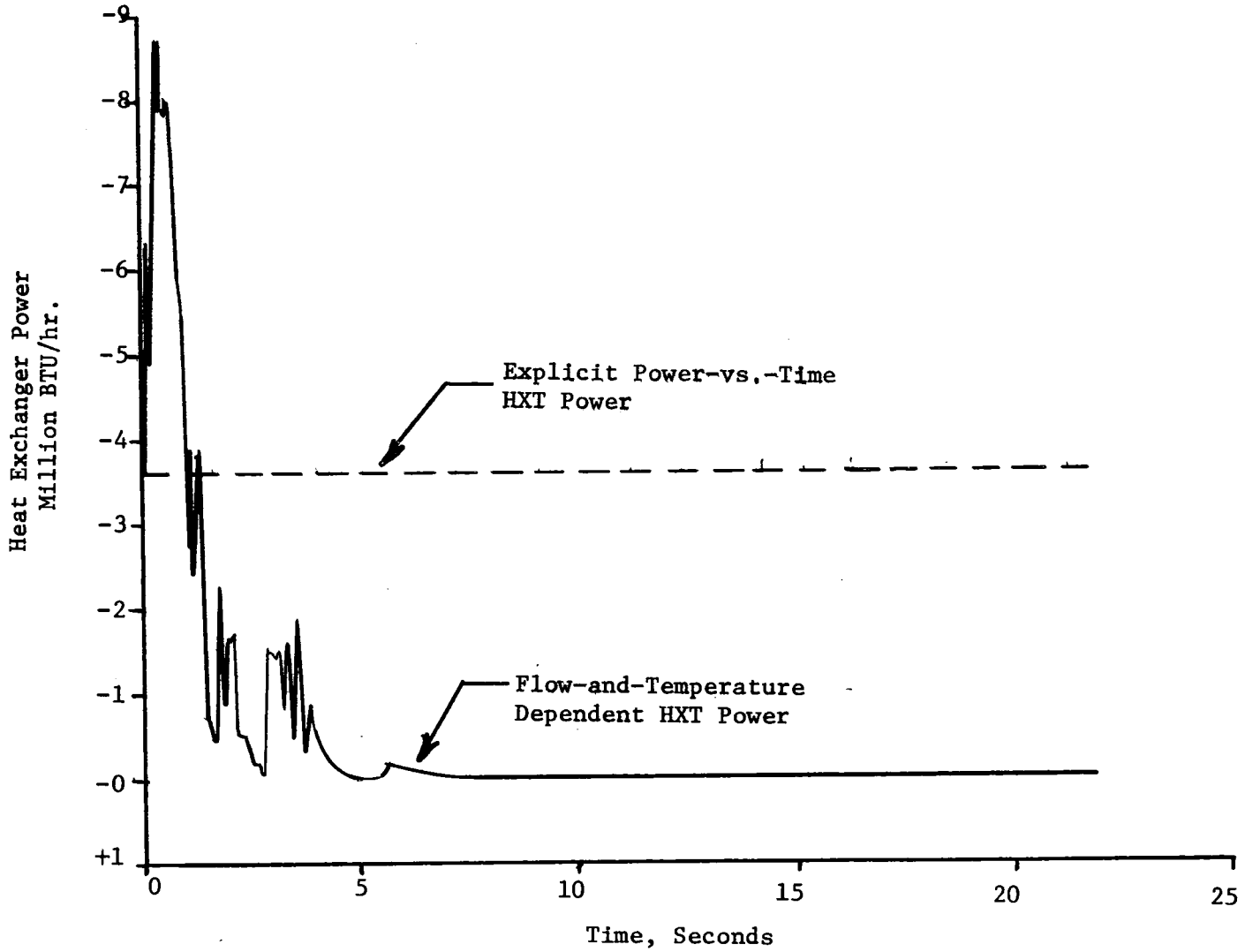


Figure 25. Heat exchanger heat removal rate--test 845.

the transient. The peak value is 2.4 times the initial steady-state value. Figure 24 compares the calculated tube bundle pressure using the two sets of assumptions. The calculated pressures are the same out to about two seconds. After two seconds, the constant-power results are about 100 psi below the flow and temperature dependent results. Figure 25 compares the calculated heat exchanger tube bundle fluid mass for the two sets of assumptions. The constant heat removal rate condenses considerable steam, giving a much higher fluid-mass in the later part of the transient.

C. RESULTS--TEST 825

System Parameters

System pressures. Figure 26 compares the calculated inlet plenum pressure with the test data. The calculated pressure is too low for the first 11 seconds, and is too high after 11 seconds. Figure 27 compares the calculated heat exchanger outlet plenum pressure with the test data. Slugs of water leaving the bottom of the plenum cause the pressure oscillations beginning at 4.8 seconds. Figure 28 illustrates this effect. The junction between volumes eight and nine is near the bottom of volume nine. The fluid is flowing from volume nine to volume eight. Volume nine has stratified bubble rise parameters, so if there is any liquid in volume nine, the fluid in the junction will be liquid. The liquid level is low and periodically drops to zero. This makes the density and the flow rate in the junction vary rapidly, causing the oscillations. A

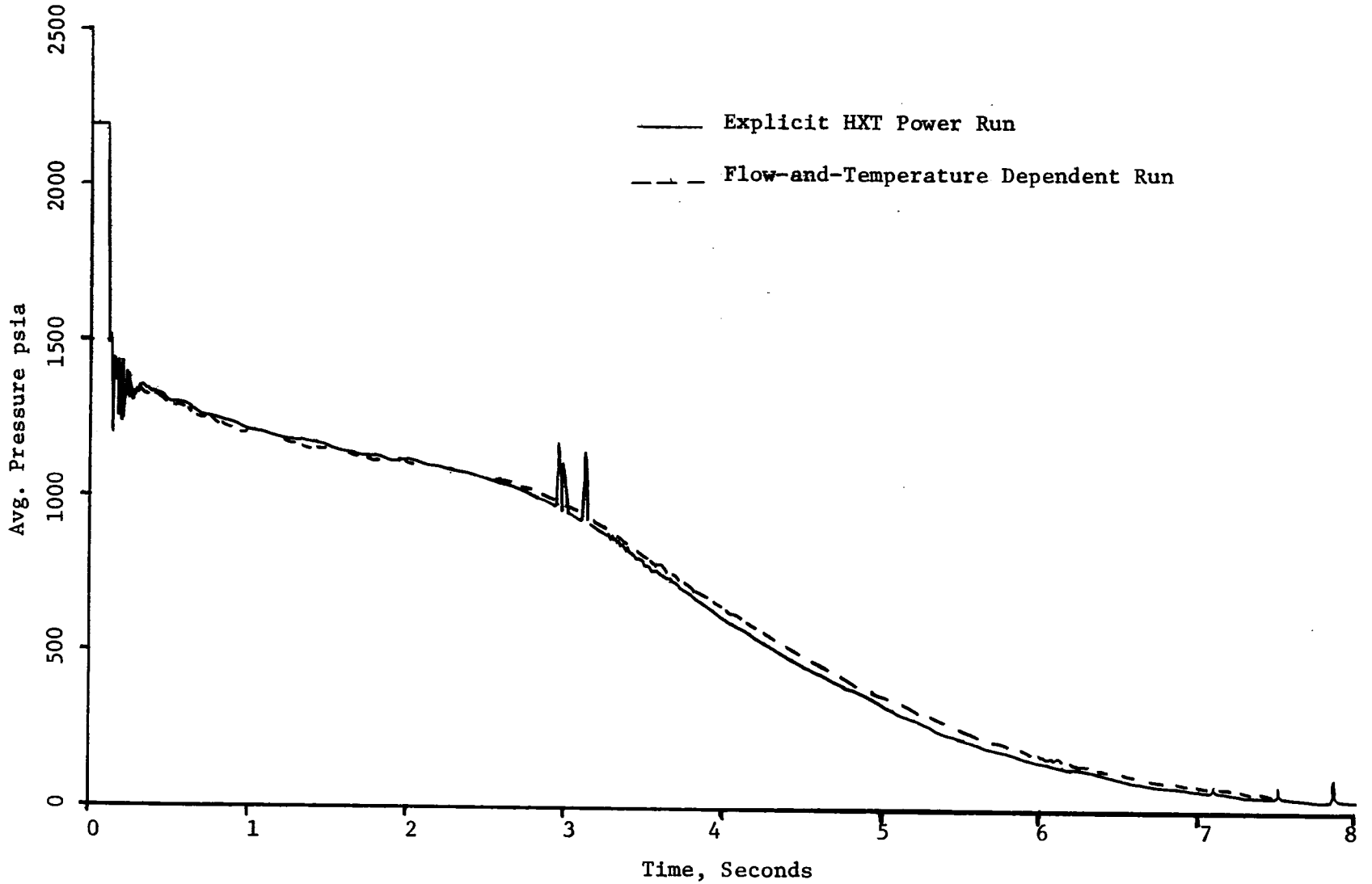


Figure 24. Heat exchanger tube bundle pressures--test 845.

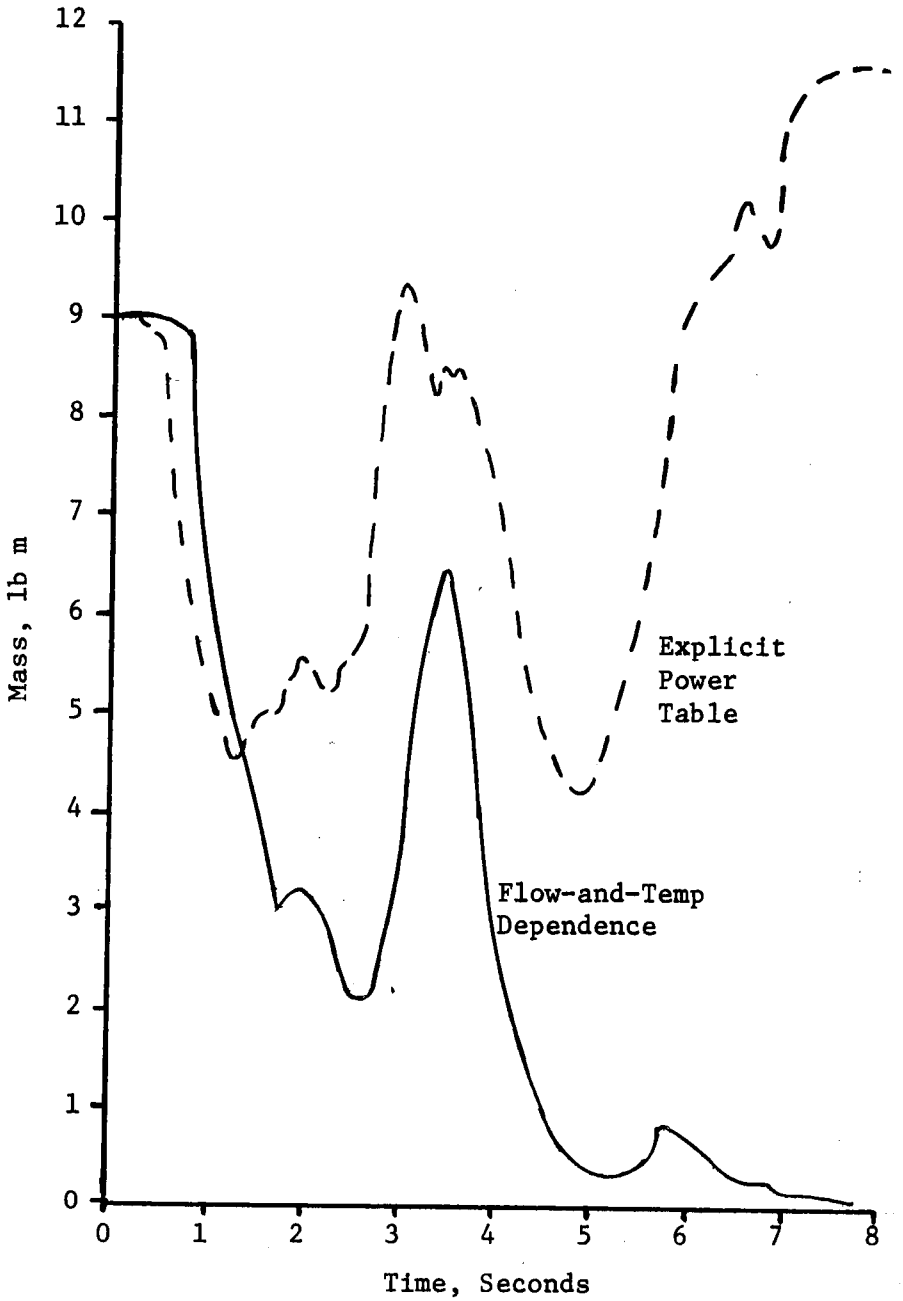


Figure 25. Heat exchanger tube bundle fluid mass--test 845.

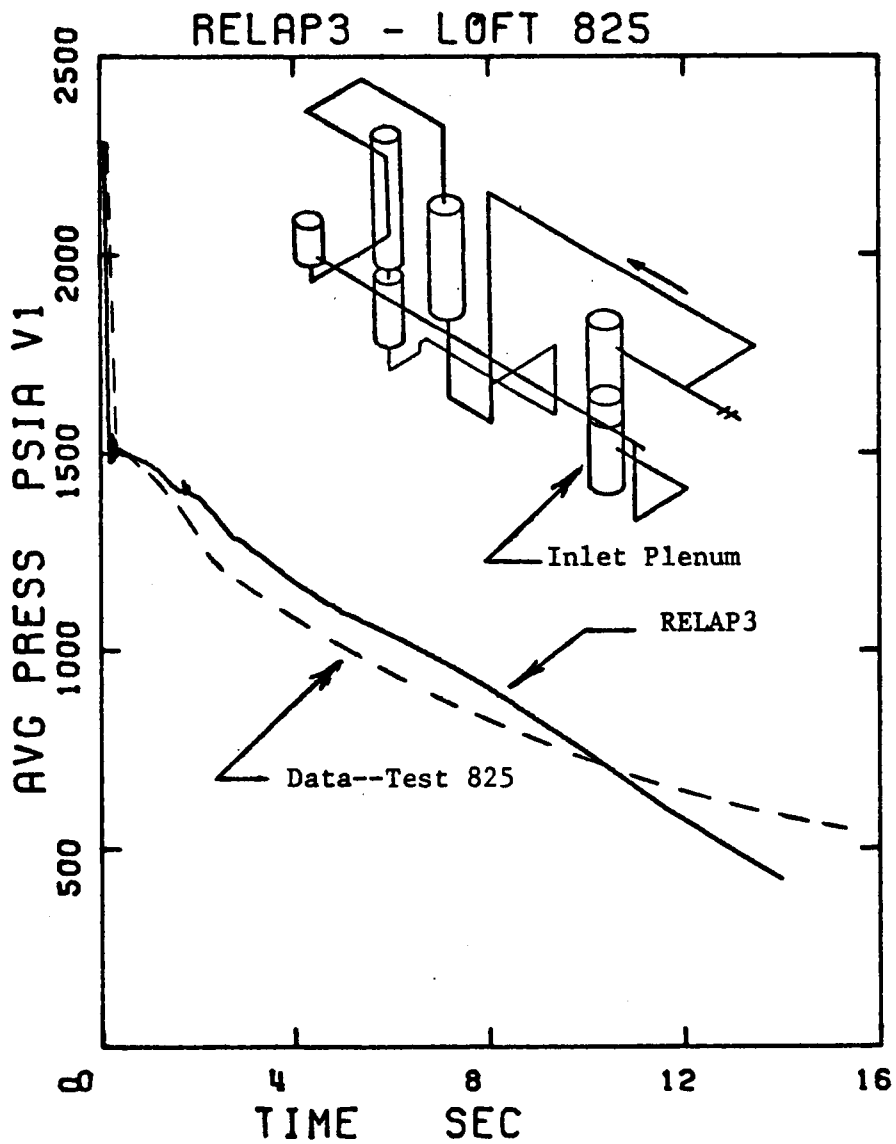


Figure 26. Inlet plenum pressure--test 825.

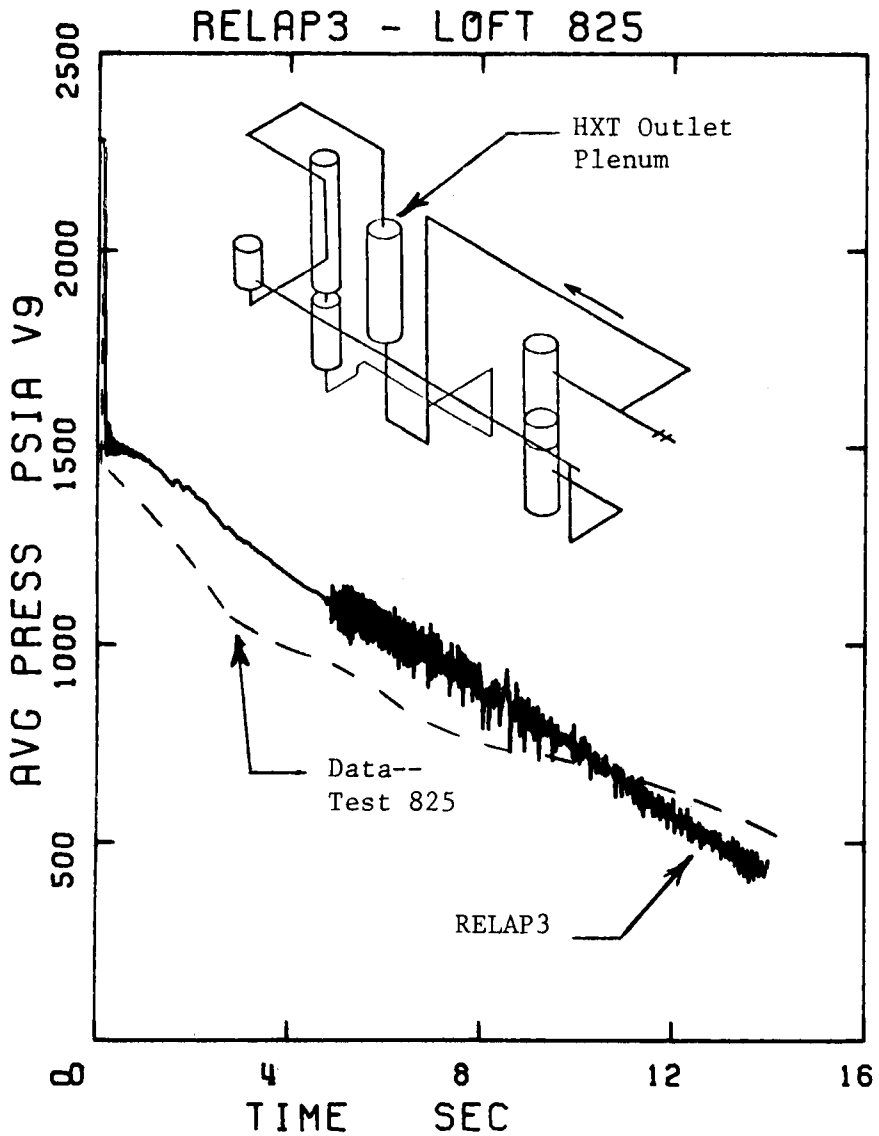


Figure 27. Heat exchanger outlet plenum pressure--test 825.

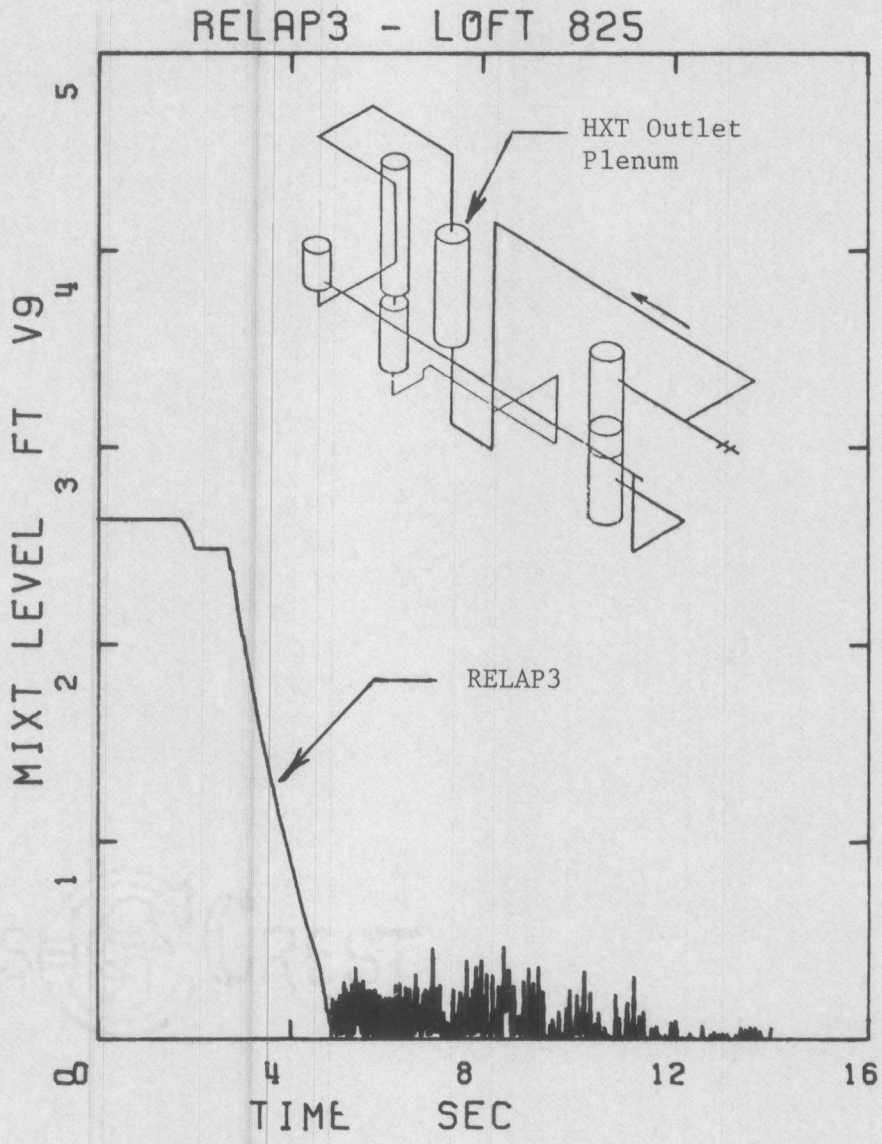


Figure 28. Heat exchanger outlet plenum mixture level--test 825.

similar effect occurs in volume seven, the heat exchanger inlet plenum. There were no such pressure oscillations in the calculations for test 845, because the heat exchanger flow is in the opposite direction for this test.

Fluid temperatures. Figure 29 compares the calculated fluid temperature in the inlet plenum with the test data. Both the calculated temperatures and the test temperatures correspond closely to the saturation temperatures.

Flow rates. Figure 30 compares the calculated core flow rate with the test data. The calculated flow is the average of the flow entering and leaving the core. The averaging was done graphically, and this process smooths the flow, eliminating the high frequency oscillations similar to those on the following figures. The oscillations are caused by alternate slugs of water and steam leaving the outlet plenum. The mixture level in the outlet plenum falls to the outlet nozzle elevation right after the rupture and remains there for a considerable time. Depending on the amount of liquid in the plenum, the mixture level can be either above or below the nozzle elevation. A slight change in mixture level makes a large change in junction flow and density. This causes the oscillations. Figure 31 compares the calculated flow rate in the outlet nozzle with the test data. Despite the oscillations, the smoothed calculated flow agrees fairly well with the data. Figure 32 compares the flow rates in the hot leg pipe, with similar results.

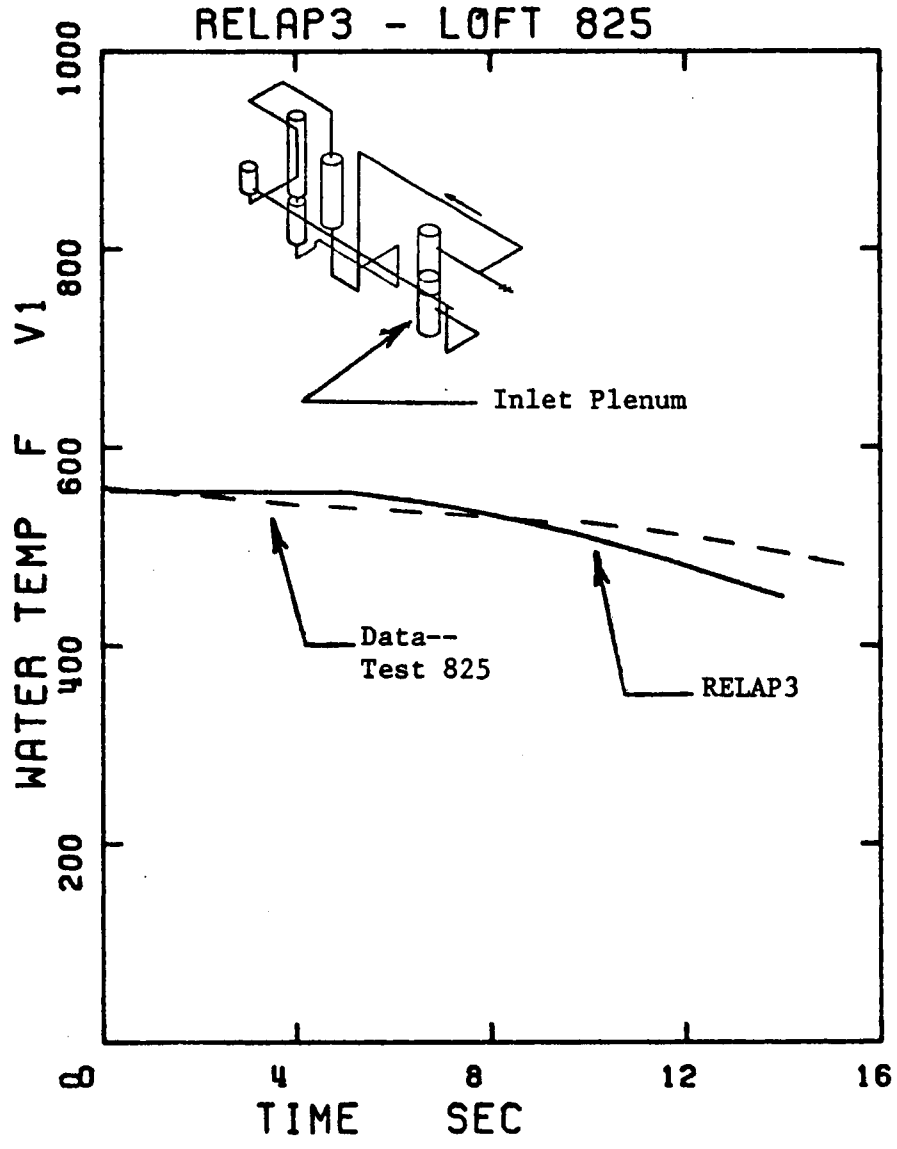


Figure 29. Inlet plenum fluid temperature--test 825.

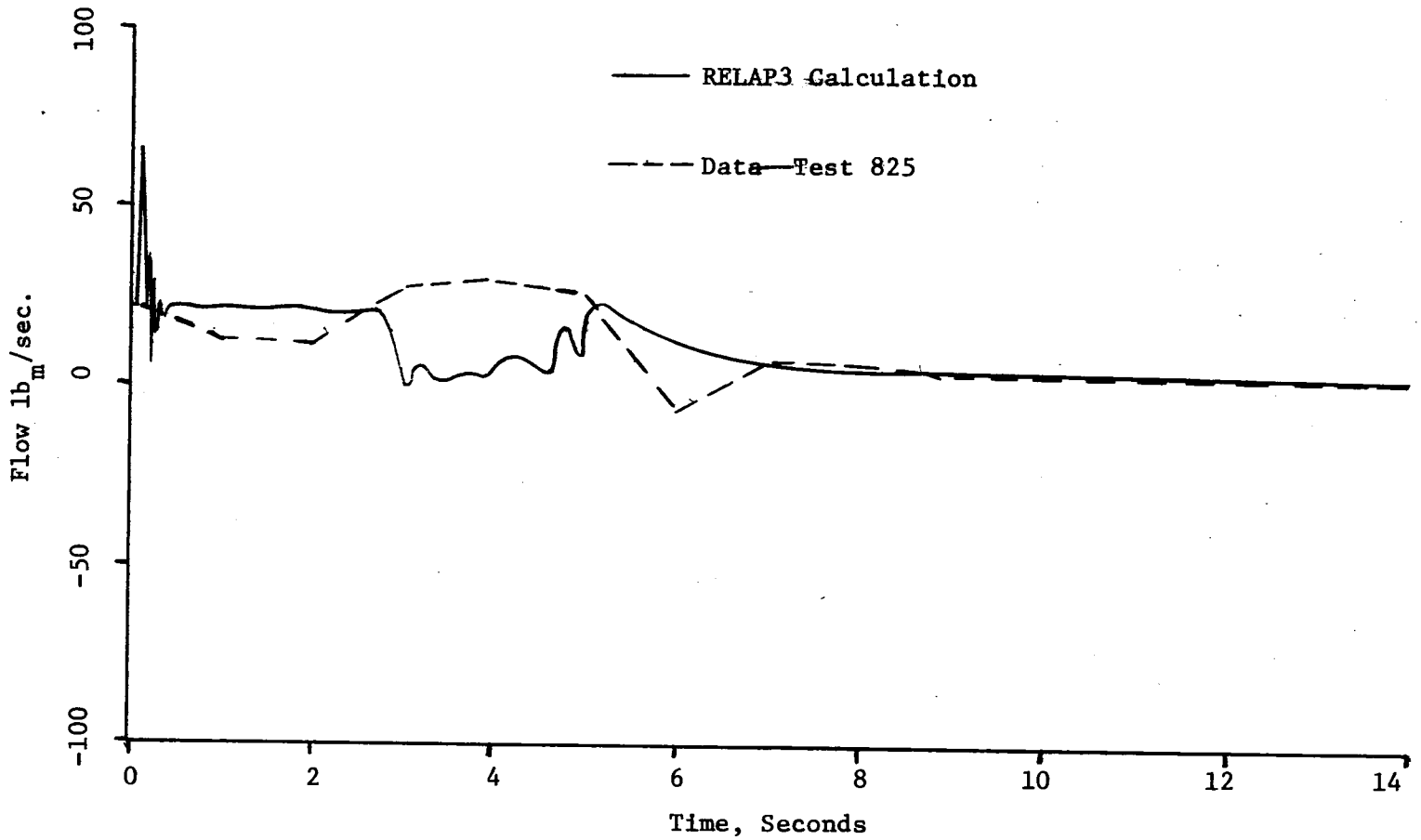


Figure 30. Core flow rate--test 825.

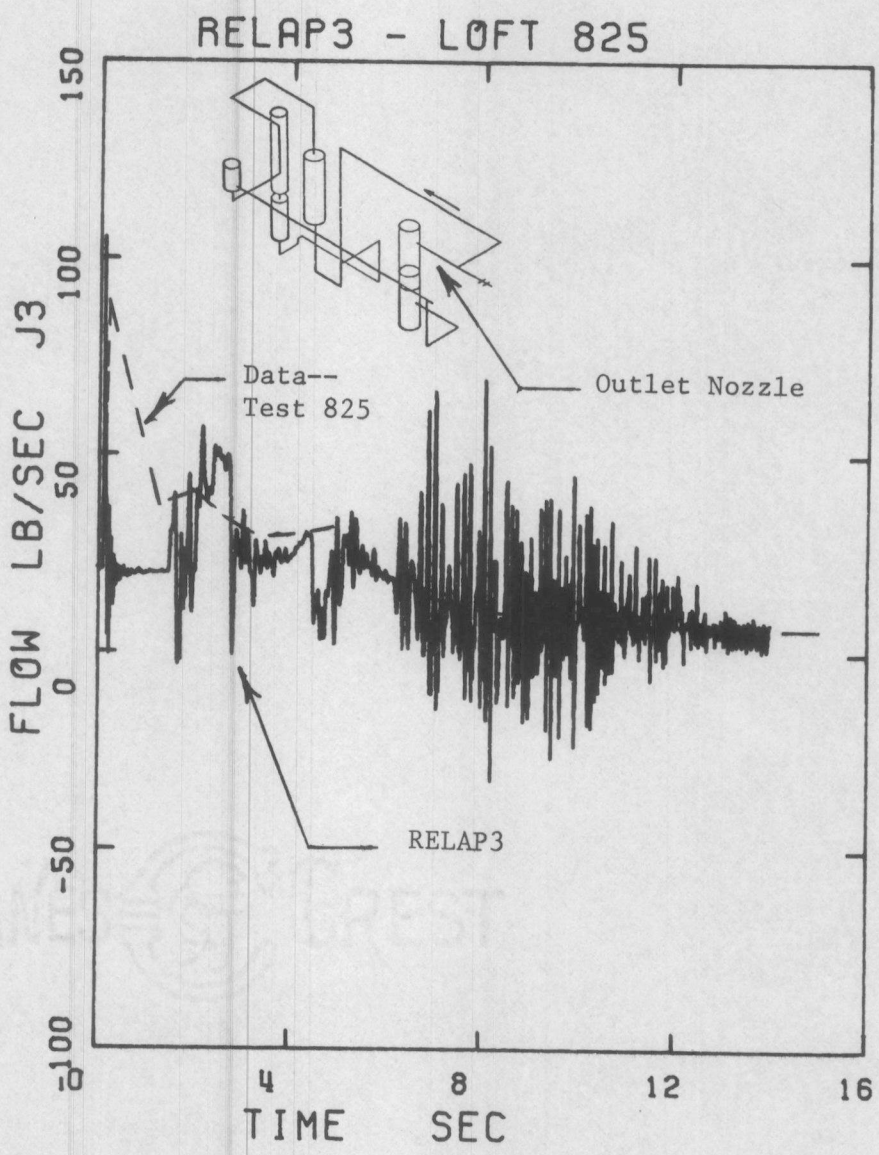


Figure 31. Outlet nozzle flow rate--test 825.

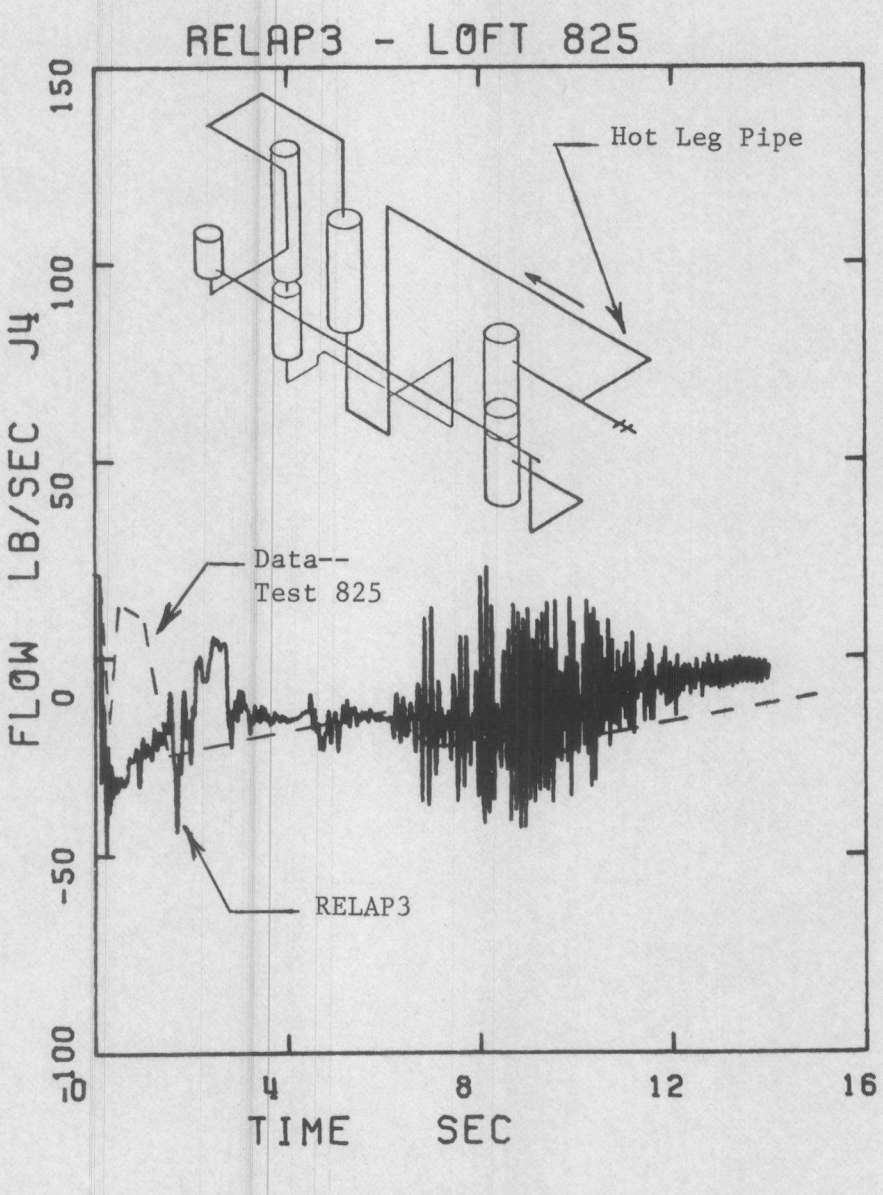


Figure 32. Hot leg pipe flow rate--test 825.

Fluid density. Figure 33 compares the calculated fluid density in the core with the test data. Once again, one must be cautious in making this comparison. The RELAP3 calculated densities are averaged over the entire core. The test data was taken at a particular line-of-sight through the core, and the two results are not necessarily comparable. Figure 34 compares the calculated fluid density in volume 12 with the test data taken at the inlet nozzle.

Core Heat Transfer

Clad temperatures. Figure 35 compares the calculated heater clad temperatures with the test data. As for test 845, RELAP3 predicts much higher clad temperatures than the actual test values. Once again, the reason is the predicted DNB time. The test DNB occurs at 12.5 seconds. RELAP3 predicts DNB at 0.1250 seconds. This makes the calculated heat transfer coefficient much lower than the real value after 0.125 seconds. The low heat transfer coefficient causes a rapid increase in calculated heater temperatures.

DNB calculations. Figure 36 shows the history of DNB calculation for test 825. The heat transfer mode oscillates between subcooled forced convection and subcooled nucleate boiling until about 0.1020 seconds. At this time the heat transfer mode switches to all subcooled nucleate boiling. The mode oscillations resume at 0.119 seconds, and they persist until DNB occurs. DNB occurs at the peak of one of the oscillations, when the heat transfer mode is subcooled nucleate boiling.

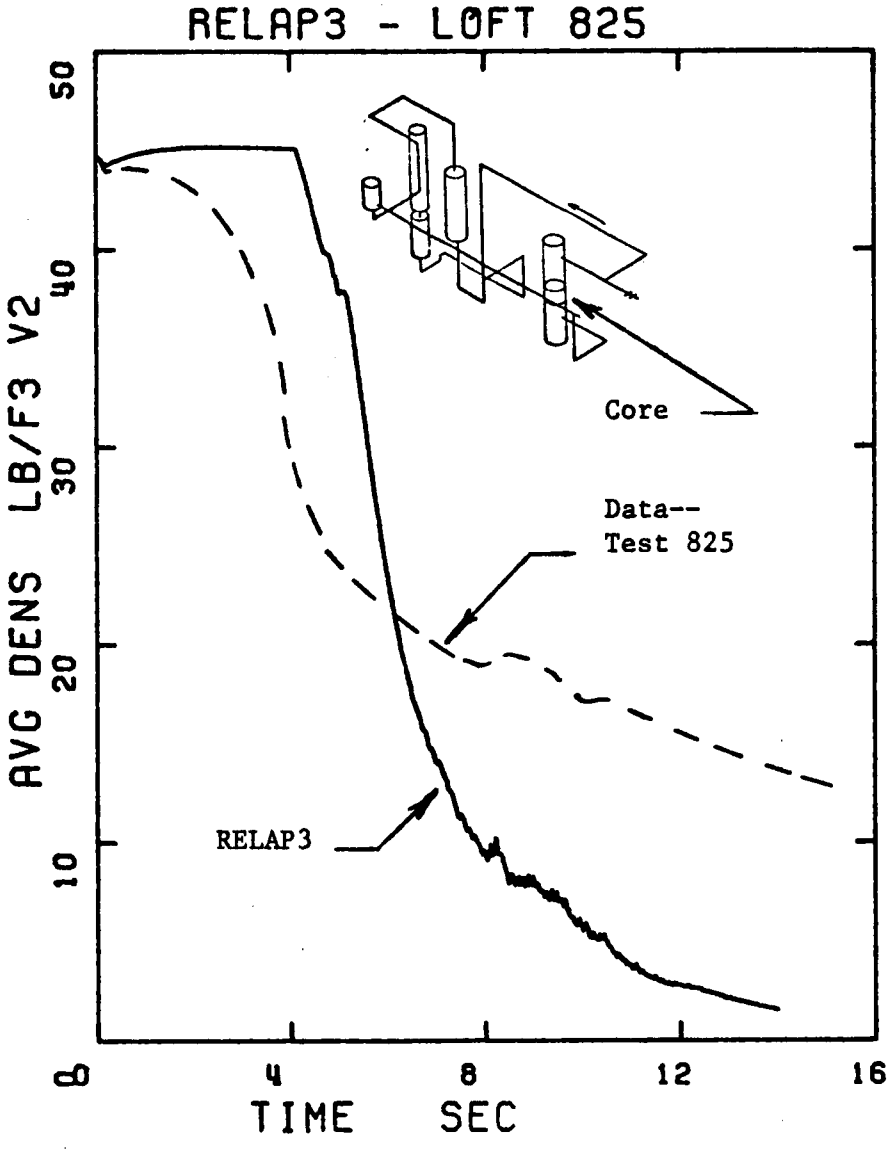


Figure 33. Core fluid density--test 825.

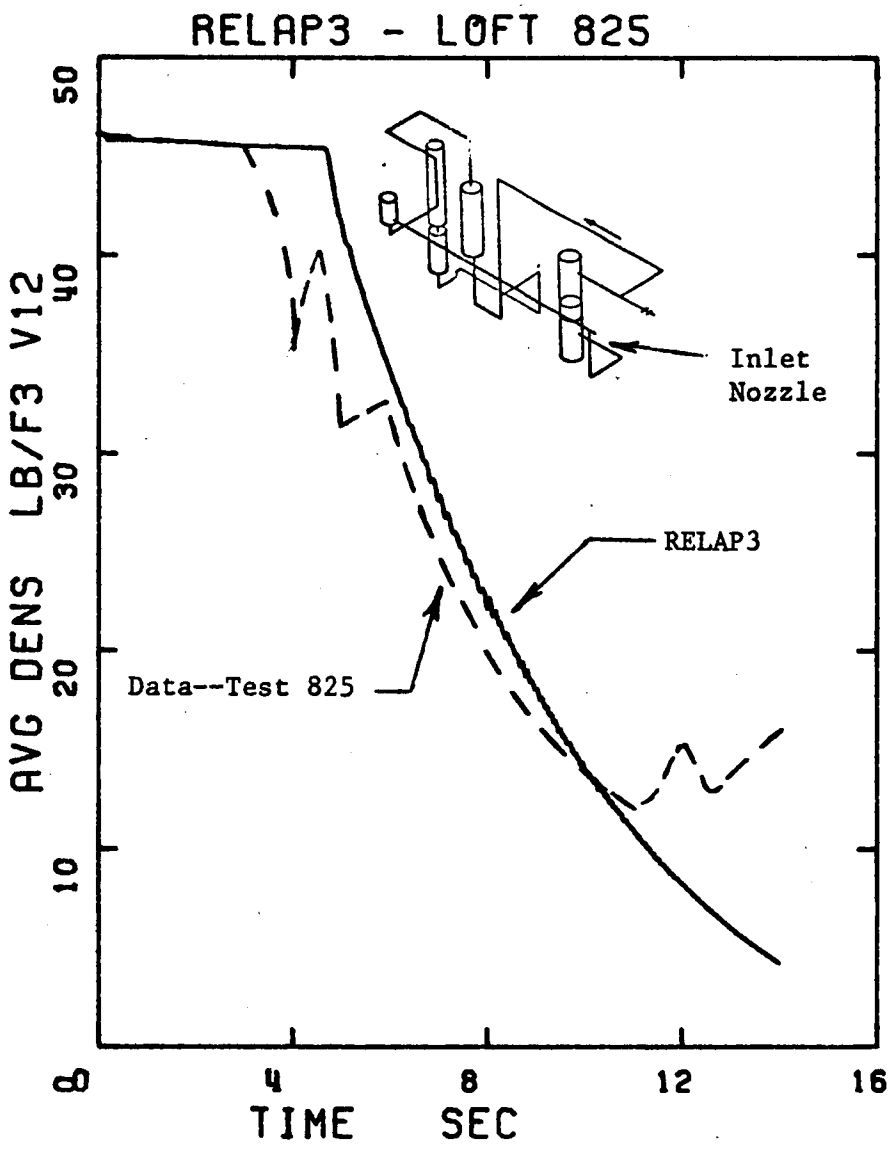


Figure 34. Inlet nozzle fluid density--test 825.

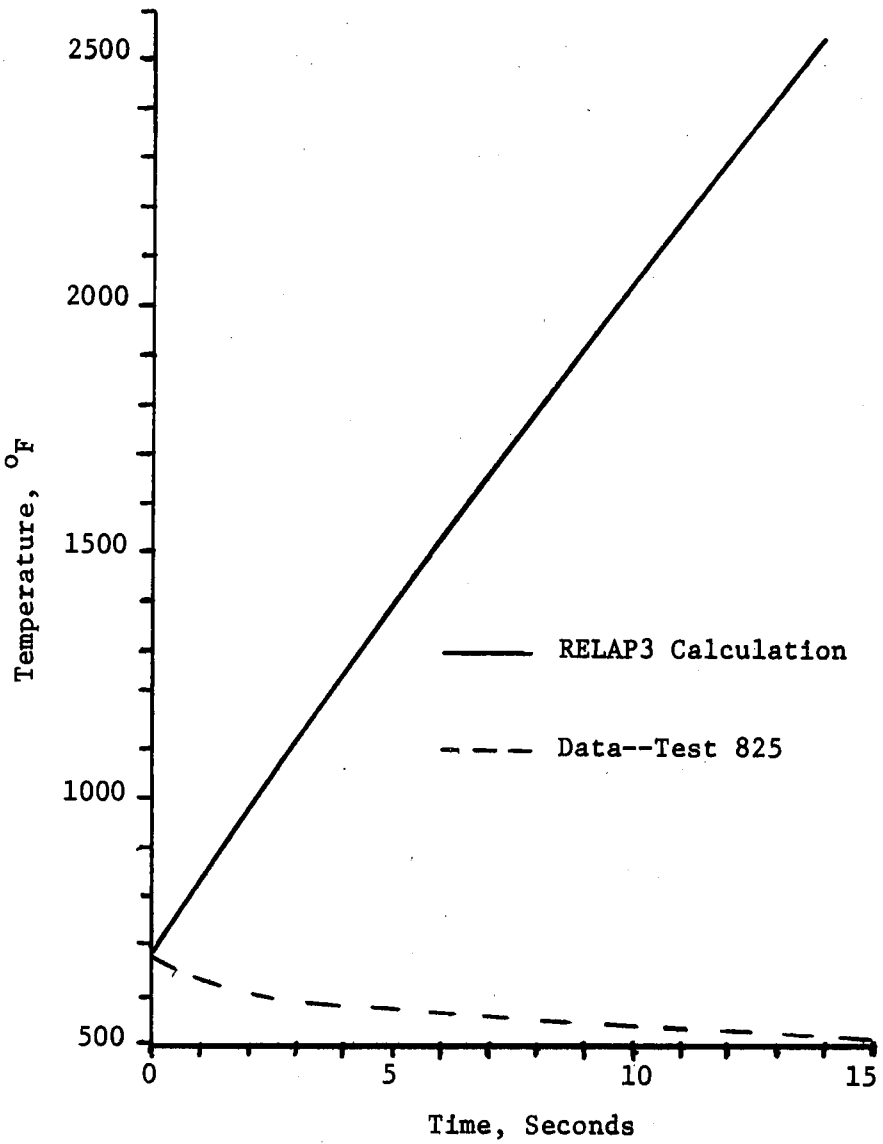


Figure 35. Clad temperatures--test 825.

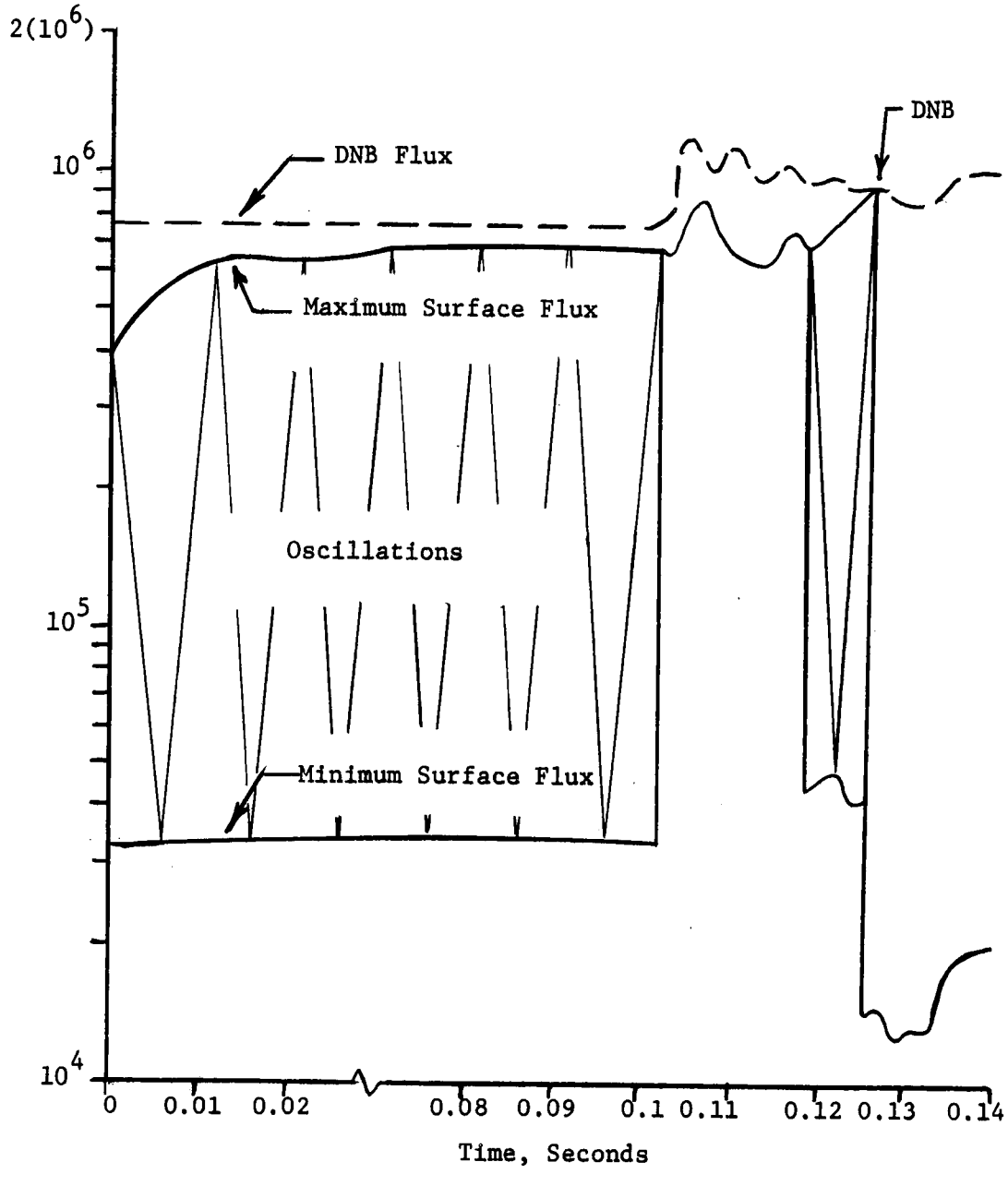


Figure 36. DNB history--test 825.

D. COMPARISON OF FLASH3 AND RELAP3 CALCULATIONS

Description of FLASH3 Calculations

Source of data. References (8) and (22) present a comparison of FLASH3 calculations with data from test 845. The FLASH3 code is described in reference (10).

Comparison of calculation models. Figure 37 shows the control volume arrangement used in the FLASH3 calculations (22). Table 10 compares the calculation methods used in the two models. The most significant differences between the two models are the control volume arrangement and the DNB correlations. The FLASH3 model has fewer control volumes, and consequently, less spatial detail of the loop piping than does the RELAP3 model. The FLASH3 calculations used the three-parameter fit DNB correlation. Reference (22) does not say what parameters were used in this correlation.

Comparison of Results

System pressure. Figure 38 compares the RELAP3 and FLASH3 calculated lower plenum pressure with the test data. The FLASH3 results are very close to the RELAP3 results.

Inlet nozzle flow rate. Figure 39 compares the RELAP3 and FLASH3 calculated inlet nozzle flow rates with the test data. FLASH3 predicts a flow reversal at about 3 seconds, which RELAP3 does not predict, and which does not appear in the test data. From four seconds to 11 seconds

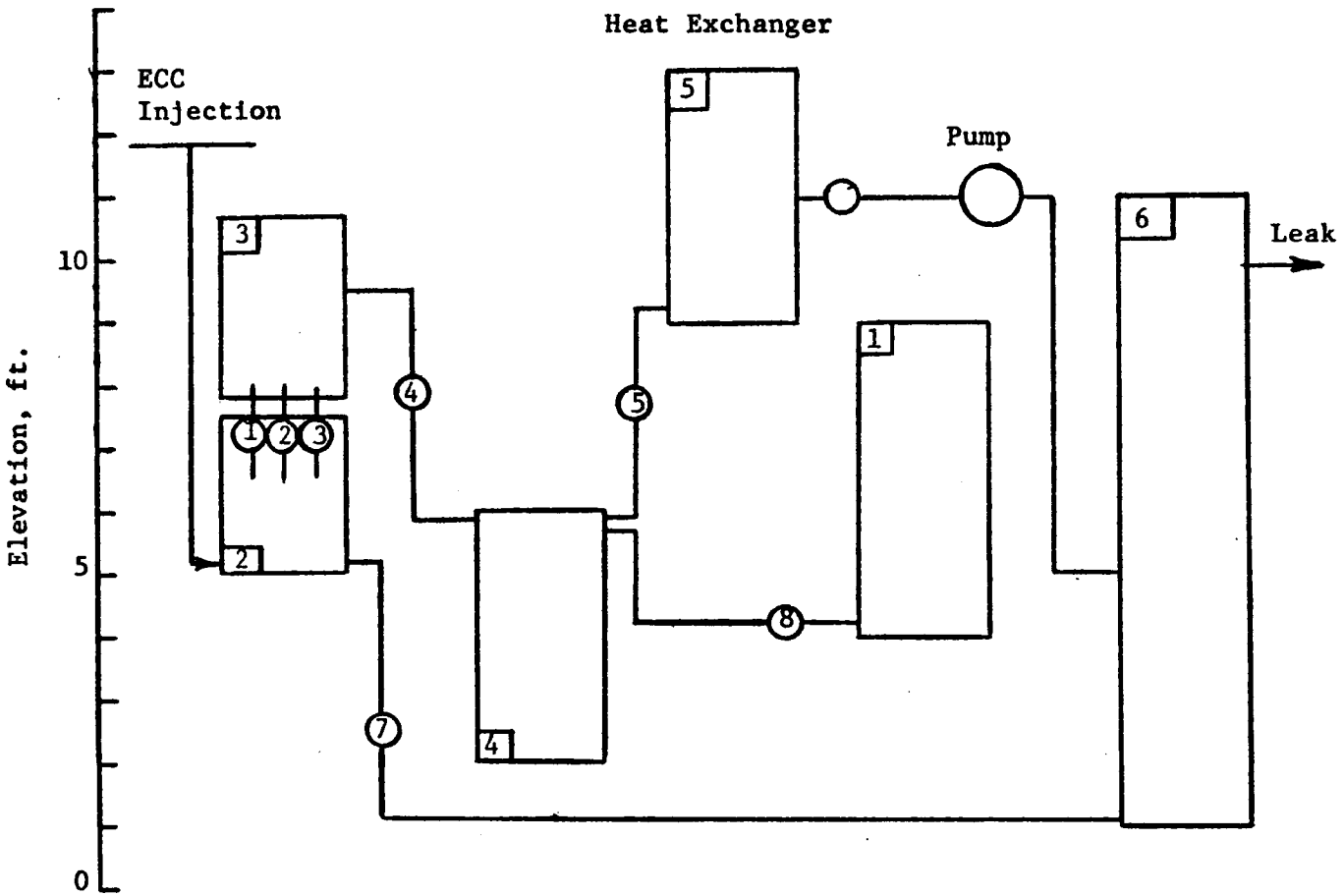


Figure 37. FLASH3 control volume arrangement (from reference 10).

TABLE 10

COMPARISON OF FLASH3 AND RELAP3 CALCULATION MODELS

Item	RELAP3	FLASH3
Number of Control Volumes	15	6
Number of Flow Paths	17	10
Number of Core Flow Paths	1	2, Plus One Bypass Path
ECC Injection Point	Cold Leg	Lower Plenum
DNB Correlation	Various	Three Parameter Fit
Leak Correlation	Moody	Moody
Discharge Coefficient	0.6	0.6

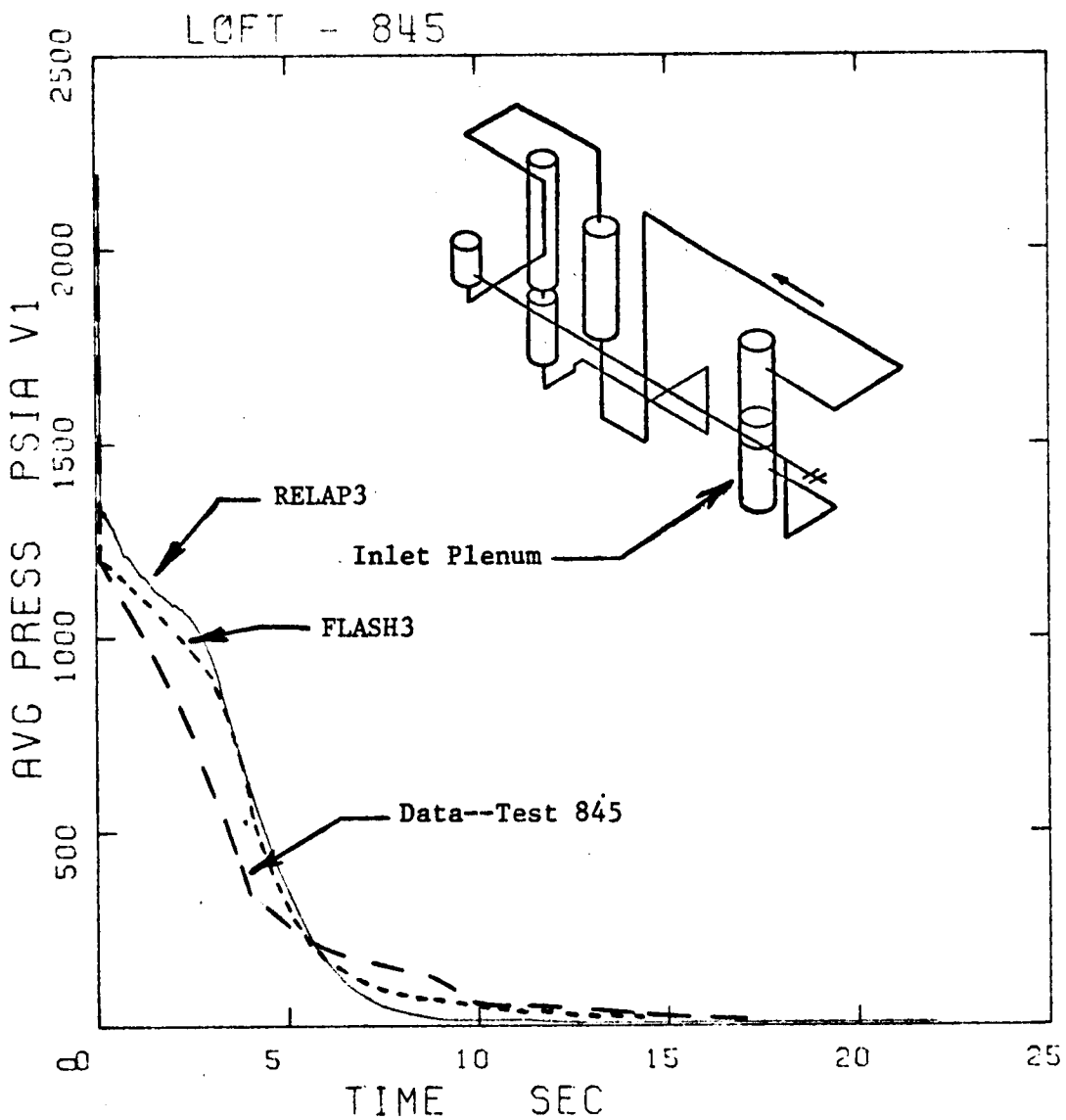


Figure 38. FLASH3 inlet plenum pressure.

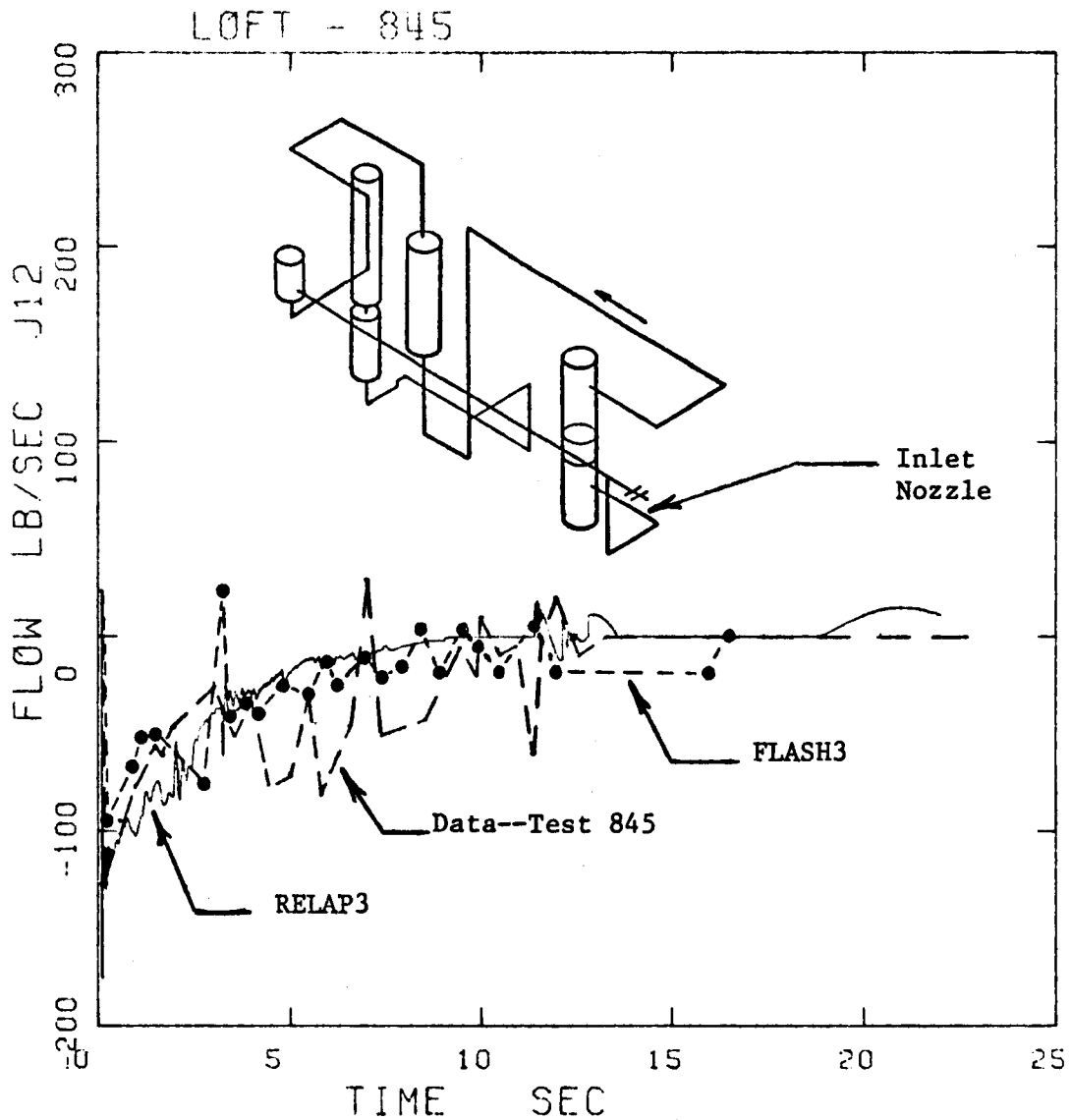


Figure 39. FLASH3 inlet nozzle flow rate.

the FLASH3 results are similar to the RELAP3 results. Between 11 seconds and 16 seconds, FLASH3 predicts a negative flow of about 20 lb/sec, which does not appear in the RELAP3 results, or in the data.

The location of the ECC injection point affects the above comparison. In the FLASH3 model, the ECC injection point is upstream of the inlet nozzle. In the RELAP3 model, the ECC is injected downstream of the inlet nozzle. From this, one would expect the FLASH3 inlet nozzle flow rate to be greater (more negative) during ECC injection. A comparison of the FLASH3 and the RELAP3 flows between 3.5 and 11.5 seconds confirms that this is so.

Core clad temperatures. Figure 40 compares the RELAP3 and FLASH3 calculated clad temperatures with the test data. The FLASH3 results agree quite well with the test data. The three-parameter fit correlation probably accounts for the good agreement, since the calculated flow rates and fluid conditions are not sufficiently different to account for the difference in results.

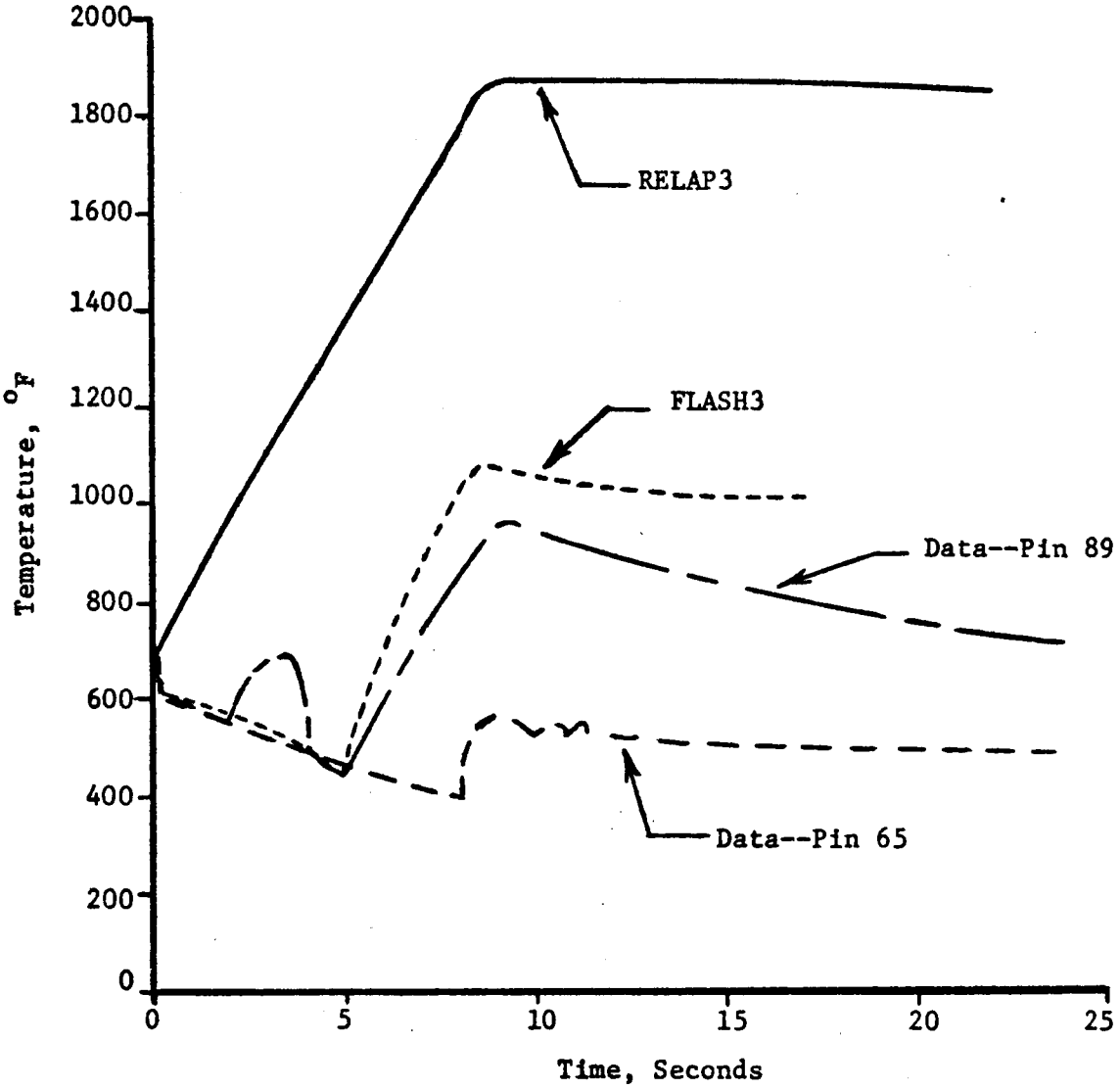


Figure 40. FLASH3 clad temperature.

IV. DISCUSSION

System Thermodynamics

Significant results. The comparisons between the RELAP3 predictions and the test data show several significant trends. Taken together, these trends give clues for some possible improvements in RELAP3. The significant trends are as follows. First, the RELAP3-predicted system pressures lie above the test data during the early part of both tests. The predicted pressures lie below the test data during the latter part of test 845. Similarly, the predicted pressures for test 825 lie below the test data after 11 seconds. Second, the RELAP3-predicted fluid temperatures for test 845 remain at saturation, while the observed fluid temperatures are above saturation after four seconds. Third, the RELAP3-predicted residual water is considerably greater than that observed in the test. This conclusion holds even if we discount the fill water that was expelled from the system by the accumulator gas in the experiment but not in the calculations. There are several effects that could help account for the three trends described above. These are discussed below.

Thermodynamic equilibrium. RELAP3 assumes thermodynamic equilibrium in a control volume. This assumption tends to bring all the fluid in the system to its saturation temperature. Any subcooled liquid or superheated vapor in the system will, in time, be eliminated. The use of a nonequilibrium model which gives a realistic rate of heat exchange

between phases should improve the fluid temperature and residual liquid predictions. The assumption of thermal equilibrium is particularly important when there is ECC injection. The RELAP3 simulation of test 845 showed that the highly subcooled ECC water causes a high rate of steam condensation in the volumes that contain ECC water. These volumes act as a sink, decreasing system pressure and drawing fluid from throughout the loop. The test results showed that much of the ECC water was ejected from the system as a subcooled liquid. Reference (6) discusses the results of a CRAFT code (23) analysis of test 845. This simulation included calculations with both equilibrium and nonequilibrium models. The nonequilibrium model greatly reduced the condensing effect of the fill water, giving a much better simulation of ECC behavior.

Phase separation. Reference (9) shows that the phase separation parameters used as input can affect both the pressure predictions and the residual water predictions. The use of different phase separation parameters might improve the calculations. The flow and pressure oscillations in the calculated results for test 825 are a result of the assumptions in the phase separation model. The oscillations would disappear if homogeneous phase separation parameters were used. This is because there would be no mixture level. A homogeneous model would eliminate the rapid variation in junction flow and density caused by the changing mixture level.

Phase separation and interphase heat transfer. The phase separation model and the interphase heat transfer model are closely

related. The degree of phase separation helps determine the rate of interphase heat transfer. If the liquid and vapor phases are well separated, the rate of interphase heat transfer may be fairly low. If, however, the phases are well mixed, the rate of interphase heat transfer is likely to be high. The RELAP3 phase separation model allows the phase separation rate to vary from rapid separation to zero separation. However, the assumption of thermodynamic equilibrium requires an infinite rate of interphase heat transfer, regardless of the phase separation rate.

Metal internal energy. RELAP3 does not consider the internal energy of the system pressure boundary. In small systems with a large surface to volume ratio, such as the semiscale loop, this stored energy can be significant. Consider the results for test 845. Excluding volumes 1, 12, and 15, RELAP3 predicts about 7 lb. of residual water. The internal energy in the pressure boundary should be enough to evaporate this much water in seconds. The fluid temperatures would then rise above saturation, in closer agreement with the test data.

Effect of noncondensible gas. RELAP3 has the capability to consider the presence of air in a control volume. However, RELAP3 apparently does not allow this air to flow from one volume to another. This makes it impossible to simulate the effects of escaping accumulator gas. Obviously, such effects can be important, and the results of the residual water calculations would be better if they were included. Reference (24) reports the results of ECC injection experiments in a glass

model system. The experiments included tests in which the apparatus was completely filled with steam, and also experiments in which air (a noncondensible) was present in the apparatus. The effects of emergency core coolant injection were considerably different for the two cases. With only steam present, the ECC injection caused depressurization as steam was condensed by the cold water. When air was present, the depressurization did not occur to the same extent.

Core Heat Transfer

Heat transfer mode oscillations. Figure 41 is a heat flux-versus-wall superheat plot for the initial conditions of test 825. This graph shows the mechanism of the heat transfer mode oscillations, which were described previously. The cause of the oscillations is the coupling of the heat transfer rate to the system pressure. The heater pin surface temperature is 662°F, which corresponds to a wall superheat of 7°F. The calculated heat flux is switching between the forced convection heat flux and the subcooled nucleate boiling heat flux. Equation (II-11) is a strong function of the system pressure. At the input initial conditions for test 825, the surface temperature is just high enough for subcooled nucleate boiling. However, in the first time step the pressure increases by about 0.3 psi. This increases T_{NB} enough so that the heat transfer mode switches to subcooled forced convection on the second time step. During the second time step the pressure decreases about 0.3 psi, and on the third time step the heat transfer mode switches back to subcooled nucleate boiling. The cycle persists indefinitely. Reducing the time step by an order of

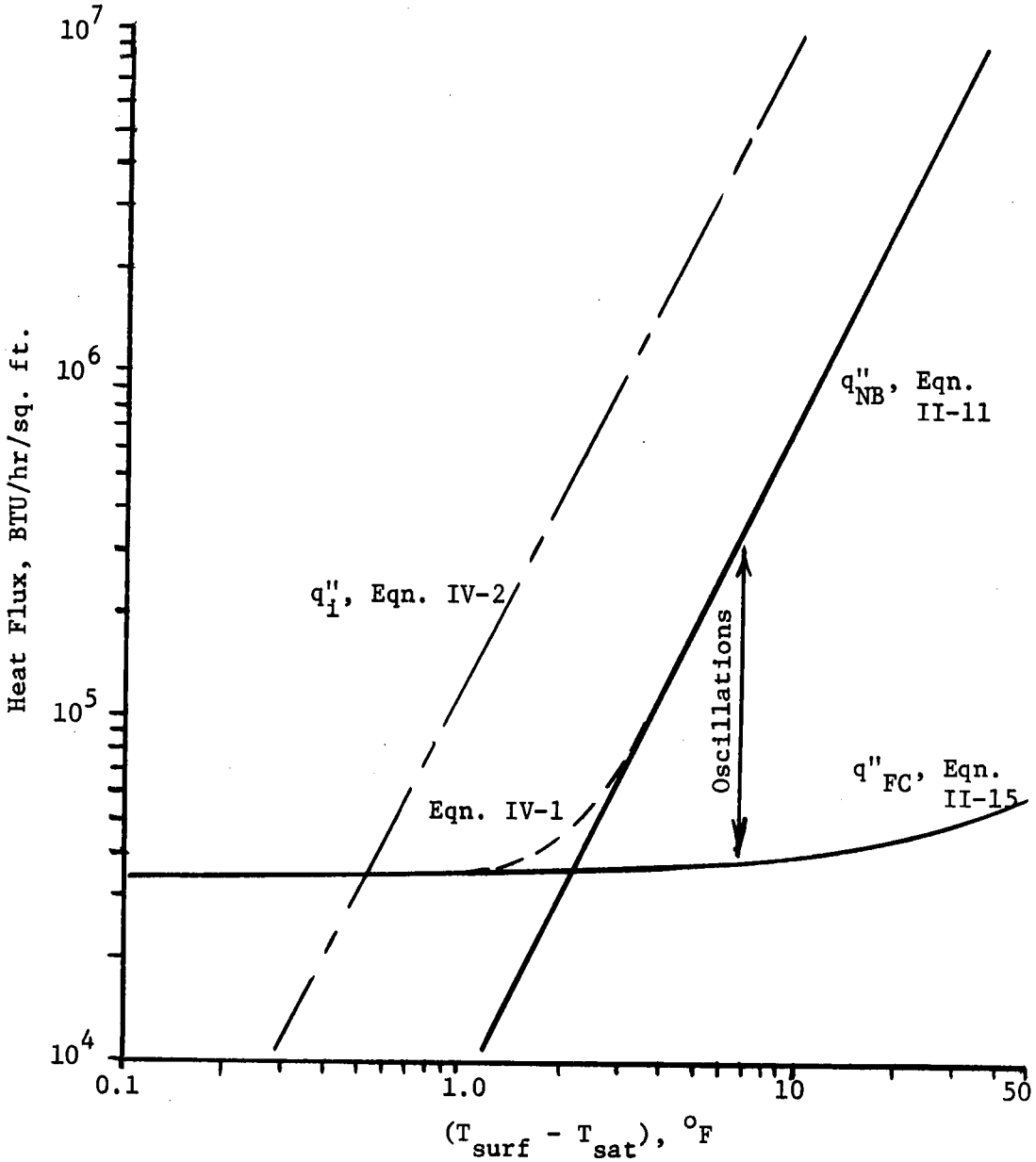


Figure 41. Heat flux diagram--test 825.

magnitude has no effect. As before, the oscillations have a period of two time steps.

Method of Bergles and Rohsenow. The heat transfer mode oscillations described above can be eliminated by using the method of Bergles and Rohsenow (25). The SATAN-4 blowdown code (14) also uses this method. In this method, if the surface heat flux exceeds the incipient boiling heat flux (see Figure 41, page 92) then the heat flux follows the transition curve shown on Figure 41. The transition heat flux can be calculated from (25):

$$q'' = q''_{FC}\left[1 + \left\{\frac{q''_{NB}}{q''_{FC}}\left(1 - \frac{q''_{NBi}}{q''_{NB}}\right)\right\}^2\right]^{1/2} . \qquad \text{(IV-1)}$$

The incipient boiling heat flux can be calculated from:

$$q''_i = 15.60\ P^{1.156}(T_{surf} - T_{sat})^{2.30/P^{0.0234}} . \qquad \text{(IV-2)}$$

In equation (IV-1) q''_{NBi} is the nucleate boiling heat flux at the incipient boiling surface temperature. This method should give a stable transition from subcooled forced convection to subcooled nucleate boiling.

DNB calculations. As we saw in Section III, RELAP3 predicts DNB much earlier in the transient than it actually occurred. The geometry of the semiscale core is not at all like the geometry used to develop the DNB correlations in RELAP3. The DNB correlations were derived from data taken in closely packed rod bundles with large length-to-diameter ratios.

The semiscale core has widely spaced heaters and a small length-to-diameter ratio. This in itself limits the accuracy of the DNB calculations. However, there are still some possible ways to improve the predictions without affecting the correlations themselves. Eliminating the heat transfer mode oscillations described above would have improved the results for test 825. The calculated flow rate in the core remains fairly large until about 2.8 seconds, except for a few momentary stoppages. If the mode oscillations were eliminated, and if the momentary dips in the flow were ignored, the calculated DNB time would be about 2.9 seconds.

Flow rate for DNB calculation. RELAP3 uses the instantaneous flow rate at each time step in the DNB calculation. The DNB calculation is a quasi-steady state calculation. Therefore, a more realistic approach would be to use a smoothed flow rate in the DNB calculation. RELAP3 predicts numerous high frequency flow variations that cannot be observed experimentally. These should be eliminated from the flow used in the DNB calculation. For example, the results for test 845 show that RELAP3 predicts core flow reversal right after rupture. The reversal takes place in such a short time that DNB does not occur. If a smoothed flow rate were used in the DNB calculation, the RELAP3 results would be better. A crude, but simple, way to smooth the flow rates would be to use the average value computed over some small backward time interval. A value like the past 0.01 seconds might work well, without any real risk of failing to predict a real DNB. Of course, the best method would be to develop a DNB correlation especially for transient applications.

Significance of FLASH3 results. The FLASH3 DNB calculations (see Section II) give core temperature results that are more realistic than the RELAP3 results. The three-parameter fit DNB correlation probably accounts for the improvement. In the three-parameter correlation, the DNB flux is not a function of the transient mass flux. The success of the FLASH correlation implies that the mass flux dependence in the RELAP3 DNB correlations is too strong, which tends to confirm the conclusions reached in the previous paragraph.

Effect of core heat transfer rate on the system. The response of the system depends in part on the rate of heat transfer from the core to the fluid. RELAP3 predicts a very low rate of heat transfer from the core to the fluid. The clad temperature results show this very clearly. A more realistic heat transfer rate in the core would probably improve the system pressure predictions. The heat transfer rate observed in the test data is enough to evaporate about one pound of water per second. The core heat transfer model in RELAP3 does produce conservative core temperatures. However, the unrealistically low rate of heat transfer to the fluid introduces an error in the system calculations. The system pressure and fluid temperature results could be improved by using a more realistic heat transfer rate.

Heat Exchanger Model

RELAP3 model. The test reports for tests 825 and 845 (references (2) and (3)) give very little information about the behavior of the heat

exchanger during the transient. However, the RELAP3 heat exchanger model contains several severe approximations. These were discussed in Section II. The RELAP3 heat exchanger heat transfer rate is likely to be unrealistic.

Effect of heat absorption rate. The comparison of the flow-and-temperature dependent heat exchanger results for test 845 with the results for constant heat exchanger power show little difference between the two in the early stages of blowdown. However, in the latter part of the blowdown, the effects can be considerable. When condensation occurs in the heat exchanger the heat transfer rate could be important, and RELAP3 should have a more accurate heat exchanger model. An accurate heat exchanger model would calculate heat transfer coefficients on both sides of the heat exchanger tubes, rather than using an initial heat transfer coefficient multiplied by a flow rate correction factor. An accurate heat exchanger model would also consider varying secondary temperatures and flow rates.

V. CONCLUSIONS

Overall Results

Cladding temperatures. The cladding temperature results are probably the most important single parameter to use in judging the accuracy of a blowdown code. RELAP3 predicts clad temperatures which are far greater than those observed experimentally. Thus, RELAP3 has a large amount of built-in conservatism.

System results. RELAP3 appears to give a reasonable approximation of the flow rates and fluid conditions during the period prior to the start of ECC injection. However, during emergency core coolant injection, the assumption of thermodynamic equilibrium in a control volume causes a high rate of steam condensation. The rapid condensation rate depressurizes the system too quickly, and alters the system flow rates and fluid mass distribution. In addition, the excessive condensation tends to increase the residual liquid in the system at the end of the transient. The lack of ability to simulate the effect of noncondensibles in the system also affected the system results for test 845. In the experiment, the probable effect of the nitrogen cover gas from the accumulator was to displace much of the residual liquid from the system. The RELAP3 model did not simulate this effect.

Heat exchanger model. The equations RELAP3 uses to calculate the heat transfer rate in the heat exchanger are very approximate, and the rate of heat transfer is likely to be unrealistic. The heat exchanger

heat transfer rate does not appear to affect any important results, but nevertheless, a more accurate model should be available.

Conclusions. The results of this research show that RELAP3 can give a reasonable prediction of experimental loss-of-coolant data, provided that the user recognizes the limitations and approximations within the computer code. The user must allow for the highly conservative core heat transfer model, the assumption of thermodynamic equilibrium, and the lack of ability to simulate the effect of noncondensibles. The heat exchanger model is an additional factor to be considered, but it appears to be of lesser importance.

Possible Areas of Improvement

Summary. The comparisons presented between the RELAP3 results and the semiscale experimental data show that there are several possible areas of investigation which could improve the RELAP3 predictions of experimental data. The most obvious of these is the core heat transfer calculation, which gives core temperatures which are much greater than the experimental values. Another obvious area of improvement is the heat exchanger heat transfer calculations, which are highly approximate. Several other areas of investigation could improve the system thermodynamic calculations.

Core heat transfer. RELAP3's present DNB calculation method is based on steady-state correlations, but it uses transient flow rates and fluid conditions as input to the DNB correlation. The DNB calculations could be improved by using time-averaged flow rates and fluid conditions

as input. Another possibility would be to develop new correlations especially for the transient application. Either of the two methods would make the pin temperature calculations more realistic. Such a change would also improve the overall system results, since the rate of heat transfer to the fluid in the core would be more nearly correct.

Heat exchanger calculations. The severe assumptions in the present RELAP3 heat exchanger model should be corrected. A more accurate model would actually calculate the heat transfer coefficients on both sides of the heat exchanger tubes, rather than using an initial heat transfer coefficient multiplied by a flow rate correction. An accurate heat exchanger model would also allow for varying secondary temperatures and flow rates.

Interphase heat transfer. The present RELAP3 code assumes thermodynamic equilibrium between phases at all times. RELAP3 should have an optional model which allows steam and water to coexist at different temperatures with a realistic rate of heat transfer between phases.

Phase separation model. The modeling of the phase separation is closely tied to the problem of interphase heat transfer. Further research on phase separation modeling could improve the RELAP3 calculations.

Noncondensible gases. RELAP3 should consider the effect of noncondensible gases in the system, if they are present. This could improve the results of the calculation, especially at the low-pressure end of the blowdown, and during emergency core coolant injection.

LIST OF REFERENCES

LIST OF REFERENCES

1. Rettig, W. H., et al. "RELAP3--A Computer Program for Reactor Blowdown Analysis," USAEC Report IN-1321 (June, 1970).

2. Olson, D. J., et al. "Semiscale Blowdown and Emergency Core Cooling Project Test Report--Tests 824 and 825," USAEC Report IN-1481 (June, 1971).

3. _____. "Semiscale Blowdown and Emergency Core Cooling Project Test Report--Test 845," USAEC Report ANCR-1014 (January, 1970).

4. Bingham, B. E. and Roberson, C. E. "Loss-of-Coolant Methods Development," Trans. ANS 14, No. 2, October, 1971.

5. Hentzen, R. D. "Nodal Sensitivity in Modeling for Large PWR System for a Loss-of-Coolant Accident," USAEC Report CONF-710302-8.

6. Jensen, W. L. "Correlation of Experimental Blowdown and Reflooding Data Using the CRAFT Code," Trans. ANS 14, No. 2, October, 1971.

7. Moore, K. V. and Gruen, G. E. "Effects of State Properties on High Pressure Compressible Hydrodynamics," USAEC Report CONF-7103026.

8. Murphy, J. H. and Redfield, J. A. "FLASH3 Analysis of the LOFT Semiscale Test 845," Trans. ANS 14, No. 2, October 17-21, 1971.

9. Slater, C. E. "Comparison of Predictions from the Reactor System Decompression Code (RELAP3) with Decompression Data from the Semiscale Blowdown and ECC Tests," USAEC Report IN-1444.

10. Murphy, J. H., et al. "FLASH3: A Fortran IV Program for the Simulation of Reactor Plant Transients in Space and Time," USAEC Report WAPD-TM-800.

11. Olson, D. J. and Van Haverbeke, J. D. "Description of the Facility and Data Acquisition System for the Heated Core Portion of the 800 Series of the Semiscale Blowdown and Emergency Core Cooling Project," USAEC Report IN-ITR-202 (July, 1970).

12. Dietz, K. A. "Quarterly Technical Report--LOFT Program Office," April 1-June 30, 1969, USAEC Report IDO-17303.

13. Heisselman, H. W. Personal communication to Dr. Julian E. Mott (May 11, 1972).

14. _____. Telephone conversation with J. R. Hamilton (June 16, 1972).

15. Bordelon, F. M. "A Comprehensive Space-Time Dependent Analysis of Loss-of-Coolant" (SATAN-4 Digital Code), USAEC Report WCAP-7750 (August, 1971).

16. Streeter, V. L. and Wylie, E. B. Hydraulic Transients. New York: McGraw-Hill Book Company, 1967.

17. Parks, C. E. et al. "Multi-Node Analysis of B & W's 2568 Mwt Nuclear Plants During a Loss of Coolant Accident," USAEC Report BAW-10034 (Rev. 1), February, 1972.

18. Goldsmith, A. et al. Handbook of Thermophysical Properties of Solid Materials. New York: MacMillan Company, 1961.

19. Southern Research Institute. "The Thermal Properties of Twenty-Six Solid Materials to 5000°F or Their Destruction Temperatures," Technical Documentary Report ASD-TDR-62-765 (January, 1963).

20. Plenum Press Handbook of High Temperature Materials. New York: Plenum Press.

21. Parker, E. F. Materials Data Book for Scientists and Engineers. New York: McGraw-Hill Book Company.

22. Murphy, J. H. and Redfield, J. A. "FLASH-3 Analysis of the LOFT Semiscale Test 845," USAEC Report WAPD-T-2474.

23. Bingham, B. E. et al. "CRAFT--Description of Model for Equilibrium LOCA Analysis Program," USAEC Report BAW-10030 (October, 1971.

24. Murphy, J. H. et al. "Glass Model Tests on Emergency Core Cooling Systems," Trans. ANS 13, 385 (1970).

25. Bergles, A. E. and Rohsenow, W. M. "The Determination of Forced-Convection Surface Boiling Heat Transfer," J. Heat Trans., August, 1964.

VITA

John Ralph Hamilton was born in Little Rock, Arkansas, on December 9, 1944. He graduated from Las Animas High School, Las Animas, Colorado, in 1963. In September, 1963, he entered the University of Arkansas, and in January, 1968, he received a Bachelor of Science degree in Mechanical Engineering.

Following his graduation from the University of Arkansas he was employed by the Babcock & Wilcox Company.

He entered the Graduate School of The University of Tennessee in September, 1971, and received the Master of Science degree with a major in Nuclear Engineering in March, 1973. He is a member of the American Nuclear Society and the American Society of Mechanical Engineers.

He is married to the former Maxine Lois Brown of Greenville, Pennsylvania.